Technical Report Documentation Page

1. Report No. FHWA/TX-09/0-5367-1	2. Government Accession No.	3. Recipient's Catalog No.
4. Title and Subtitle Recommendations for the Use of Precast Deck Panels at Expansion Joints		5. Report Date November 2008 6. Performing Organization Code
7. Author(s) Sharon L. Wood, James O. Jirsa, Oguzhan Bayrak, Lewis S. Agnew, Jr., C. Adam Boswell, Alan R. Kreisa, Kristen S. Donnelly, and Bryan Bindrich		8. Performing Organization Report No. 0-5367-1
9. Performing Organization Name and Address Center for Transportation Research The University of Texas at Austin 3208 Red River, Suite 200 Austin, TX 78705-2650		10. Work Unit No. (TRAIS) 11. Contract or Grant No. 0-5367
12. Sponsoring Agency Name and Address Texas Department of Transportation Research and Technology Implementation Office P.O. Box 5080 Austin, TX 78763-5080		13. Type of Report and Period Covered Technical Report 9/2005–8/2008 14. Sponsoring Agency Code

15. Supplementary Notes
Project performed in cooperation with the Texas Department of Transportation and the Federal Highway Administration.

16. Abstract

Prestressed concrete panels have been used by the bridge construction industry in the state of Texas for many years to increase construction speed and improve safety and economy. At expansion joints, cast-in-place concrete is used and requires temporary formwork and slows construction. In a previous TxDOT project (0-4418), a full-scale bridge deck was constructed that included precast panels at a 0^o skew. The results indicated that the precast panel system provided adequate strength and reduced construction costs compared with the traditional cast-in-place details at the expansion joint. In this investigation (TxDOT Project 0-5367) two areas not covered in Project 0-4418 were studied: fatigue performance of bridge decks using precast panels at the expansion joints and the use of precast panels at skewed expansion joints. Fatigue response of precast panels under loading at the expansion joint in 0^o skew bridges was excellent. Skewed precast panels at expansion joints were tested under static and fatigue loads. Two skew angles were tested: 30^o and 45^o. Six specimens were constructed and subjected to a total of eleven tests. Loads were applied at midspan of the skewed end of each specimen, and some specimens were also loaded at joint between trapezoidal (skewed) panels and an adjacent rectangular panel. The skewed panels performed well. Design recommendations for implementation of skewed panels were developed.

17. Key Words	18. Distribution Statement
precast panels, skewed expansion joints, concrete, bridge, deck, slab, shear, fatigue	No restrictions. This document is available to the public through the National Technical Information Service, Springfield, Virginia 22161; www.ntis.gov.

19. Security Classif. (of report)	20. Security Classif. (of this page)	21. No. of pages	22. Price
Unclassified	Unclassified	124	

Form DOT F 1700.7 (8-72) Reproduction of completed page authorized

Recommendations for the Use of Precast Deck Panels at Expansion Joints

Sharon L. Wood
James O. Jirsa
Oguzhan Bayrak
Lewis S. Agnew, Jr.
C. Adam Boswell
Alan R. Kreisa
Kristen S. Donnelly
Bryan Bindrich

CTR Technical Report:	0-5367-1
Report Date:	November 2008
Research Project:	0-5367
Research Project Title:	Development of Simple Bridge Deck Details at Expansion Joints
Sponsoring Agency:	Texas Department of Transportation
Performing Agency:	Center for Transportation Research at the University of Texas at Austin

Project performed in cooperation with the Texas Department of Transportation and the Federal Highway Administration.

Center for Transportation Research
The University of Texas at Austin
3208 Red River
Austin, TX 78705

www.utexas.edu/research/ctr

Disclaimers

Author's Disclaimer: The contents of this report reflect the views of the authors, who are responsible for the facts and the accuracy of the data presented herein. The contents do not necessarily reflect the official view or policies of the Federal Highway Administration or the Texas Department of Transportation (TxDOT). This report does not constitute a standard, specification, or regulation.

Patent Disclaimer: There was no invention or discovery conceived or first actually reduced to practice in the course of or under this contract, including any art, method, process, machine manufacture, design or composition of matter, or any new useful improvement thereof, or any variety of plant, which is or may be patentable under the patent laws of the United States of America or any foreign country.

Notice: The United States Government and the State of Texas do not endorse products or manufacturers. If trade or manufacturers' names appear herein, it is solely because they are considered essential to the object of this report.

Engineering Disclaimer

THIS REPORT IS NOT INTENDED FOR CONSTRUCTION, BIDDING,
OR PERMIT PURPOSES.

James O. Jirsa, Texas P.E. #31360
Research Supervisor

Acknowledgments

This research project was funded by the Texas Department of Transportation (TxDOT) under Project No. 0-5367. The support of the project director, Walter R. (Ray) Fisher, III, and project panel members David Hohmann; Dean Van Landuyt; John Holt; Joe Roche; Jason Tucker; and Lewis Gamboa is greatly appreciated.

Products

Research Product P1, Design Recommendations is included in the Appendix of this report. Limits on the geometry of the panels are discussed in Section A.1. Recommended reinforcement is presented in Section A.2. Issues related to construction of the PC panels and of the composite bridge deck are summarized in Section A.3 and Section A.4, respectively.

Table of Contents

List of Figures

List of Tables

Chapter 1. Introduction

1.1 Background

The Texas Department of Transportation (TxDOT) has, in recent decades, dedicated considerable resources to improving bridge construction methods. Evolving from this effort is the current practice of using prestressed concrete panels in bridge decks. The use of these panels eliminates the majority of formwork for concrete bridge decks, decreases construction time, and reduces construction costs.

Prestressed concrete panels in bridges span from girder to girder and run the length of the bridge, as shown in Figure 1.1. Precast panels are 4 in. thick and are topped with a 4-in. cast-in-place slab. The entire 8-in. deep composite section comprises the bridge deck. In the past, precast concrete panels have been placed at 4 ft. away from the expansion joint in the bridge deck and traditional forming techniques have been used to cast a 10-in. I-beam thickened slab (IBTS) adjacent to the expansion joint. Cross sections of precast panels used at expansion joints are provided in Figure 1.2.

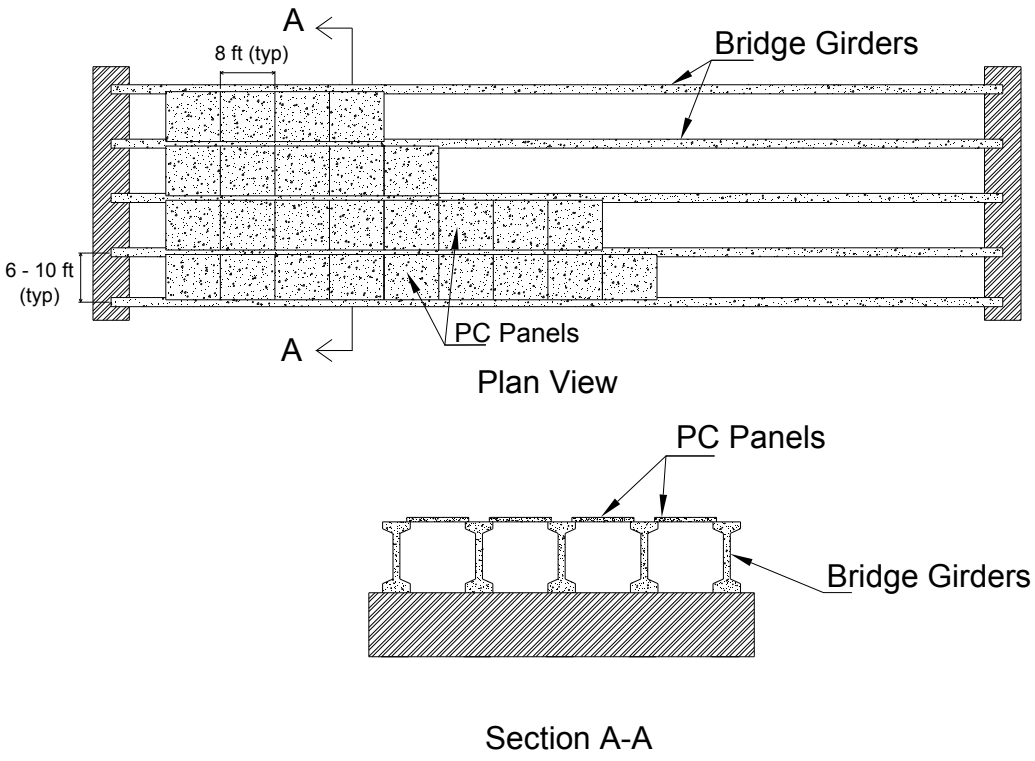

Figure 1.1: Placement of Precast Panels in Bridge Deck Construction

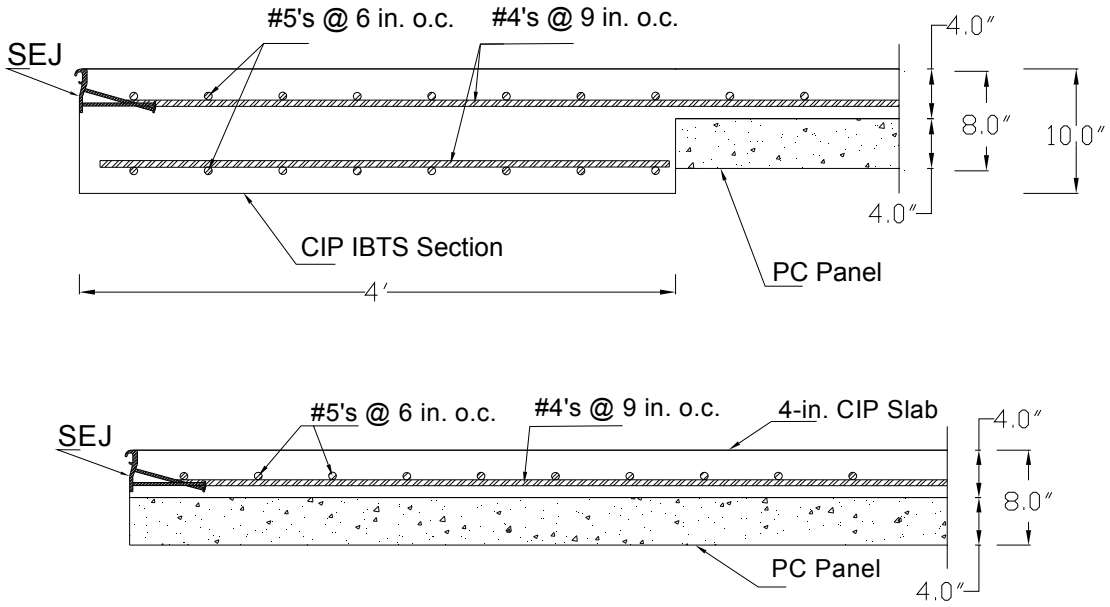

Figure 1.2: Comparison of Traditional IBTS Detail at Expansion Joint (top) and Precast Panels at Expansion Joint (bottom)

Skewed expansion joints in bridge decks present a unique challenge for precast panel bridge deck systems. Precast panels are generally rectangular in shape and, as shown in Figure 1.3, leave trapezoid-shaped gaps at the end of the deck adjacent to the expansion joint. Current bridge construction practices call for the use of stay-in-place sheet metal forms or timber forming methods to construct the IBTS detail at the end of the bridge deck.

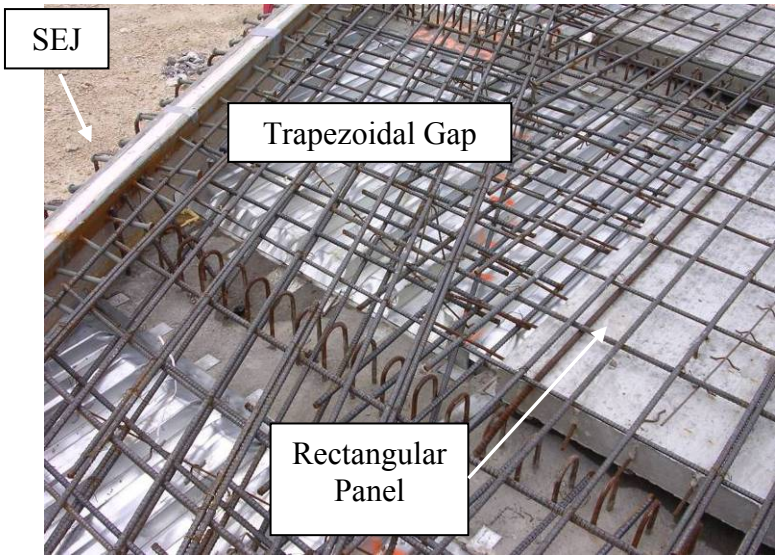

Figure 1.3: Trapezoidal Gap Adjacent to Skewed Expansion Joint

In TxDOT project 0-4418, a full-scale bridge deck with 0^o skew was constructed and it was concluded that the precast panel system provided adequate strength and reduced construction costs compared with the traditional cast-in-place details at the expansion joint. The bridge deck was subjected to monotonic loads to failure. Although one specimen had 45^o expansion joints, rectangular precast panels could not be placed to the joint. Recommendations were made for studies needed to better understand the behavior of precast panels in a broad range of applications. Fatigue loading of precast panels at the expansion joint was recommended as well as the use of trapezoidal precast panels at expansion joints in skewed bridge decks.

1.2 Project 0-5367

The purpose of Project 0-5367 was to evaluate the fatigue performance of precast panels use in perpendicular and skewed bridges. For skewed PC panels, the work done earlier on non-skewed expansion joints was to extended to skewed edges so that panels could be used throughout the length of a bridge deck. In consultation with fabricators, contractors, and bridge engineers, details of skewed (trapezoidal) panels were to be developed and evaluated and guidelines for the implementation of skewed panels prepared.

Chapter 2. Overview of Experimental Program

The primary objective of this research project was to develop simple bridge deck details in the vicinity of expansion joints. Details incorporating precast concrete (PC) panels and a cast-in-place topping slab were selected for investigation because of the excellent measured response during TxDOT Project 0-4418 (Coselli et al. 2006) and because the PC panels act as stay-in-place formwork, thereby increasing worker efficiency and safety at the construction site. The experimental program was focused on answering two basic questions about the behavior of constant thickness bridge decks using PC panels with a cast-in-place topping slab:

1. Is fatigue damage likely to occur under service loads if the precast panels are placed up to the expansion joint edges of bridge decks?
2. What configurations of precast panels are appropriate for skewed edges of bridge decks?

As discussed in Chapter 1, previous research using precast panels along the entire length of the bridge deck included only static loading. Question 1 addresses the concern that the long-term serviceability of a bridge deck may be limited if the expansion joint detail with PC panels is susceptible to fatigue damage. Question 2 addresses the issue that a large portion of bridges within Texas are skewed. Approximately 50% of the prestressed I-girder bridges and approximately 35% of all bridges have skewed supports. Therefore, the development of appropriate PC panels for skewed bridges would eliminate the need for special formwork at expansion joints in nearly all bridges in Texas.

The experimental program was divided into two phases. In Phase 1, the research team evaluated the fatigue performance of the precast panels in rectangular test specimens. In Phase 2, the research team evaluated the strength and stiffness of skewed test specimens under monotonically applied loads. One skewed test specimen was also subjected to fatigue loads in Phase 2. All specimens were constructed using full-size PC panels and expansion joint rails. The configuration of the test specimens and the primary experimental parameters used in each phase of the investigation are summarized in this chapter.

2.1 Fatigue Response of PC Panel Detail at Rectangular Expansion Joints

The three specimens tested during TxDOT Project 0-4418 (Coselli et al. 2006) were constructed at full-scale and each specimen included four longitudinal girders and a 32-ft wide bridge deck. Wheel loads were applied at multiple locations on each specimen to evaluate the behavior of the expansion joint details under both positive and negative moment. A similar configuration was considered during this project. However, the research team concluded that testing smaller sections of a full-scale bridge deck was a better investment of time and resources. The smaller specimens were more economical to construct, and several specimens could be built more efficiently than one large bridge deck. Multiple test specimens would also allow for the repeatability of the test results to be evaluated.

Similarly to TxDOT Project 0-4418, the specimens tested in this project were designed to evaluate the behavior of the expansion joint details under both positive and negative moment. The geometry of the two test specimen configurations is shown in Figure 2.1 through Figure 2.4. Precast concrete beams with an overall length of 8 ft were spaced at 10 ft on center in both types of specimens. A single PC panel spanned between the two beams in the positive moment

specimens (Figure 2.1) and two panels were used in the negative moment specimens (Figure 2.3). The sealed expansion joint (SEJ) rail was used along one edge of each specimen. A single wheel load was applied at midspan of the edge with the SEJ for the positive moment specimen. Two wheel loads were place symmetrically with respect to the center beam in the negative moment specimens.

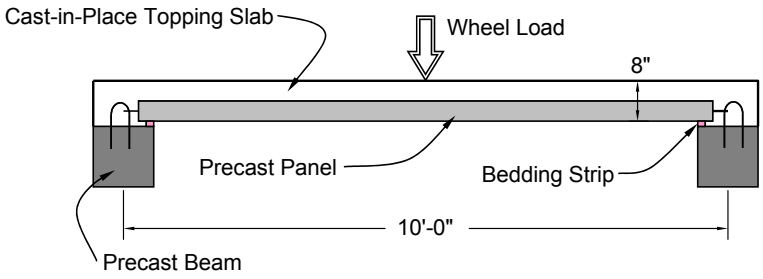

Figure 2.1: Cross Section of Positive Moment Specimens

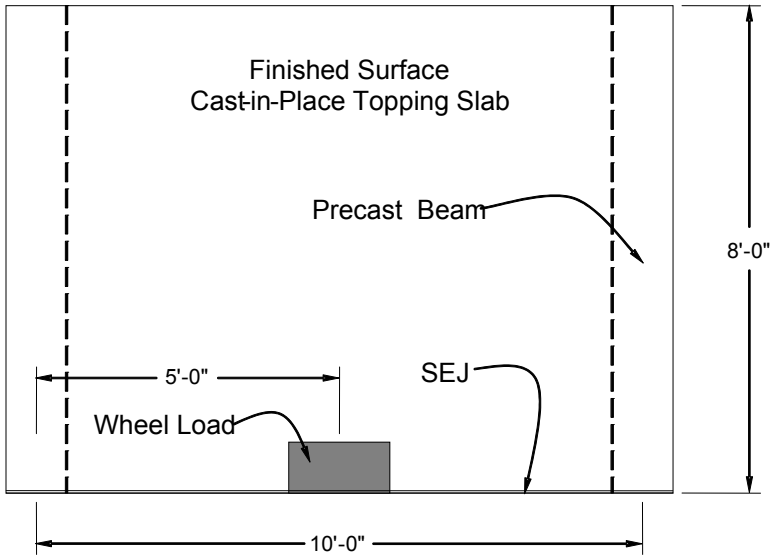

Figure 2.2: Plan View of Positive Moment Specimens

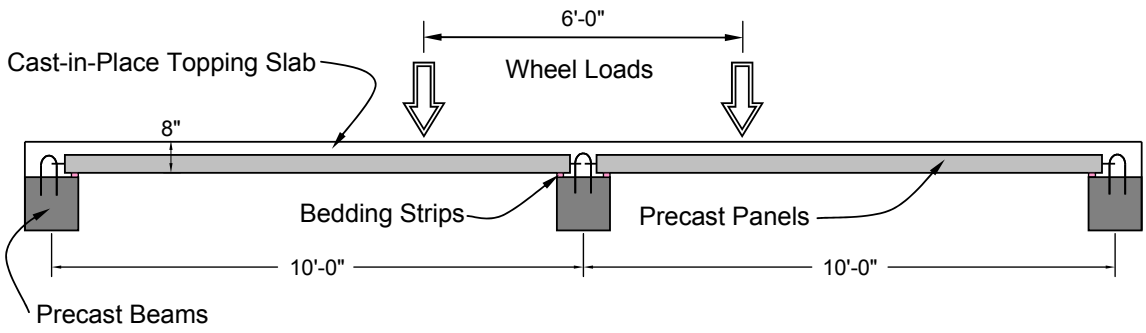

Figure 2.3: Cross Section of Negative Moment Specimens

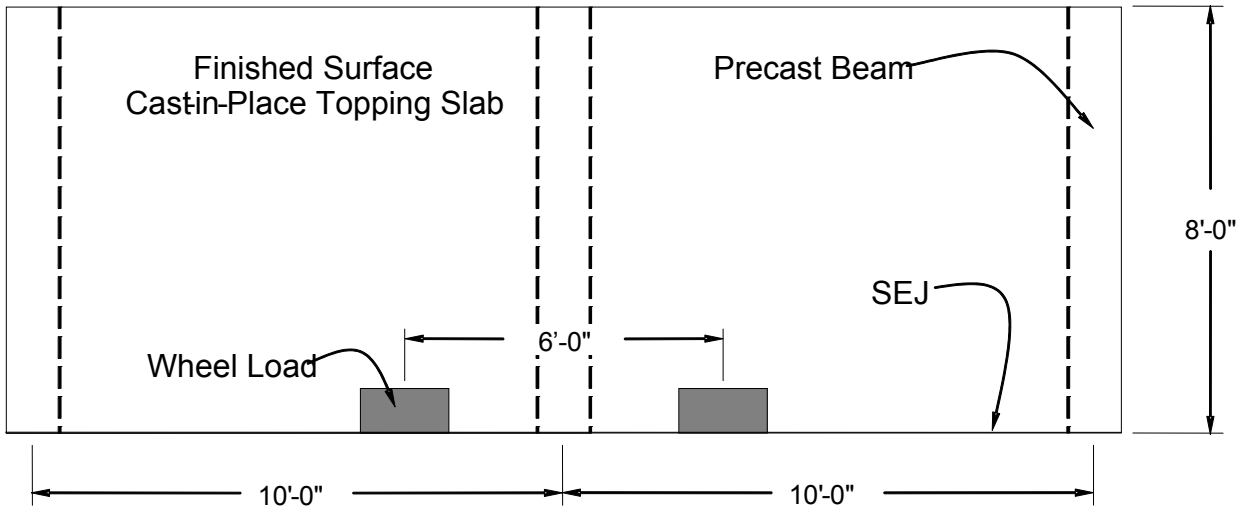

Figure 2.4: Plan View of Negative Moment Specimens

Agnew (2007) conducted 2D and 3D linear analyses to demonstrate that the response of the test specimens under service loads was comparable to that of a prototype bridge deck. A bridge deck with four longitudinal girders was selected as the prototype for this study (Figure 2.5). The overall thickness of the deck was assumed to be 8 in. and the center-line spacing of the longitudinal girders was taken as 10 ft. The results of a 2D analysis were used to determine the transverse location of the axle loads that generated the largest positive and negative moments (Figure 2.6).

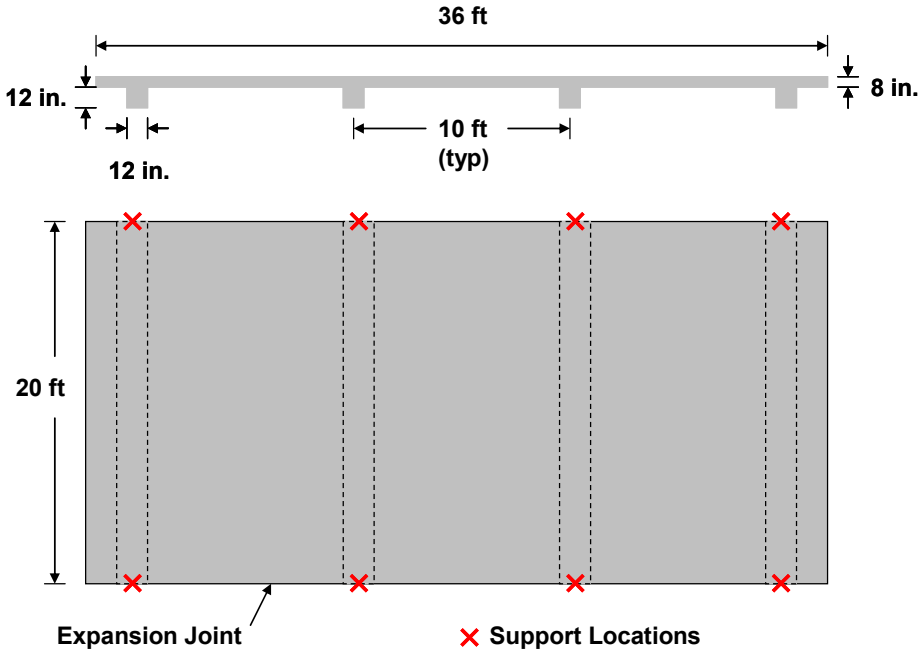

Figure 2.5: Configuration of Prototype Bridge Deck

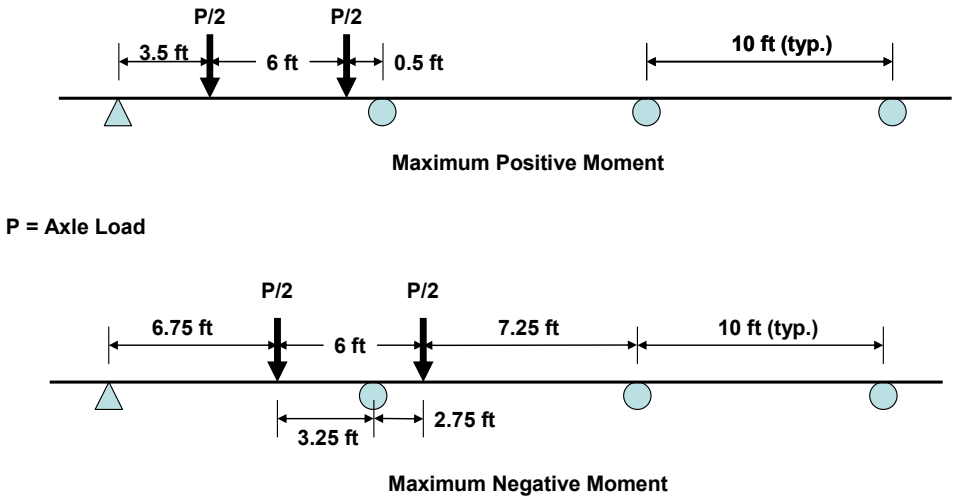

Figure 2.6: Transverse Locations of the Axle Loads Corresponding to Maximum Positive and Negative Moments in the Bridge Deck

The rear axle of the HL-93 Design Truck and the HL-93 Design Tandem were then applied to a 3D, elastic model of the prototype bridge deck. Axle locations corresponding to the maximum positive moment are shown in Figure 2.7 and Figure 2.8 for the design truck and design tandem, respectively. In each case, one axle was positioned adjacent to the expansion joint rail to maximize the moment at this critical location. Calculated values of the maximum principal stresses from these analyses are summarized in Table 2.1. For both positive and

negative moment, the HL-93 Design Tandem produced larger calculated compressive stresses, while the HL-93 Design Truck produced larger calculated tensile stresses.

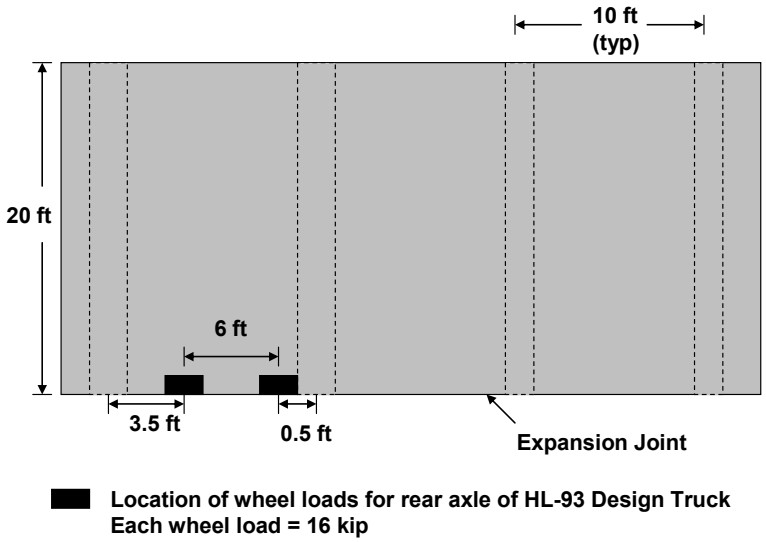

Figure 2.7: Location of HL-93 Design Truck that Generates Maximum Positive Moment in Prototype Bridge Deck

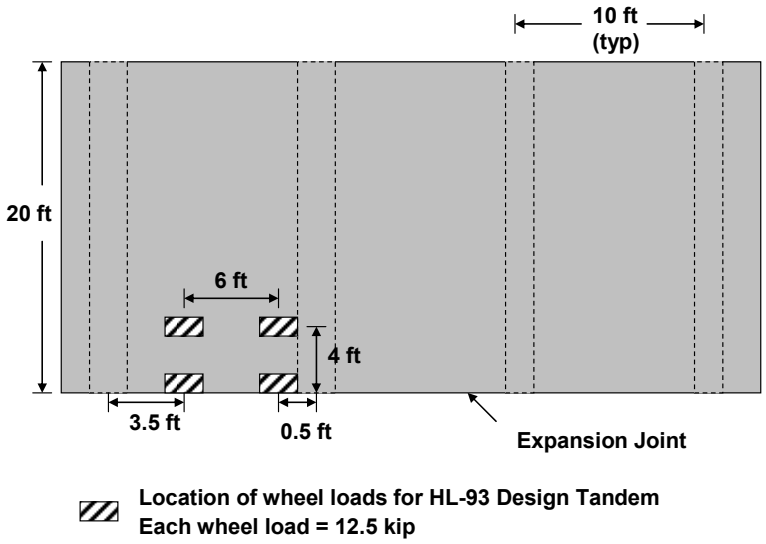

Figure 2.8: Location of HL-93 Design Tandem that Generates Maximum Positive Moment in Prototype Bridge Deck

Table 2.1: Maximum Values of Principal Stress from Elastic Finite Element Analyses of Prototype Bridge Deck

Parameter	Load Placed to Maximize Positive Moment		Load Placed to Maximize Negative Moment	
	HL-93 Design Truck	HL-93 Design Tandem	HL-93 Design Truck	HL-93 Design Tandem
Compressive Stress (psi)	555	581	617	620
Tensile Stress (psi)	498	492	522	466

The test specimens were then analyzed using both the rear axle from the HL-93 Design Truck and the HL-93 Design Tandem. As shown in Figure 2.2 and Figure 2.4, the wheel loads for the rear axle of the HL-93 Design Truck were placed adjacent to the SEJ. A second set of wheel loads was positioned at the center of the panel for the HL-93 Design Tandem loading.

Maximum calculated values of the principal stresses are summarized in Table 2.2 and Table 2.3 for the positive moment and negative moment specimens, respectively. For the test specimens, the rear axle of the HL-93 Design Truck generated larger stresses than the HL-93 Design Tandem. In addition, the calculated stresses in the test specimens were 3 to 12% larger than the corresponding stresses in the prototype bridge deck. Based on these analyses, the stresses induced in the test specimens were considered to be representative of those induced in the prototype bridge deck, and the rear axle load from the HL-93 Design Truck was selected as the loading configuration for the entire test program.

Table 2.2: Maximum Values of Principal Stress from Elastic Finite Element Analyses of Positive Moment Specimen

Parameter	Load Placed to Maximize Positive Moment	
	HL-93 Design Truck	HL-93 Design Tandem
Compressive Stress (psi)	648	603
Tensile Stress (psi)	544	508

Table 2.3: Maximum Values of Principal Stress from Elastic Finite Element Analyses of Negative Moment Specimen

Parameter	Load Placed to Maximize Negative Moment	
	HL-93 Design Truck	HL-93 Design Tandem
Compressive Stress (psi)	682	640
Tensile Stress (psi)	540	485

2.1.1 Experimental Program

Four rectangular specimens were subjected to fatigue loading during the first phase of this investigation. Two positive moment and two negative moment specimens were tested (Table 2.4). The design, construction, and measured response of these specimens are discussed in detail by Agnew (2007). In addition to the geometry of the specimens, the primary experimental variable was the amplitude of the fatigue load.

Table 2.4: Primary Experimental Parameters Tested during First Phase of Investigation

Specimen	Configuration	Fatigue Load		
		Designation	Type	Value (kip)
1	Positive Moment	Service Vehicle	Wheel	6
2	Positive Moment	Design Truck	Wheel	16
3	Negative Moment	Design Truck	Axle	32
4	Negative Moment	Overload Truck	Axle	46

The amplitude of the fatigue loads was initially selected to represent service-level traffic loadings. Because the specimens exhibited excellent fatigue response, the fatigue loads were increased in subsequent specimens. Service-level axle loads were determined from weigh-in-motion (WIM) data from IH 35 South of San Antonio (Wood et al. 2007). A histogram of axle weights measured over a 50-day period is shown in Figure 2.9, and the effective axle weight corresponding to this distribution of axle loads is 12 kip. Wheel loads were applied to the two positive moment specimens 1 and 2. The applied fatigue load for specimen 1 (6 kip) corresponds to one half of the effective axle load from the WIM data. The amplitude of the fatigue load was increased to one half the rear axle load from the HL-93 Design Truck (16 kip) for specimen 2.

The full axle load was distributed to two wheel loads, which were symmetrically placed with respect to the center beam, for the negative moment specimens. The fatigue load for specimen 3 corresponded to the rear axle of the HL-93 Design Truck (32 kip). The fatigue load was increased to represent an overload truck for specimen 4 (46 kip).

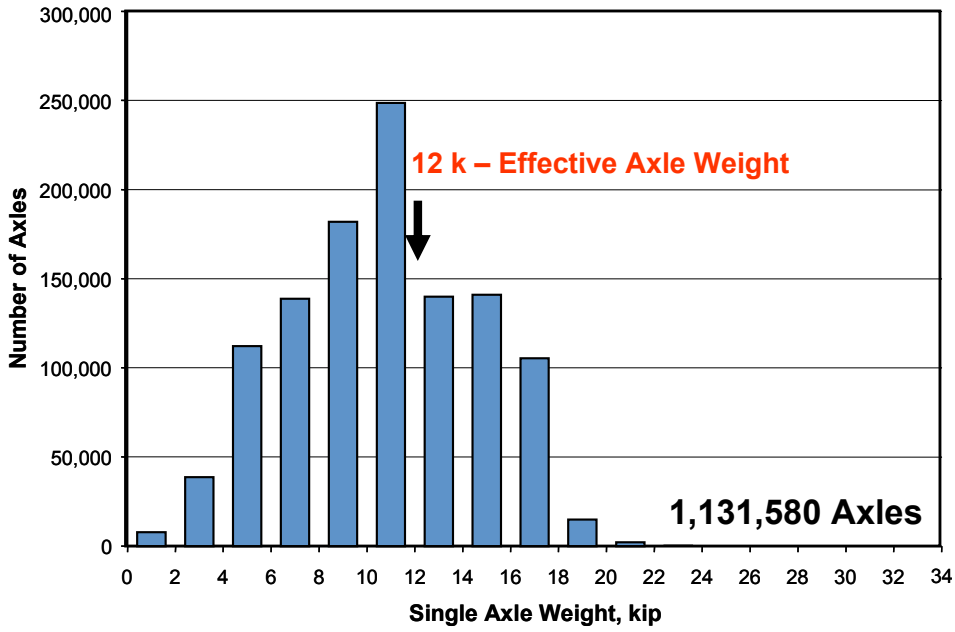

Figure 2.9: Histogram of Weigh-In-Motion Data (Wood et al. 2007)

2.1.2 Testing Protocol

Each of the test specimens experienced at least 5 million loading cycles during the fatigue test. Because it was not possible to measure the strain and displacement response of the

specimens during the fatigue tests; the fatigue tests were stopped periodically to perform static tests. Displacements and strains were recorded during these periodic static tests and were used to monitor changes in the stiffness of the test specimens during the fatigue tests. At the conclusion of the fatigue tests, each specimen was loaded statically to failure.

Flexural cracks were not observed in any of the test specimens under the fatigue loads. After at least 2 million fatigue cycles, the two positive moment specimens were subjected to a static overload that caused flexural cracks to form. The fatigue tests were then resumed. It is anticipated that an overload vehicle could cause cracking of the PC panels in a bridge, and the measured response of the specimens before and after cracking was used to determine if the cracked panels were more susceptible to fatigue damage. The actuator used for the fatigue tests did not have sufficient capacity to induce flexural cracks in the negative moment specimens. Therefore, it was not possible to compare the fatigue response of the uncracked and cracked negative moment specimens.

2.2 Response of PC Panel Detail at Skewed Expansion Joints

During the second phase of the investigation, six specimens with skewed expansion joints were tested. A trapezoidal PC panel was positioned adjacent to the expansion joint rail in all specimens. The primary experimental variables included the angle of the skew, the arrangement of the prestressing strand within the trapezoidal PC panel, and the number of panels in the test specimen (Table 2.5). Three test specimens were constructed using panels with a 45º skew and three specimens were constructed using panels with a 30º skew.

Table 2.5: Primary Experimental Parameters Tested during Second Phase of Investigation

Specimen	Skew Angle (degree)	Strand Pattern in Skewed Panel	Number of Trapezoidal Panels	Number of Rectangular Panels	Number of Locations Tested
5	45	Fanned	1	0	1
6	45	Parallel to Skew	1	1	2
7	45	Parallel to Skew	1	1	1
8	30	Parallel to Skew	1	1	2
9	30	Parallel to Skew	1	1	2
10	30	Parallel to Skew	2	1	3

Four of the six test specimens in the second phase of the investigation were constructed using two PC panels as shown in Figure 2.10. Specimen 5 was constructed with only the trapezoidal panel and specimen 10 was constructed with two trapezoidal panels and a center, rectangular panel. All specimens tested during the second phase of the investigation were subjected to positive moment. Specimen 7 was subjected to fatigue loading. Monotonically applied loads were applied to all other test specimens.

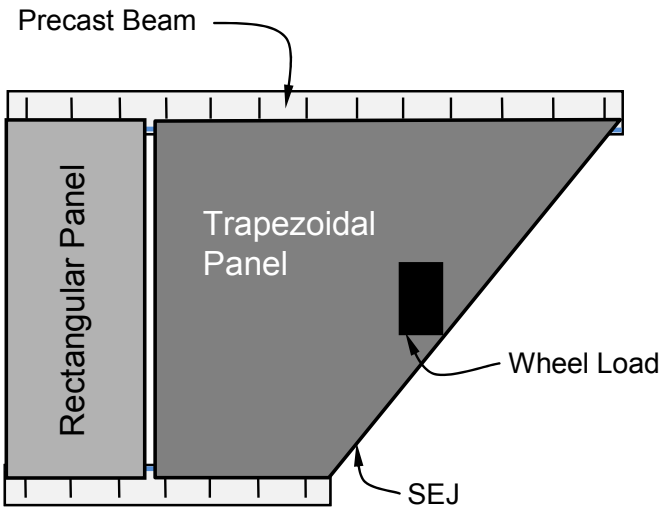

Figure 2.10: Configuration of Test Specimens with Two PC Panels

Specimen 5 was constructed using a fanned arrangement of the prestressing strand in the trapezoidal panel, which was selected to provide a uniform distribution of prestress within the panel. However, as discussed in Chapter 3, this strand pattern dramatically increased the complexity of constructing the trapezoidal PC panel. An alternate arrangement of strands was developed to address the construction issues where the strands were positioned parallel to the skew. This arrangement of strand was used in all other test specimens. One consequence of the parallel strand pattern is that the rectangular corner along the long side of the trapezoidal panel is not prestressed. The test specimens were also subjected to wheel loads in the vicinity of this nonprestressed corner as shown in Figure 2.11.

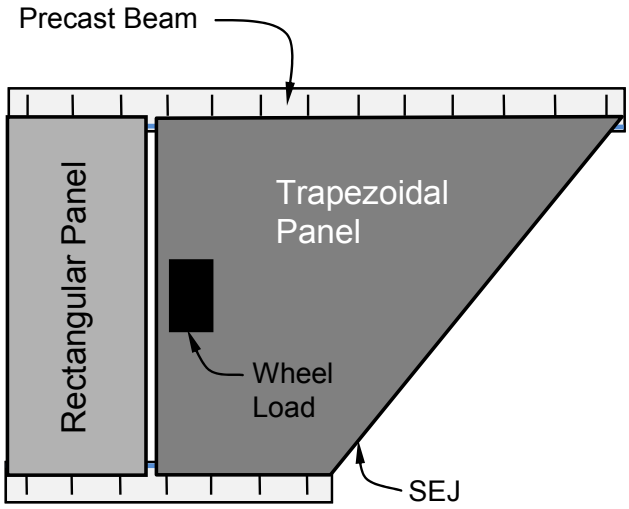

Figure 2.11: Location of Secondary Wheel Load for Trapezoidal Panels with Parallel Strands

Chapter 3. Design of Trapezoidal PC Panels

The objective of the experimental program was to evaluate the constructibility and practicality of producing skewed prestressed panels for use at expansion joints. In the investigation of a new product, many variables may need to be tested or held constant. The areas of primary concern included the skew angle, panel dimensions, and prestressing strand arrangement. Additional variables included prestressing force, concrete release strength, and supplementary deformed reinforcing bars for bursting or flexural reinforcement.

3.1 Preliminary Design

In September 2006, the research team held a joint meeting with representatives from TxDOT's bridge division, local precast concrete panel fabricators, and bridge construction contractors. The objective was to determine if contractors had an interest in skewed panels, if the fabricators could produce such panels, and if the requirements of TxDOT's bridge division could be satisfied. At the joint meeting, the discussion was open for any ideas from TxDOT, fabricators, or contractors. The main topics discussed were the panel geometries and methods of reinforcement. Several basic concepts came from this meeting and set the initial outline from which planning could proceed. A follow-up meeting held in November 2006 with the TxDOT representatives to establish the test parameters.

3.1.1 Panel Geometry

The most feasible panel geometries presented were:

- **Option 1**: One large trapezoidal panel (Figure 3.1). Using a single panel to make the skew angle transition would require the fewest custom panels and minimize construction awkwardness. However, panels with large angles and widths cannot be produced on current prestressing beds and would require construction of new, wider ones. Also, depending on the orientation of the prestressing, some of the strands may have embedment lengths shorter than required to transfer forces into the panel. Areas with such strands might not provide the necessary strength.
- **Option 2**: System of two, smaller trapezoidal panels (Figure 3.2). By breaking up the skew angle transition into two panels, each panel would be small enough to fabricate on current prestressing beds. As well, smaller angles on each panel may result in fewer strands lacking the proper embedment length. The downside to this method is that twice as many custom panels are required and construction crews have to manage the placement of more awkwardly shaped panels.
- **Option 3**: Quadrilateral panel with parallel sides at expansion joint followed by trapezoidal panel (Figure 3.3). By making the edge panel a parallelogram, current prestressing beds could be used with skewed formwork. However, the second, trapezoidal shaped panel would still require a new casting bed for large skew angles and beam spacing, just like that in Option 1. The main benefit of this method would be to ensure a fully prestressed panel at the expansion joint. Furthermore, regions in the trapezoidal panels containing strands without sufficient embedment would be away from the expansion joint.

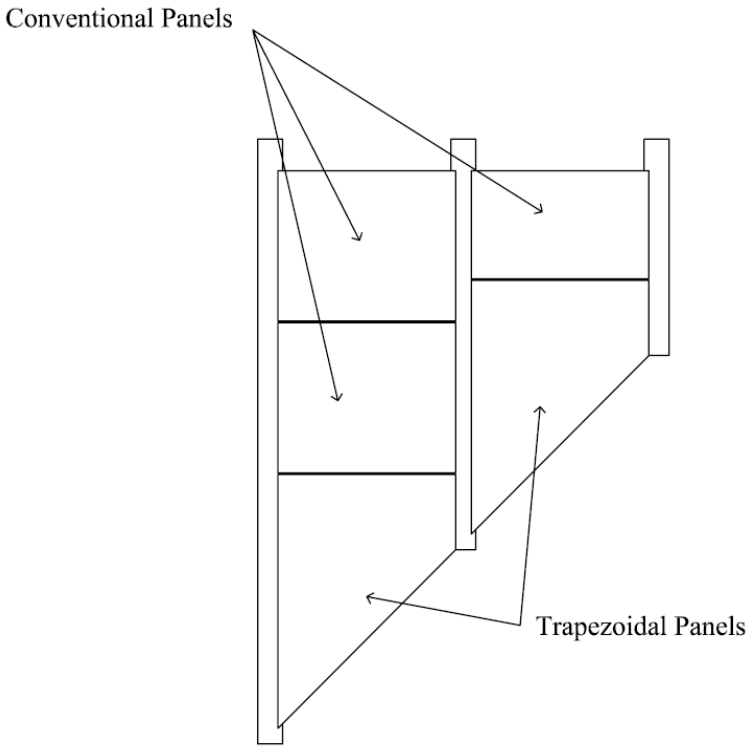

Figure 3.1: Option 1—Single trapezoidal panels

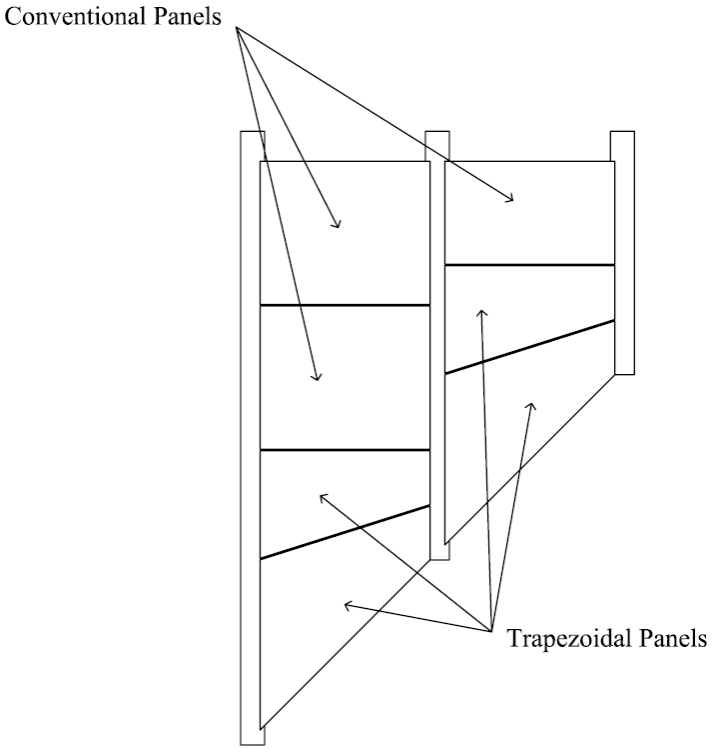

Figure 3.2: Option 2—Combination of two trapezoidal panels

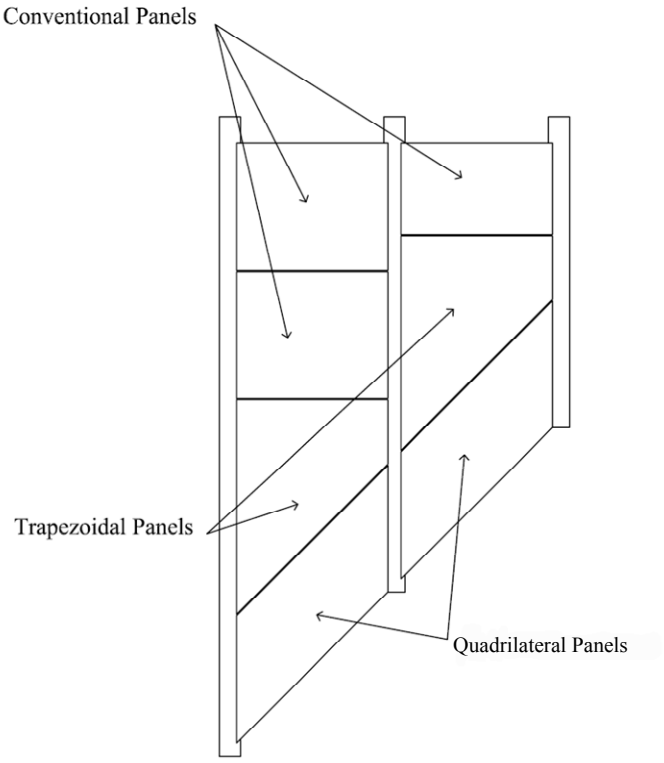

Figure 3.3: Option 3—Combination of quadrilateral and trapezoidal panels

3.1.2 Reinforcement Alternatives

As mentioned in the panel options, the trapezoidal shaped panels have several different reinforcement alternatives. Considering typical casting bed layouts, prestressing strands could be oriented either perpendicular to the girders, parallel to the girders, or parallel with the skewed expansion joint. In each case, supplemental reinforcement would need to be placed at locations without effective prestressing. Figures 3.4 and 3.5 show different prestressing arrangements with the supplementary deformed reinforcement that would be needed. Another alternative that would not require any additional deformed bars is shown in Figure 3.6. By flaring the strands throughout the panel, strands are parallel to both the skewed and non-skewed ends. In each figure, strands that do not meet the embedment length requirement were omitted to show partially prestressed locations. Furthermore, typical temperature and shrinkage reinforcement required for panels is not shown.

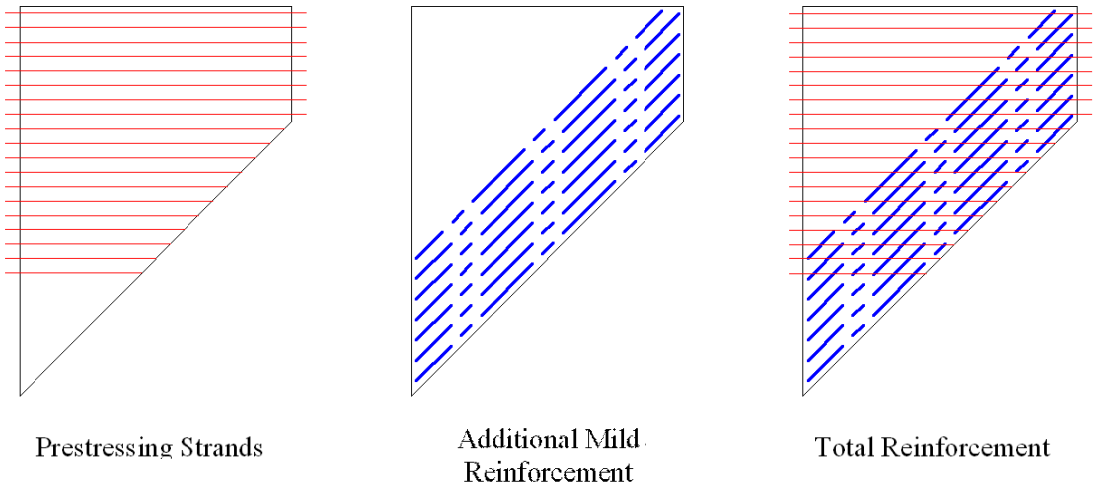

Figure 3.4: Strands oriented perpendicular to the girders

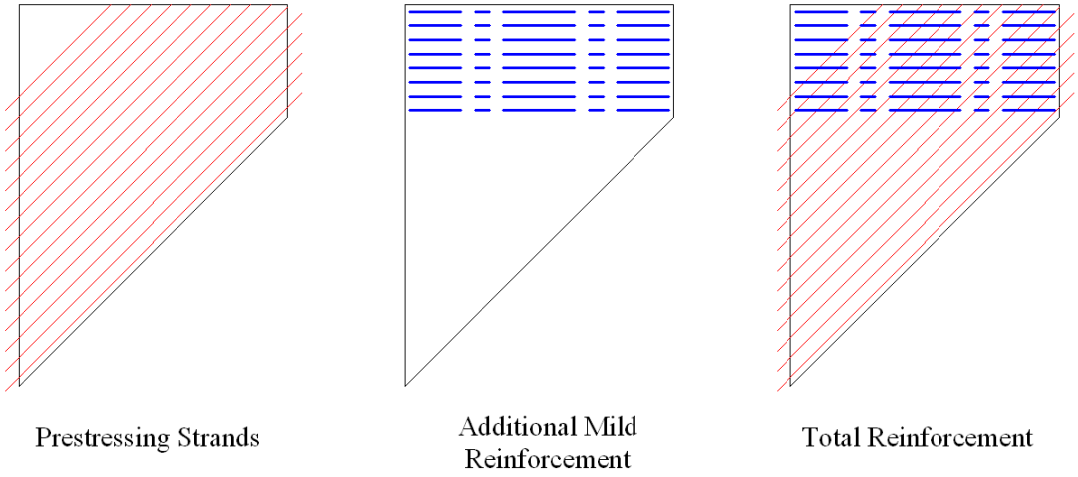

Figure 3.5: Strands oriented parallel to the skewed end

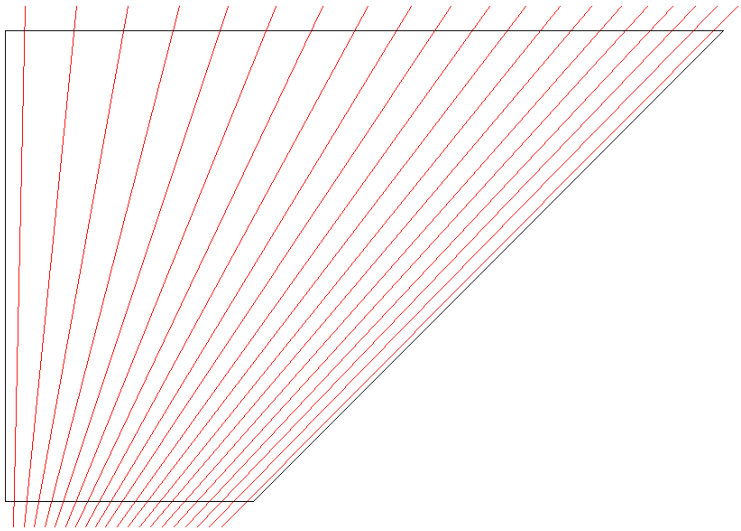

Figure 3.6: Strands fanned throughout panel

In addition to prestressed panels, a conventionally reinforced panel and a post-tensioned panel using Dywidag bars were discussed. The conventionally reinforced panel option was eliminated due to crack control requirements under the weight of the cast-in-place topping slab. Cracking would most likely occur and TxDOT engineers did not find that acceptable. The post-tensioned panel was rejected, as well, because of complications with anchorage and bar sizes.

3.1.3 Construction Issues

In general, contractor and fabricator representatives expressed support for the possibility of using skewed panels. However, they indicated that there were limitations on their capabilities that would restrict using some of the proposed alternatives. Additionally, TxDOT, as the owner of the structures, has established standards for the panels currently being used.

3.1.3.1 Contractor Requests

The contractors were in unanimous agreement that using skewed panels at expansion joints would benefit the construction process. The panels would eliminate the additional time used to form and shore the current IBTS detail, as well as the time required to remove such forms. In certain circumstances, such as over water, removal of formwork from the underside of the bridge can become costly and time consuming. Additionally, eliminating the temporary hole in the unfinished bridge deck before the formwork is in place at expansion joints could reduce insurance costs and create a safer work environment. The contractors also claimed they would willingly pay a premium, if necessary, for the specialty panels. The primary requests were to use a single panel and limit the panel weight to 6,000 pounds. Using a single panel between each girder would reduce the handling and setting of awkward panels. By limiting the weight of the panels, the contractors would not have to upgrade the cranes or other equipment currently used to place panels. The contractors also rejected the idea to saw cut standard panels to custom angles because saw blades wear down quickly while cutting through prestressing strands.

Another area of concern associated with using panels at expansion joints was the permitted spacing between panels. Using the current IBTS detail, formwork can easily be

constructed to match the location of the end panel (Figure 3.7a). With a precast panel, however, geometric control in setting panels becomes more important because the panel dimensions on site are fixed. A strip of compressible foam, known as backer rod, is typically used to fill any gaps between panels up to 3/4 in., but a gap in this situation could become too large if the geometry control is not accurate (Figure 3.7b). One proposed alternative is to saw-cut two conventional rectangular panels on site for a custom fit (Figure 3.7c). Because the cut would be oriented parallel to the strands, the saw blade would last longer.

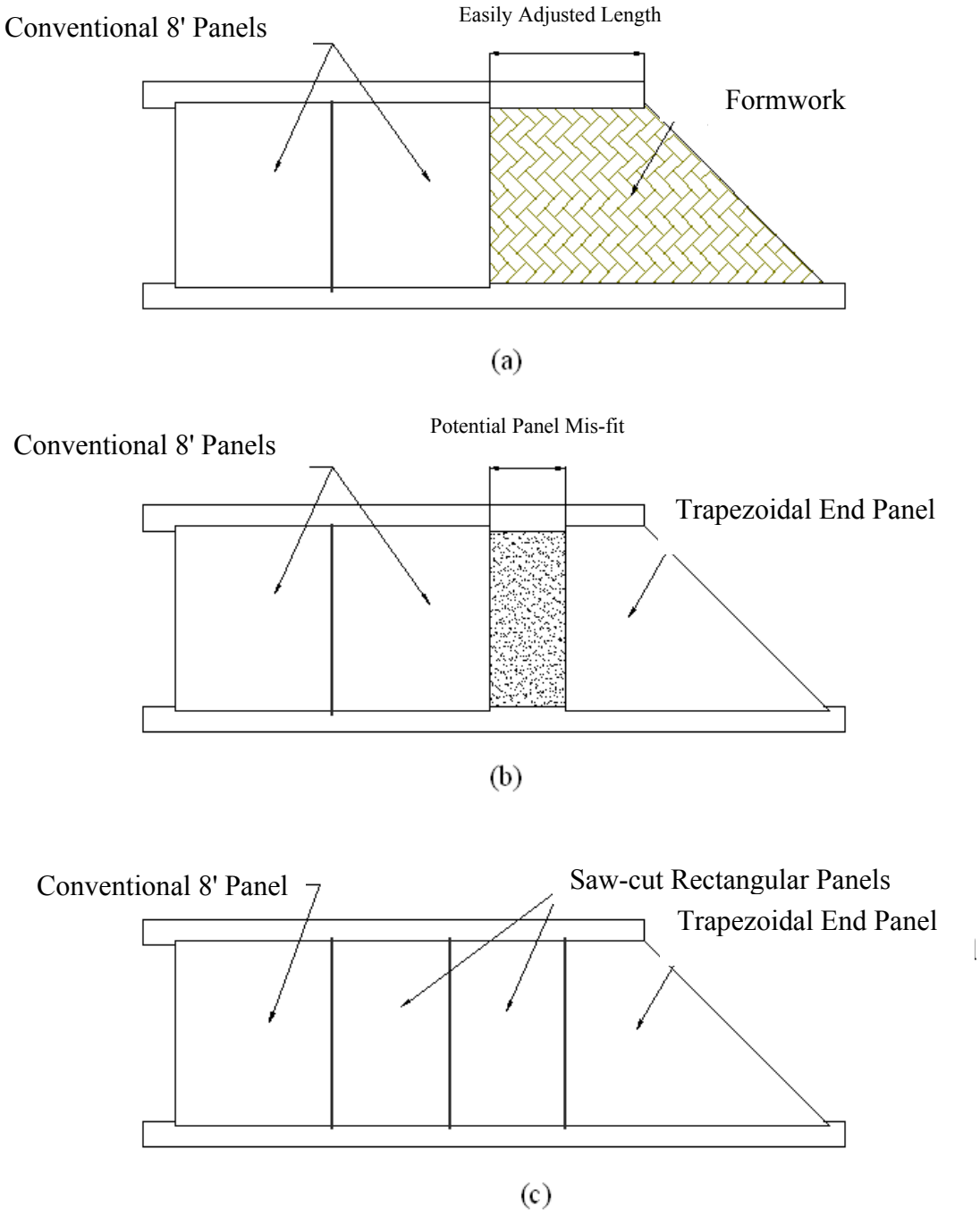

Figure 3.7: (a) Current construction techniques (b) Construction issue with end panels (c) Possible solution using two field-sawn panels

3.1.3.2 Fabricator Capabilities

The fabricator representatives indicated that producing skewed panels would not be difficult. They could easily produce custom wooden formwork for a given panel geometry as well as de-bond any strands necessary. De-bonding would be required if strands do not meet the minimum embedment length needed to transfer the prestressing force. The main problem they

face is that the long lines used at the prestressing plants to produce the panels are permanently set to an 8 ft. width due to shipping restrictions. Anything wider than 8 ft. would necessitate special truck permits and cost extra money. However, many fabricators agreed that if the contractors were willing to pay the premium for the skewed panels, they would construct a new, wider casting bed to accommodate a wider panel dimension. Moreover, the fabricators claimed they could handle the shipping restrictions. These capabilities are dependent on the skewed panels having strands parallel to one another. For the fanned prestressing strand alternative, no fabricator input was given. It was assumed that specialty casting beds would need to be constructed that would preclude mass production similar to current long-line methods.

3.1.3.3 TxDOT Requirements

The TxDOT bridge division representatives suggested that the panels utilize the current precast concrete panel standards as much as possible. This included concrete strength, the prestressing strand size, additional mild steel reinforcement, concrete release strength, panel thickness, and all bedding strip requirements (Figures 3.8 and 3.9). The other main variables were panel width, skew angle, and the short edge bearing length. Regardless of fabrication technique, the requirements needed to be flexible enough to accommodate variable skew angles and beam spacing. Current construction practice utilizes bedding strips with 40 or 60 psi strength, therefore, the TxDOT representatives wanted to keep bearing pressures within this range so that special materials need not be specified. Additionally, TxDOT expressed their concern for crack control at service load and preferred to see the prestressing strands parallel to the skewed end of the panels.

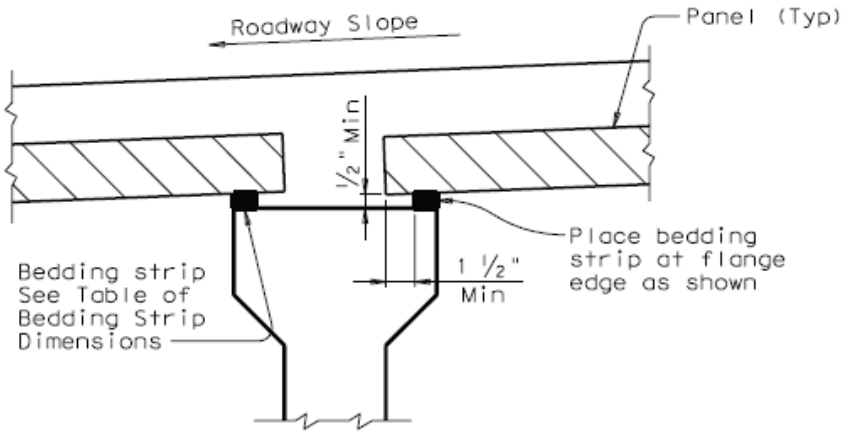

NORMAL GRADING DETAIL (1)

Showing Prestressed Concrete I-Beams.
(Other Beam Types Similar)

TABLE OF BEDDING STRIP DIMENSIONS

WIDTH	HEIGHT (2)	
	Min	Max
1" (Min)	½"	2"
1 ¼"	½"	2 ½"
1 ½"	½"	3"
1 ¾"	½"	3 ½"
2" (Max)	½"	4"

Figure 3.8: Prestressed concrete panel bearing details

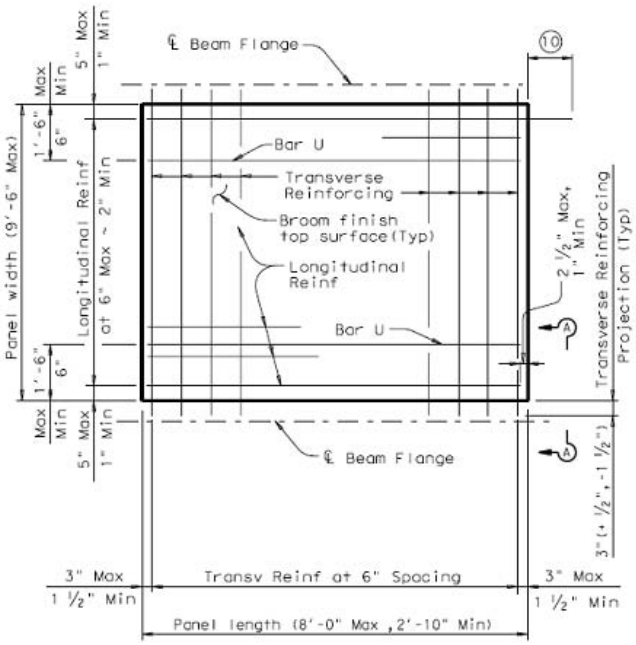

TYPICAL PANEL PLAN

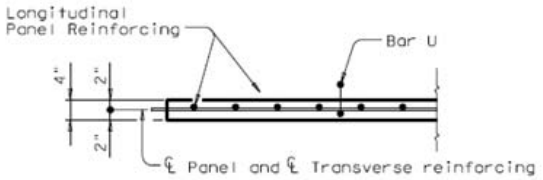

SECTION A-A

FABRICATION NOTES:

All concrete for panels is to be Class H. Use Class H (HPC) concrete for panels if required elsewhere in plans. Release strength f'ci=4000 psi. Minimum 28 day strength f'c=5000 psi.

Remove laitance from top panel surface.

A minimum of 90 percent of the top surface area shall have the required broom finish.

Shop drawings for the fabrication of panels will not require the Engineer's approval if fabrication is in accordance with the details shown on this standard.

A panel layout which identifies location of each panel shall be developed by the fabricator. Permanently mark each panel in accordance with the panel layout. A copy of the layout is to be provided to the Engineer.

TRANSVERSE PANEL REINFORCEMENT:

For panel widths over 5', use ⅜" or ½" Dia (270k) prestressing strands with an initial tension of 16.1 kips per strand.

For panel widths over 3'-6" up to and including 5', use ⅜" or ½" Dia (270k) prestressing strands with an initial tension of 16.1 kip per strand. Optionally, #4 Grade 60 reinforcing bars may be used in lieu of prestressed strands.

For panel widths up to 3'-6", use #4 Grade 60 reinforcing bars (prestressed strands are not allowed).

Place transverse panel reinforcement at panel centroid and space at 6" Max.

LONGITUDINAL PANEL REINFORCEMENT:

Any of the following options may be used for longitudinal panel reinforcement:

1. (#3) Grade 60 reinforcing steel at 6" Max Spacing. No splices allowed.
2. ⅜" Dia prestressing strands at 4 ½" Max Spacing (unstressed). No splices allowed.
3. ½" Dia prestressing strands at 6" Max Spacing (unstressed). No splices allowed.
4. Deformed Welded Wire Reinforcement (WWR) (ASTM A497) providing 0.22 sq in per foot of panel width. Wires larger than D11 not permitted. Provide transverse wires to ensure proper handling of reinforcing. One splice per panel is allowed. See WWR Splice Detail.

No combination of longitudinal reinforcement options in a panel is allowed.

Place longitudinal panel reinforcement above transverse panel reinforcement.

Figure 3.9: Prestressed concrete panel standard details

3.1.4 Selected Designs

Considering all of the options and opinions presented at the meetings, two types of skewed panels were selected to investigate. Because of the contractor requests, both types would be single trapezoidal panels that encompass the entire skew angle. The first alternative selected was the fanned prestressing pattern. The second alternative has the prestressing parallel to the skewed edge with additional reinforcement perpendicular to the girders.

The current TxDOT maximum girder spacing is 10 ft. on center with a 9 ft. clear span between top flanges. With the minimum overhang of a precast panel over a flange equal to 3 in., the maximum panel width becomes 9 ft. 6 in. A new line of girders, TX- sections, that will soon be utilized in bridge designs permits girder spacing to extend up to 11 ft. on center. However, the new girders have wider top flanges creating an 8 ft. clear span between flanges. Therefore, a worst case condition of a 9 ft. 6 in. panel width was selected. Sketches of the two panel design options are shown in Figure 3.10.

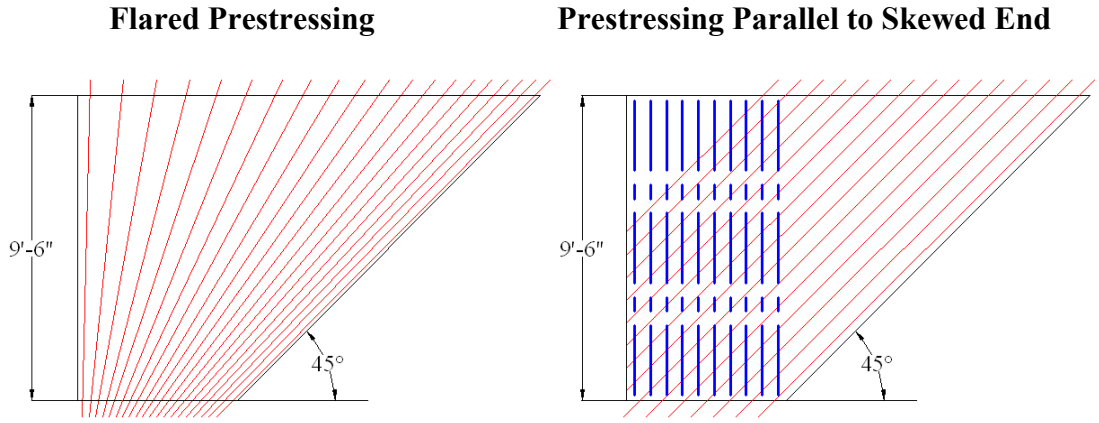

Figure 3.10: Selected design alternatives

In order to select a skew angle for design, bridge survey data from all bridges in Texas provided by TxDOT was reviewed. As seen in Table 3.1, targeting a 45º skew angle would encompass 98% of all bridges and 96% of prestressed I-girder bridges. This clearly covers a majority of bridge designs, therefore a 45º skew angle was chosen for the test program. Histograms showing the number of bridges with given skew angles are shown in Figures 3.11 and 3.12.

Table 3.1: Distribution of Skewed Bridges in Texas

	Pretensioned I-Girders		All Bridges	
Skew Angle	Number	%	Number	%
0°	3,877	48	21,376	64
≤ 15°	5,095	67	24,058	74
≤ 30°	6,310	85	28,003	87
≤ 45°	7,055	96	31,164	98
Total Number of Bridges	8,004		33,201	

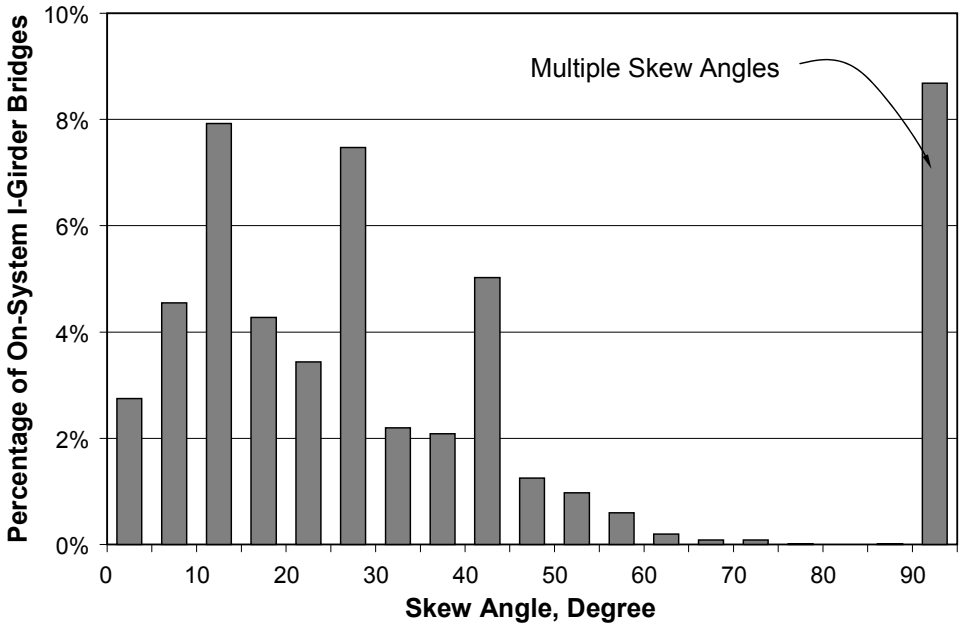

Figure 3.11: Distribution of Skewed Pretensioned I-Girder Bridges in Texas (Van Landuyt 2006)

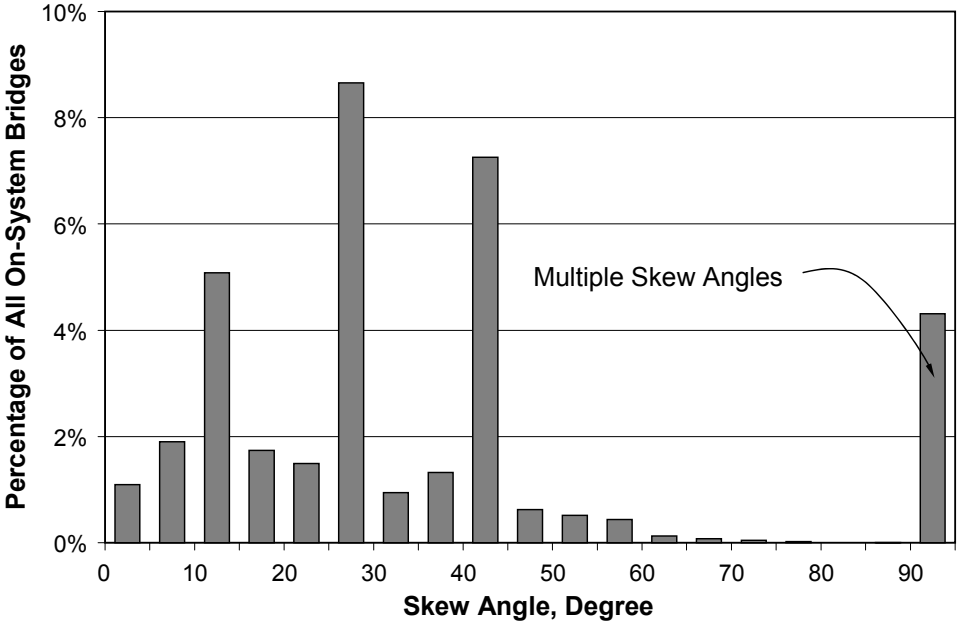

Figure 3.12: Distribution of Skewed Bridges in Texas (Van Landuyt 2006)

Lastly, the short edge bearing length was determined based on bearing pressure calculations. For these calculations, the weight of the panel was conservatively assumed to have equal distribution to each girder. Furthermore, the bearing pressures were taken as equal along the length of each girder. Both 40 psi and 60 psi foam bedding strips are used in bridge construction, but 40 psi foam was selected as the more critical case. When using the TxDOT

specified minimum short edge length for rectangular panels of 34 in., bearing pressures for panels with large skew angles exceed 40 psi as shown in Table 3.2. Using the data shown in Table 3.3 the minimum bearing length of 55.8 in. for a 45º skew panel was rounded up to 60 in. for simplicity.

Table 3.2: Bearing pressures using TxDOT minimum 34 in. bearing length

Bearing Pressures Using 34" Short Edge Length				
Angle (degrees)	Short Edge Length (in)	Panel Weight (lbs)	Total Load (lbs)	Pressure (psi)
45	34	3602	7204	53
40	34	3239	6478	48
35	34	2926	5851	43
30	34	2648	5297	39
25	34	2398	4796	35
20	34	2167	4334	32
15	34	1950	3901	29
10	34	1744	3487	26
5	34	1543	3086	23

Table 3.3: Minimum short edge bearing lengths for 40 psi and 60 psi bedding strips

Required Short Edge Lengths				
Angle (degrees)	Foam Strength (psi)	Panel Weight (lbs)	Total Load (lbs)	Short Edge Length (in)
45	40	4466	8932	55.8
40	40	3747	7495	46.8
35	40	3127	6254	39.1
30	40	2578	5157	32.2
45	60	3367	6734	28.1
40	60	2825	5650	23.5
35	60	2357	4715	19.6
30	60	1944	3888	16.2

3.2 Fanned Prestressing Pattern

The first two specimens were designed using the fanned prestressing pattern so that the entire panel was fully prestressed. The basic arrangement of the strands for this alternative is shown in Figure 3.6. The following sections describe the final design.

3.2.1 Strand Layout

As noted previously, the width of the panel was set to 9 ft. 6 in. with a 45 º skewed end and 60 in. short edge length. This set the basic geometry from which to design the prestressing strand locations. The goal for this design was to produce a uniform peak stress along the length

of the panel when loaded with fresh concrete during deck placement. Casting the topping slab for the deck was seen as a critical loading condition for the panel since it carries the entire load. Keeping the panel uncracked during this phase is essential to satisfactory long term performance. Once the topping slab is cured, the panel and slab act compositely.

In the fanned pattern, the embedment length of each individual strand varies. This leads to slight differences in seating loss, elastic shortening, creep and shrinkage, and strand relaxation. Analysis using the strip method with trapezoidal-shaped sections was done to determine the exact spacing between strands. Because the strips analyzed were trapezoidal, the effective prestressed area varied along the length of the strip. This led to a non-uniform prestressed force from one edge of the panel to the other. The strand spacing on the short edge of the panel was set to 3 in. on center to reduce local stresses and provide more space for the chuck and barrel anchoring assemblies. The selected strand spacing is shown in Figure 3.13.

Using ACI 318-05, the maximum allowable tensile stress in prestressing steel due to the jacking force is 0.94 times the yield stress. The yield stress for prestressing strands is approximately 0.85 times the ultimate strength. Using 270 ksi prestressing steel, the maximum allowable stress becomes 215.7 ksi, which equals a jacking force of 18.3 kips on a 3/8 in. strand with cross sectional area of 0.085 in^2. Because seating losses are much more critical for shorter strands, a target jacking force of 18 kips was selected instead of the 16.1 kips specified on the precast panel standard drawings. A seating loss of 1/4 in. was assumed, which could reduce the strand stress by as much as 20% for short strands. Creep and shrinkage coefficients of 2.9 and 0.0008 were selected and modified for a 60 day time frame to 1.56 and 0.000417, respectively.

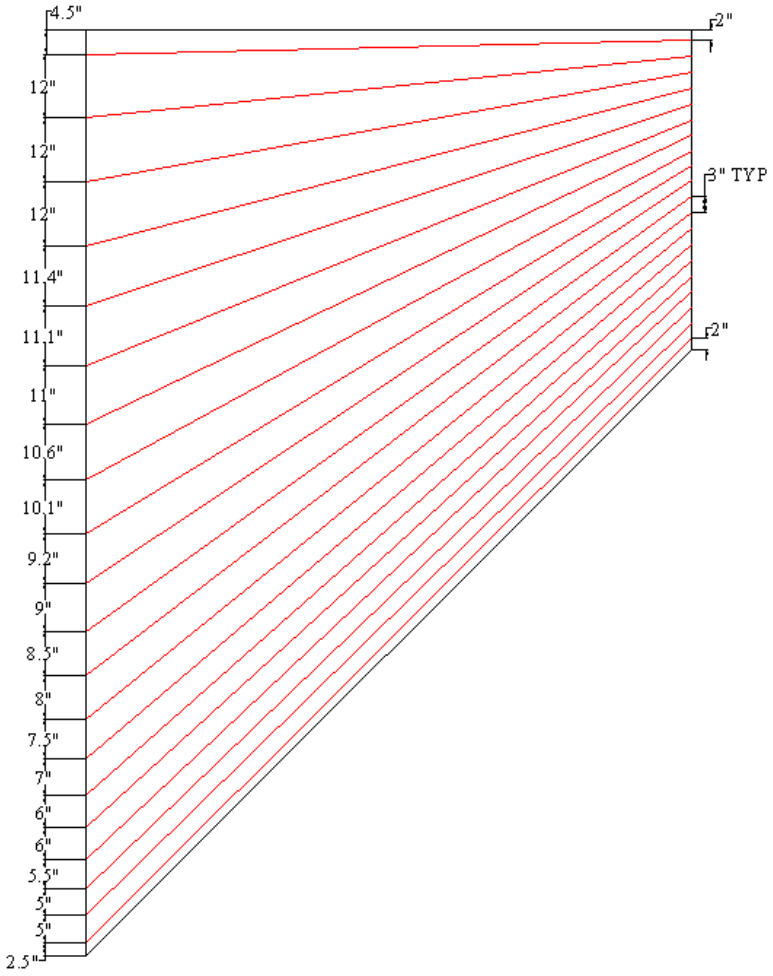

Figure 3.13: Strand spacing for fanned strand pattern

3.2.2 Additional Mild Reinforcement

In the fanned prestressing pattern, no two strands within the panel were parallel to each other. It was believed that this varying vector of compressive load would result in a splitting action between strands. No additional bursting steel is required for the current panels, but it is typical in other prestressing applications to prevent rupture and control cracking. To account for these conditions, #3 bars bent 180º (hairpins) were placed between strands. A single hairpin bar could span the gap between several strands, so an equal number of bars to strands were not necessary. The hairpins arrangement, shown in Figure 3.14, was chosen so that they crossed the strands as close to orthogonal as possible.

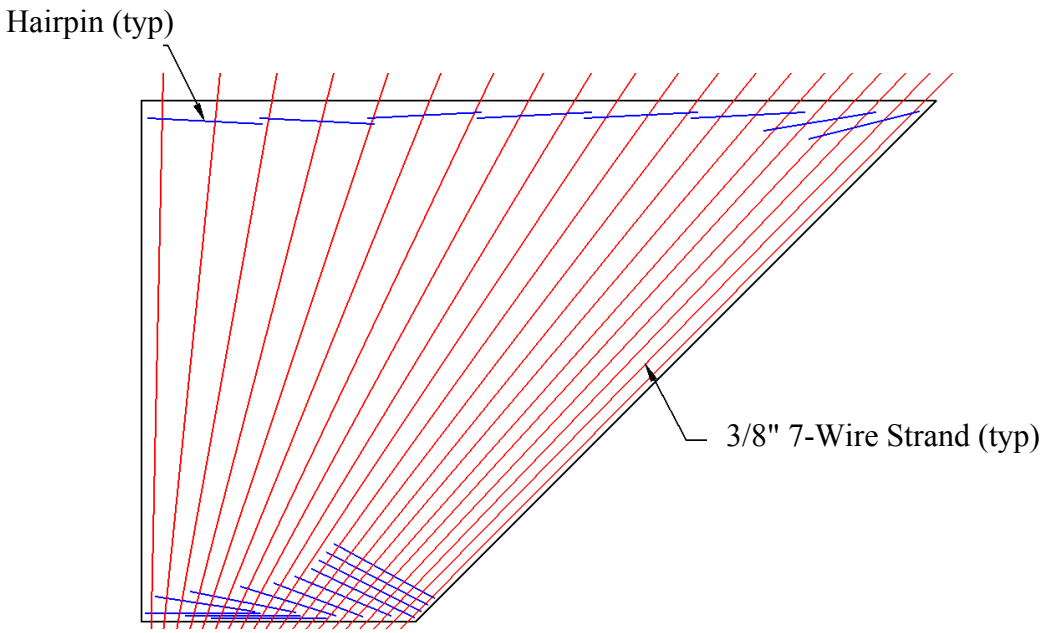

Figure 3.14: Hairpin layout for fanned strand pattern

The first test specimen had 12 hairpins on the short edge and 8 on the long edge. Because the strands were spaced much further apart on the long edge, fewer hairpins were necessary. The second test specimen did not contain any hairpins in order determine whether they were necessary. To fulfill the longitudinal panel reinforcement requirements, #3 deformed bars spaced at 6 in. on center were used in each test specimen.

3.2.3 Release Strength

The TxDOT standard for concrete release strength in precast panels is 4,000 psi. Because of the high local compressive force at the obtuse and acute angles in the skewed panel, the first test specimen had a target release compressive strength of 5000 psi. The target compressive strength at release for the second specimen was 4,000 psi in order to match the current TxDOT standard for precast panels.

3.3 Parallel Prestressing Pattern

The second set of test specimens was designed with a prestressing arrangement in which the strands are parallel to one another as well as the skewed end. To account for partially prestressed or non-prestressed portions of the panel due to lack of strand embedment, supplemental deformed reinforcement was placed in this region.

3.3.1 Panel and Strand Geometry

Similar to the fanned prestressing panels, the width of these panels was set to 9 ft. 6 in. to capture the largest beam spacing possible. Likewise, a skew angle of 45º was chosen to include a majority of bridges in Texas. The first test specimen with the parallel strand arrangement had a short edge length of 60 in. to maintain continuity with the fanned strand panels. Because this

strand arrangement facilitates fabrication of smaller panels, the short edge length was reduced to 45 in. in a second specimen for comparison.

The motivation behind the strand layout was to match the current precast panel standard and casting lines at fabrication plants. Therefore, the strand spacing for the parallel pattern was set at 6 in. on center. A triangular region of the panel contains strands that do not meet the required embedment length to transfer the prestressing force. Using ACI 318-08 equation 12-4, 3/8 in. strands tensioned to 16.1 kips require approximately 24 in. of embedment to transfer the force. Fabricators typically use a de-bonding agent or simply wrap the strand when no force transfer is desired. For these test specimens, any strand that would have an embedment length less than 48 in. was omitted (24 in. from each face of the panel). As a result, the first test specimen with a 60 in. short edge length required 14 strands spaced at 6 in. The second test specimen only required 12 strands since the short edge length was 15 in. shorter. The strand layouts for both designs are shown in Figure 3.15.

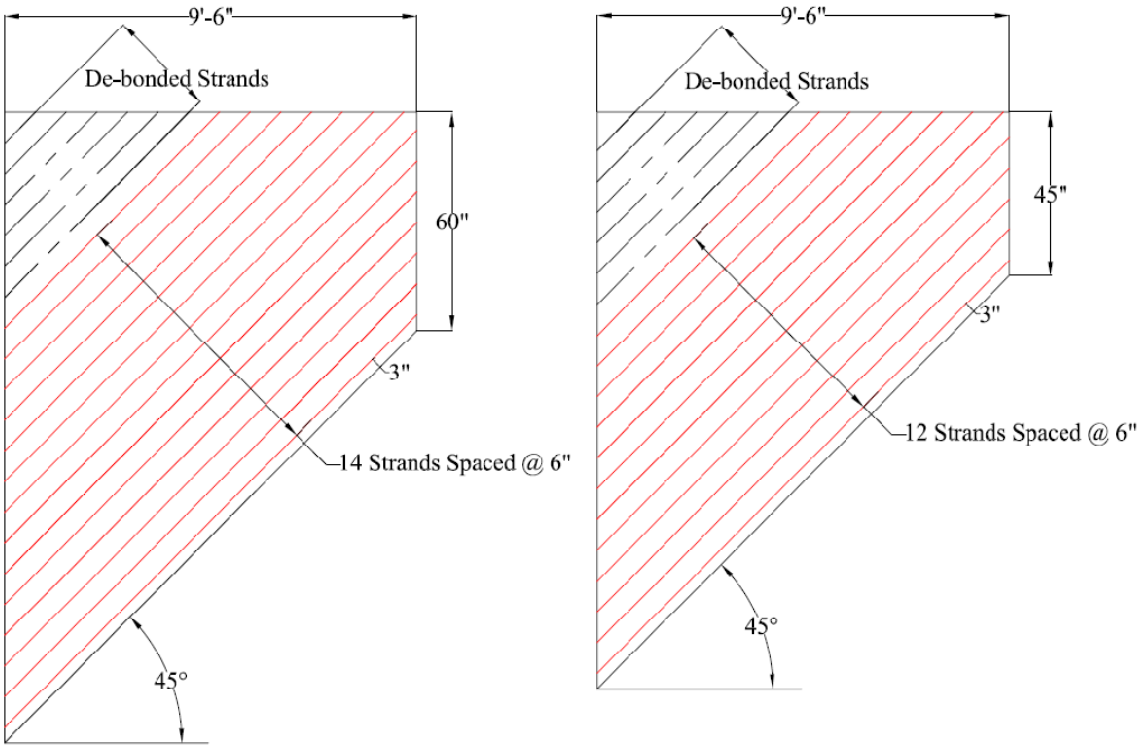

Figure 3.15: Parallel strand panel designs

3.3.2 Additional Mild Reinforcement

The strand spacing in these test specimens matched that of the TxDOT standard panels, so no additional bursting steel was used. However, these test specimens contained an entire corner region where no prestressing was present. To account for this, additional transverse mild steel reinforcing was used. To achieve a higher bending strength, the bars were placed beneath the prestressing strands. However, due to cover restrictions, the size of the bar was limited. The final design consisted of placing #4 bars with a 4 in. center to center spacing parallel to the non-skewed end. The number of bars used was selected to cover the entire non-prestressed region. The first specimen with the 60 in. short edge contained 14 transverse bars and the second

specimen with a 45 in. short edge used 11 transverse bars. To fulfill the longitudinal reinforcement requirements, #3 deformed bars spaced at 6 in. were used in each test specimen. The ordinary reinforcing layouts for both designs are shown in Figure 3.16.

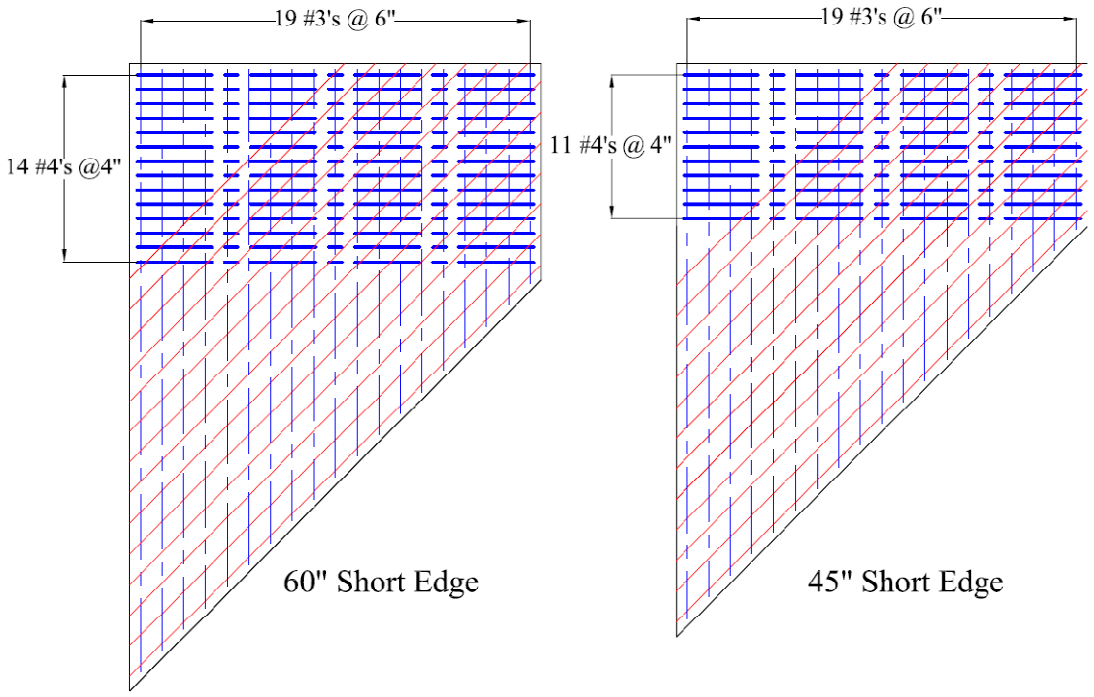

Figure 3.16: Additional deformed bars in parallel strand panels

3.3.3 Commercial Fabrication

In addition to the four test specimens fabricated by the researchers, another set of test specimens was fabricated by a precast plant. The design matched the 45º skew parallel strand pattern specimens, but because the precasting beds used for panels were only 8 ft. wide, the geometry of the panels was restricted. A skew of 30º was selected which limited the short edge length to 45 in. However, for this skew angle, the bearing pressure on the bedding strip was deemed to be satisfactory. Figures 3.17 through 3.21 show the set of drawings sent to the precast concrete plant for fabrication.

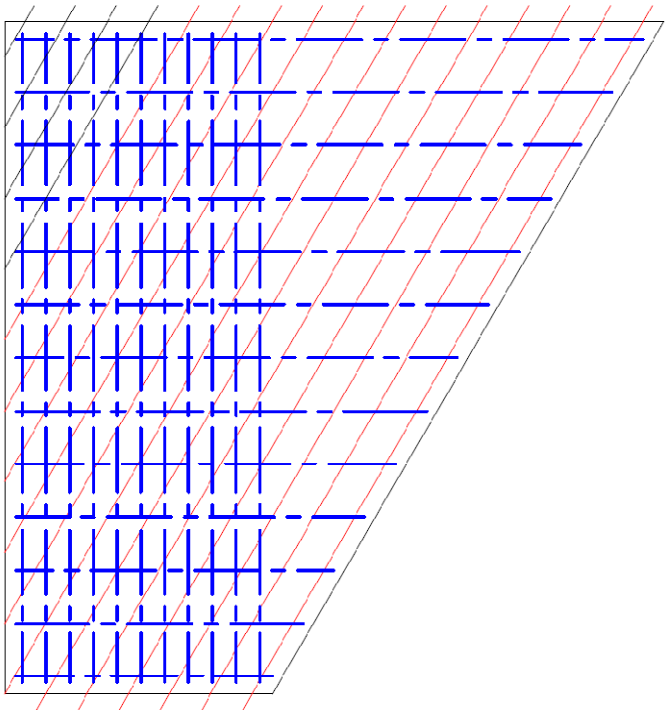

Figure 3.17: 30° skew panel general view

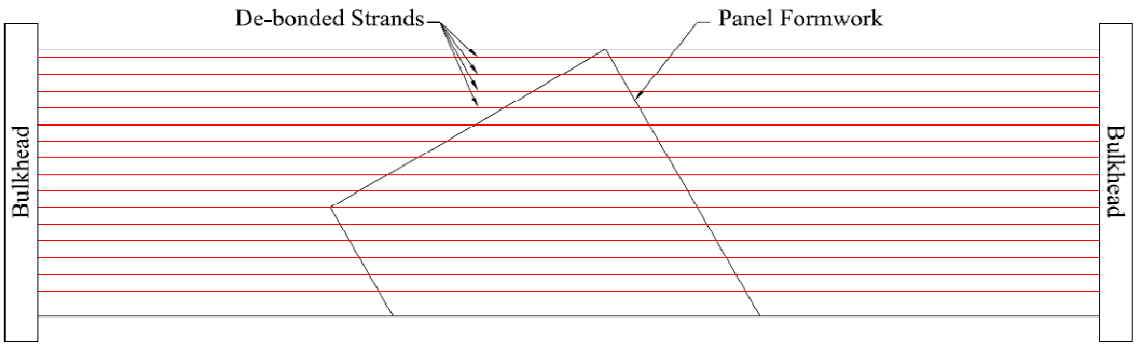

Figure 3.18: 30° skew panel arrangement in prestressing bed

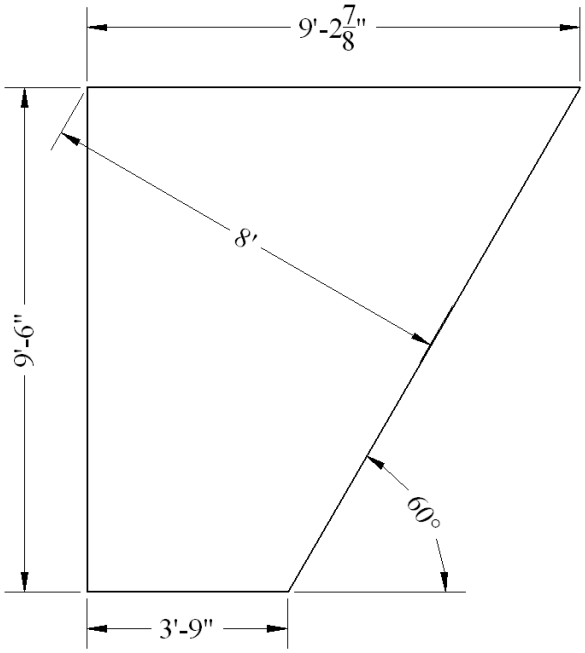

Figure 3.19: 30° skew panel dimensions

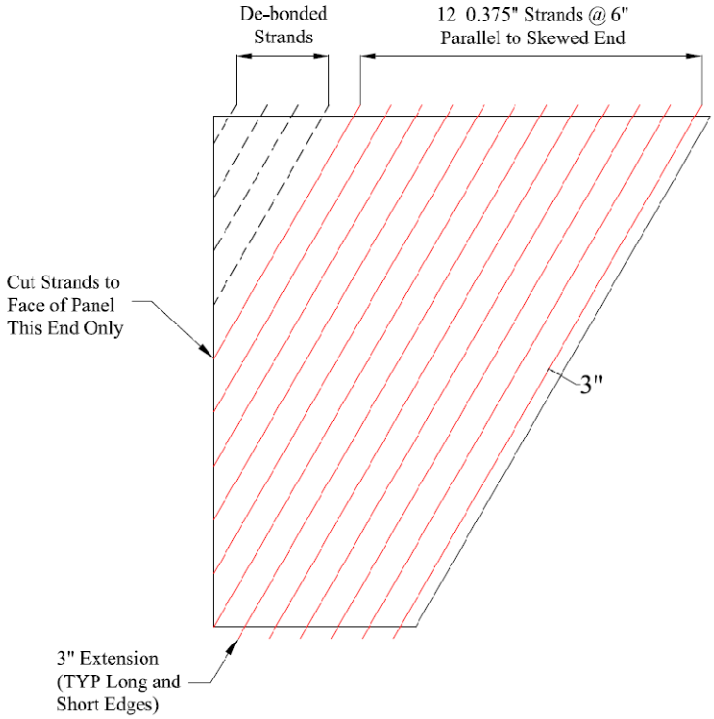

Figure 3.20: 30° skew panel prestressing

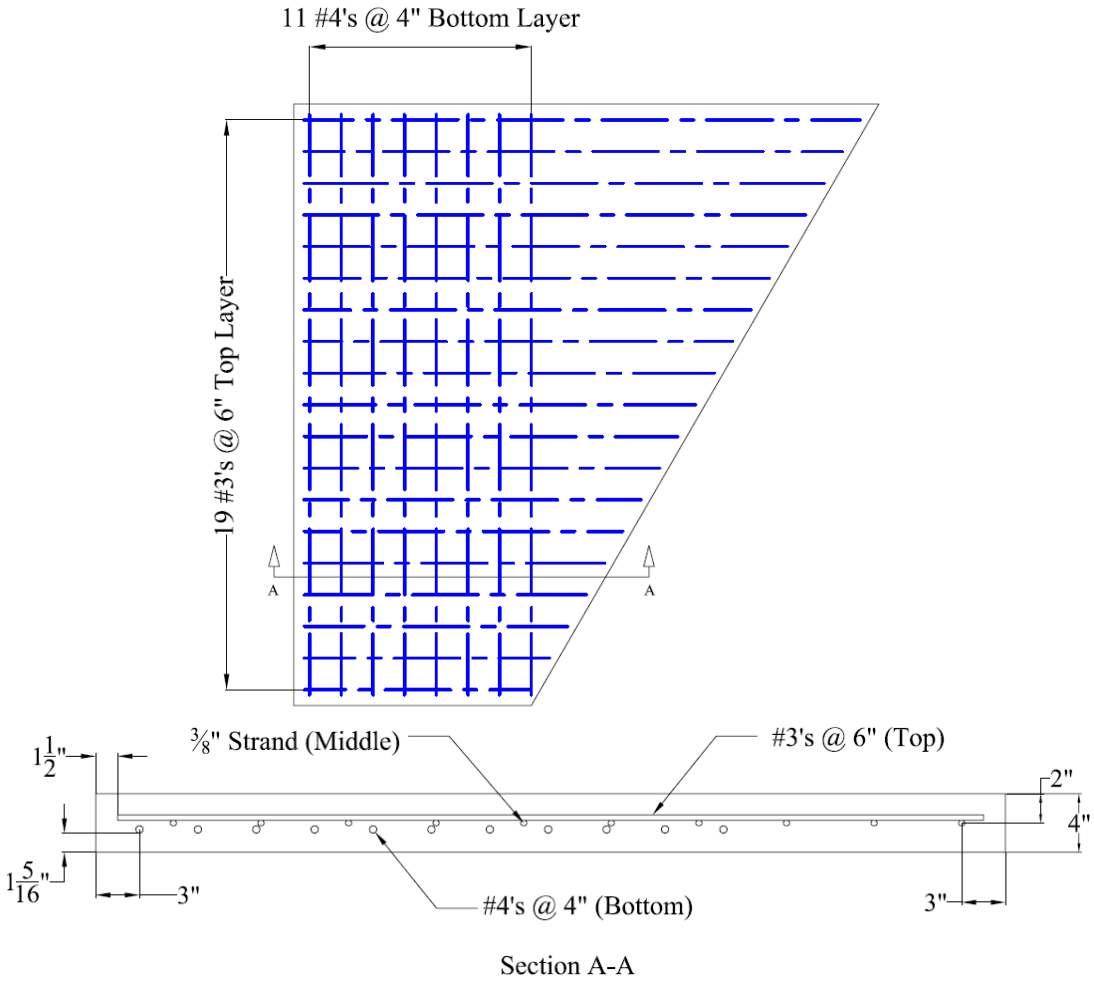

Figure 3.21: 30º skew panel ordinary reinforcing layout and detail

3.4 Design Summary

A total of eight prestressed panels were produced using five different designs. All 45º skew panels were fabricated within Ferguson Laboratory. The 30º skew panels were commercially fabricated. Table 3.4 provides a summary of all panels produced. The nomenclature used to identify the panels is as follows: 1) 30º (30) or 45º (45) skew, 2) Fanned (F) or Parallel (P) strands, 3) 45 in. (45) or 60 in. (60) short edge bearing length. The number following the dash identifies additional panels that have the same parameters. For example, the second panel that had a 45º skew, a fanned prestressing pattern, and a 60 in. short edge length, is designated 45F60-2.

Table 3.4: Summary of panel designs

Panel Name	Skew Angle (Degrees)	Short Edge Length (Inches)	Strand Pattern	Supplementary Reinforcement	Release Strength (psi)	Used in Test Specimen
45F60-1	45	60	Fanned	Hairpins	5000	5
45F60-2	45	60	Fanned	None	4000	
45P60-1	45	60	Parallel	Flexural	4000	6
45P45-1	45	45	Parallel	Flexural	4000	7
30P45-1	30	45	Parallel	Flexural	4000	8
30P45-2	30	45	Parallel	Flexural	4000	9
30P45-3	30	45	Parallel	Flexural	4000	10A
30P45-4	30	45	Parallel	Flexural	4000	10B

Chapter 4. Design and Construction of Test Specimens

In typical TxDOT bridge construction practice, the PC panels are placed on top of the PC bridge girders. The PC panels are placed along the length of each side of bridge girders as shown in Figure 4.1 (see also Figure 3.8). Standard TxDOT details for PC beams are shown in Figure 4.2

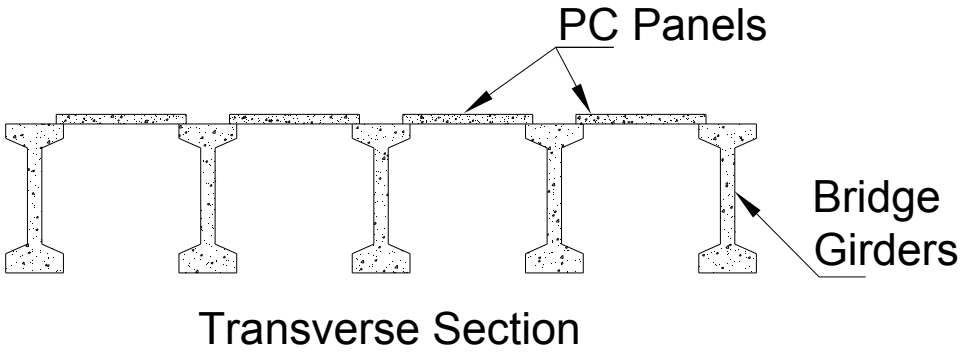

Figure 4.1: Typical Placement of PC Panels on Edge of PC Girders

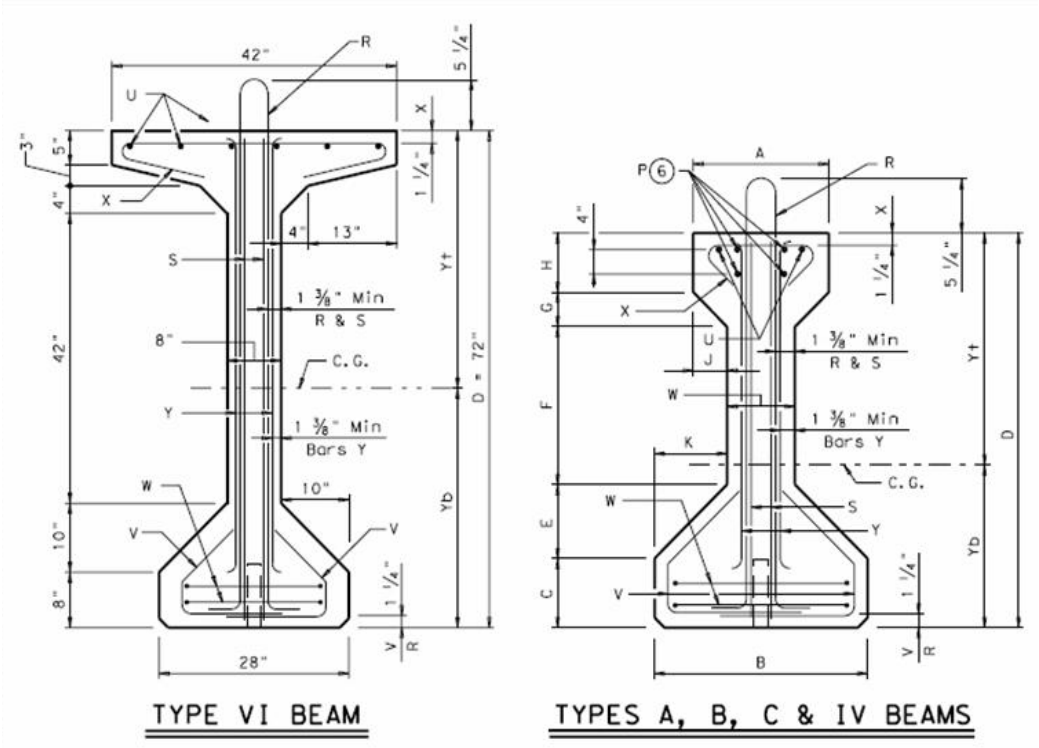

TABLE OF BEAM DIMENSIONS AND SECTION PROPERTIES

BEAM TYPE	A in.	B in.	C in.	D in.	E in.	F in.	G in.	H in.	J in.	K in.	W in.	Yt in.	Yb in.	AREA in.²	I in.⁴	Weight plf
A	12	16	5	28	5	11	3	4	3	5	6	15.39	12.61	275.4	22,658	287
B	12	18	6	34	5 ¾	14	2 ¾	5 ½	2 ¾	5 ¾	6 ½	19.07	14.93	360.3	43,177	375
C	14	22	7	40	7 ½	16	3 ½	6	3 ½	7 ½	7	22.91	17.09	494.9	82,602	516
IV	20	26	8	54	9	23	6	8	6	9	8	29.25	24.75	788.4	260,403	821
VI	See section for beam dimensions											35.60	36.40	1,084.4	732,586	1,130

Figure 4.2: Cross Section of Typical PC Girder Dimensions (TxDOT)

4.1 Support Details for Test Specimens

4.1.1 Precast Supporting Beams

For the test specimens, the support supporting beams for the PC panels were cast with shear reinforcement protruding from the top of the beams to develop composite action between the girder and the CIP topping slab. The beams were designed to have a top width that would represent the top flange dimensions of typical TxDOT beams. A 12-in. width was selected because it provided sufficient bearing area for the PC panel. The depth of the beam was designed to be 12-in. because the required nominal capacity was low. Dimensions of the precast beam are shown in Figure 4.3.

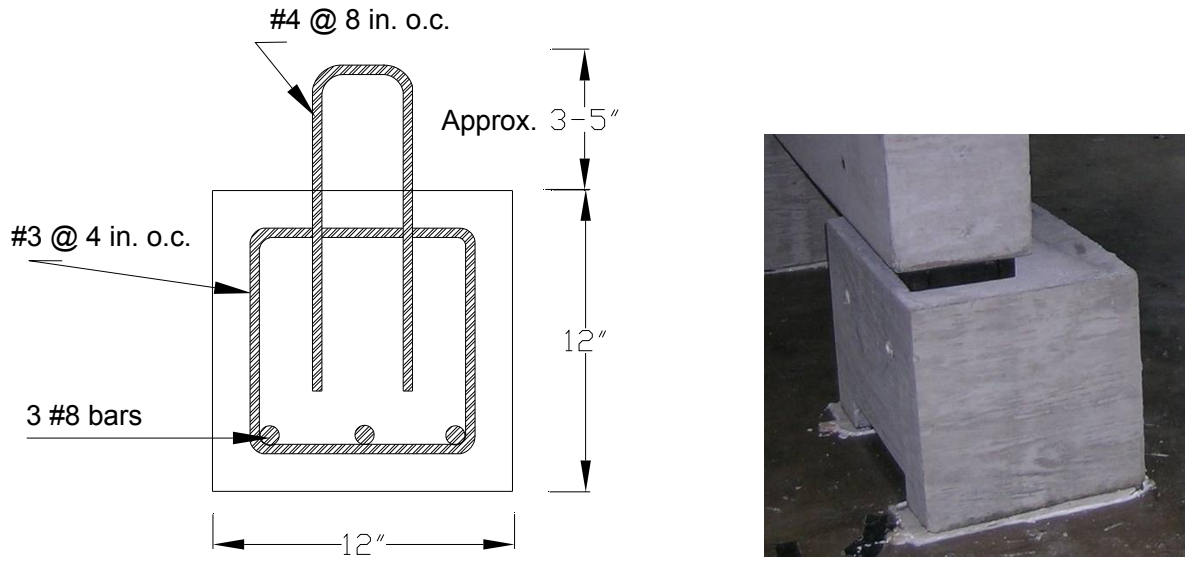

Figure 4.3: Cross Section and Support of Precast Beams

TxDOT bridge girders typically are supported by steel reinforced, elastomeric bearing pads at the ends of the simply-supported bridge spans. To reproduce these conditions, the test specimens incorporated this same construction detail. Bearing pads (2.5-in. thick, 9-in. wide, and 13-in. long) were used at the ends of all the precast beams (Figure 4.3).

4.1.2 Bedding Strips

When the PC panels are placed on top of the bridge girders, the panels bear upon a continuous foam strip, or bedding strip, that is glued to the edges of the top flanges of the PC girder. Part of the panel extends beyond the bedding strip towards the center of the beam which creates a gap that allows the cast-in-place concrete to flow underneath the panel to provide uniform bearing. In the field, the bedding strips are cut from sheets of Foamular 400, a type of extruded polystyrene insulation manufactured by Owens Corning. As shown in Figure 3.8, the height and width of the bedding strips are varied in the field to account for camber in the prestressed girders or the grading of the bridge deck surface. At expansion joints, the typical dimensions of bedding strips approach the maximum allowable dimensions listed in Figure 3.8, because, if the top surface of the bridge deck is level, and the panels bear directly on the beams, the camber in the beams will cause a thicker slab at the supports and a thinner slab at mid-span. The most severe condition corresponded to the minimum bedding strip height that would make it more difficult to place concrete underneath the panel. Initially, a 1-in. wide by ½-in. tall bedding strip was chosen, but during construction of some specimens, the bedding strip was heavily compressed and deemed unacceptable. The bedding strip dimensions and the compression strength of the polystyrene were increased.

Another factor is the overhang distance of the PC panel past the bedding strip. The minimum allowable overhang distance is 1 ½-in. The overlap distance in the test specimens was 1½-in since that represented the most critical case. The construction photograph (Figure 4.4) of the bedding strip detail shows that the panel overlap exceeded 1 ½ in. and had to be repositioned accordingly.

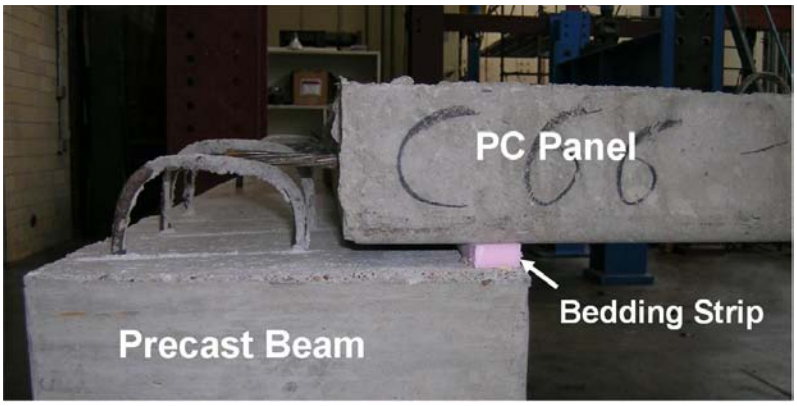

Figure 4.4: Test Specimen Bedding Strip with PCP in Place

4.2 Construction of PCPs

The girder spacing was 10 ft in all test specimens. Therefore, PC panels with a width of 9 ft 6 in. were selected.

4.2.1 Specimens with Rectangular Prestressed Concrete Panels (PCP)

The rectangular panels for the tests in Phase 1 were 8 ft long, which is the typical length. The panels were 4 in. thick and contained 3/8-in. diameter prestressed steel strands at 6 in. on center in the transverse direction (see Figure 4.5). Ordinary reinforcement in the transverse and longitudinal directions met the requirements shown in Figure 3.9. All panels were constructed by a local prestressed concrete producer.

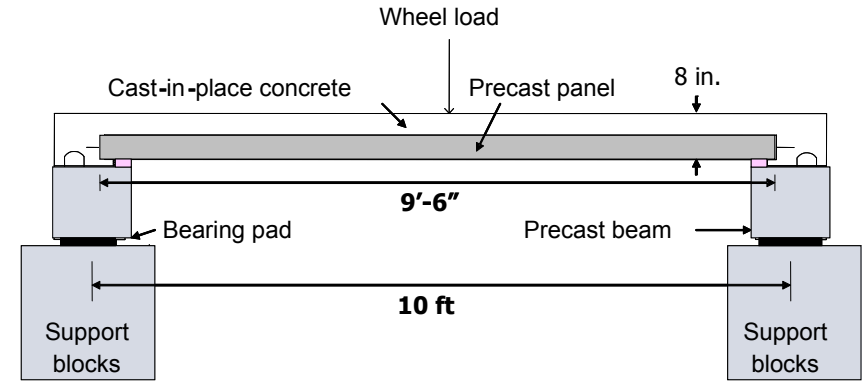

Cross Section

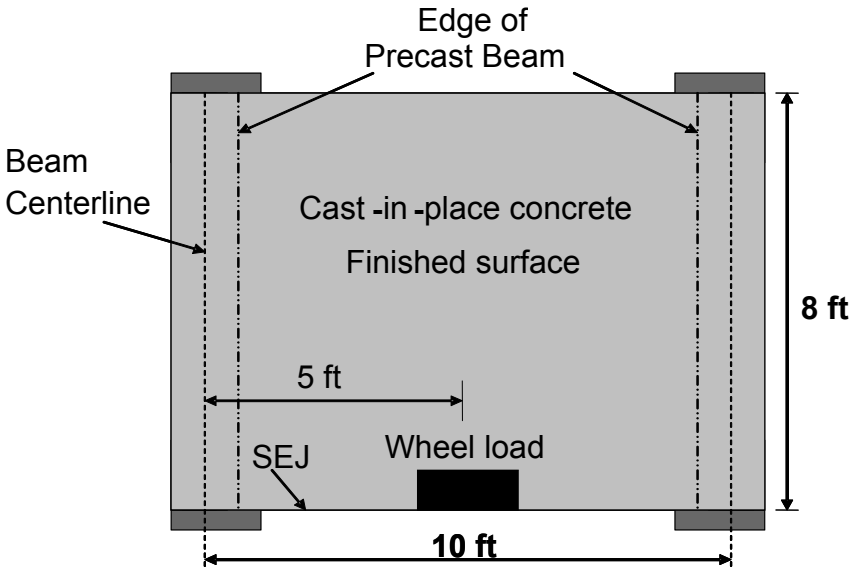

Plan View

Figure 4.5: Details of Specimens 1 and 2

4.2.2 Specimens with Trapezoidal Prestressed Concrete Panels (Skewed PCP)

The design of the skewed precast panels was described in Chapter 3. The construction details can be seen in the following figures. A stressing bed was fabricated in the laboratory and attached to the rigid test floor. Stressing operations were monitored using load cells and strain gages on some strands. Typical seating losses were between 1/8 in. and 3/16 in., lower than the assumed 1/4 in. This resulted in higher net forces than anticipated, but close to the value specified by TxDOT. After the strands were stressed, the formwork for the panels was completed and the deformed reinforcing bars were placed and tied. For all panels, #3 bars were placed with 6 in. center-to-center spacing above the strands parallel with the short and long edges of the panel. This arrangement is one of the longitudinal panel reinforcement options for temperature and shrinkage crack control. The panels with a fanned strand pattern did not require any additional flexural reinforcement because they were fully prestressed. However, to control cracking due to bursting stresses, hairpins were placed in Panel 45F60-1. Because there was no

visible cracking after the release of P45F60-1, no hairpin bars were placed in 45F60-2. Panels with 45º skew angels are shown ready for casting in Figures 4.6 and 4.7.

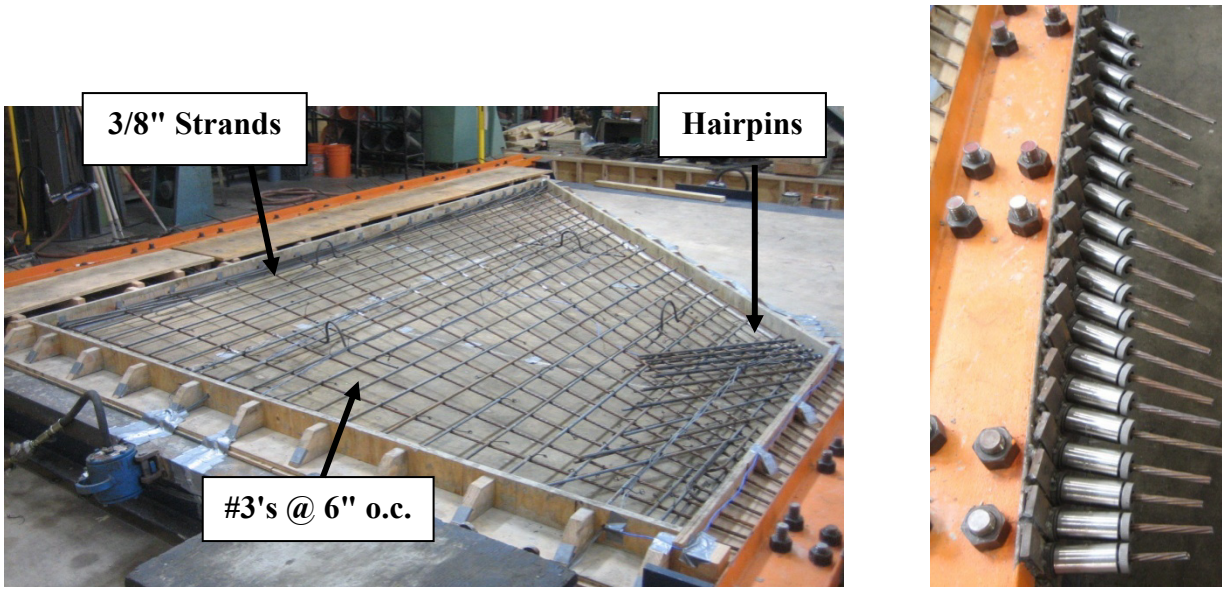

Completed formwork, strand layout and reinforcement *Congestion of strands at short end*

Figure 4.6: Fanned Strand Layout for Panel 45F60-1 (with hairpins) and 45F60-2 (no hairpins)

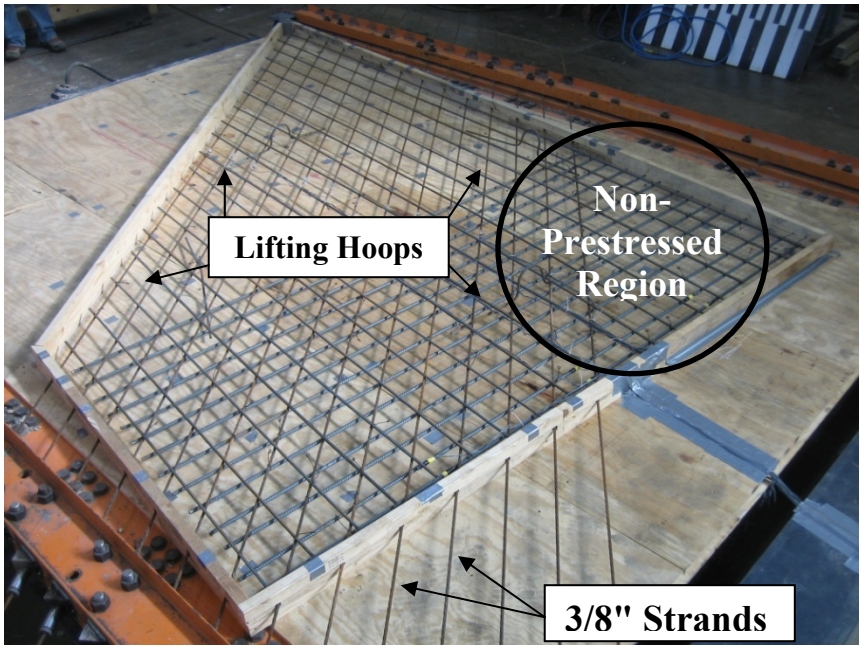

Figure 4.7: Parallel Strand Layout for Panels 45P60-1 and 45P45-1

The precast panels were constructed using Type III cement, which is typical of construction practices in commercial precast yards. The mixture design corresponds to a specified 28-day strength of 5,000 psi; however, cylinders tested at 28 days were approximately

8,000 psi. The concrete was placed and spread evenly with hoes and trowels. Screeds were used to create a level surface even with the tops of the forms. Due to the shallow depth of the concrete, ordinary stinger vibrators were not used. Instead, compressed air form vibrators mounted on the casting bed were used to vibrate the concrete. The panels were not trowel finished because a rough surface is specified on precast panels. When the concrete began to set, a broom was dragged across the surface to produce a TxDOT "standard broom finish" as shown in Figure 4.8.

Figure 4.8: Broom Finish Produced in Laboratory

The concrete strength at 28 days and at time of release is shown in Table 4.1

Table 4.1: Summary of concrete release and 28-day strengths

Panel	Strength at Release (psi)	Time (hours)	28-Day Strength (psi)
45F60-1	5120	19	8830
45F60-2	4430	9	10200
45P60-1	4100	19	8800
45P45-1	4120	26	8530

All of the 30º skewed panels were produced by a precast concrete fabricator. The bottom half of the edge forms were placed prior to tensioning the strands. The edge forms were made from a split 2x4 with 1/2 in. plywood strip spacers between strands. After the strands were tensioned, the strands with short embedment lengths were de-bonded by wrapping them in a plastic tube and sealing it with duct tape. Next, the additional flexural reinforcement was placed beneath the strands and tied into place. Rather than cutting each longitudinal #3 bar prior to installation, the iron workers tied over-length bars into place and then cut them to length with large bolt cutters. All reinforcing for both panels was completed in approximately 25 minutes. Once all of the reinforcement was tied, the top half of the wooden formwork was nailed into place. To keep the formwork from moving, small clamps were placed on the strands to brace the wood. The 30º skew panels were then ready for casting. Figure 4.9 shows a 30º panel in the

casting bed with all the strands and reinforcing bars in place. No details regarding concrete strength at release or at 28 days were available.

Figure 4.9: Panels 30P45-1 and 2 in Casting Yard

Casting the panels in the long lines common in prestressed concrete plants is a very quick process. The concrete was placed from the truck into the casting bed. The laborers then spread the concrete around the panel with shovels and dragged a vibrating screed across the top to create a level surface. The entire process took less than 4 minutes for both panels. Approximately 10 minutes later, a broom was used to create a roughened surface on the panels. Typically during the casting process at this precast plant, the lines are flooded to cure the panels when the panels are completed. It is possible that flooding may tend to reduce the surface roughness of a "standard broom finish." Panels 30P45-1 and 2 did not have a rough surface and in some places the concrete surface was quite smooth. The surface of Panels 30P45-3 and 4 is shown in Figure 4.10.

Figure 4.10: Broom Finish Produced in Casting Yard

4.3 Construction Sequence for Test Specimens

All specimens, with the exception of Specimen 10, were built following the sequence shown in Figure 4.11. The layout of panels for Specimen 10 is shown in Figure 4.12. All specimens consisted of the same key elements. The longitudinal beams were placed with a clear spacing of 9'-0". The 4 in. thick PCPs spanned between longitudinal beams and a 4-in topping slab was cast-in-place.

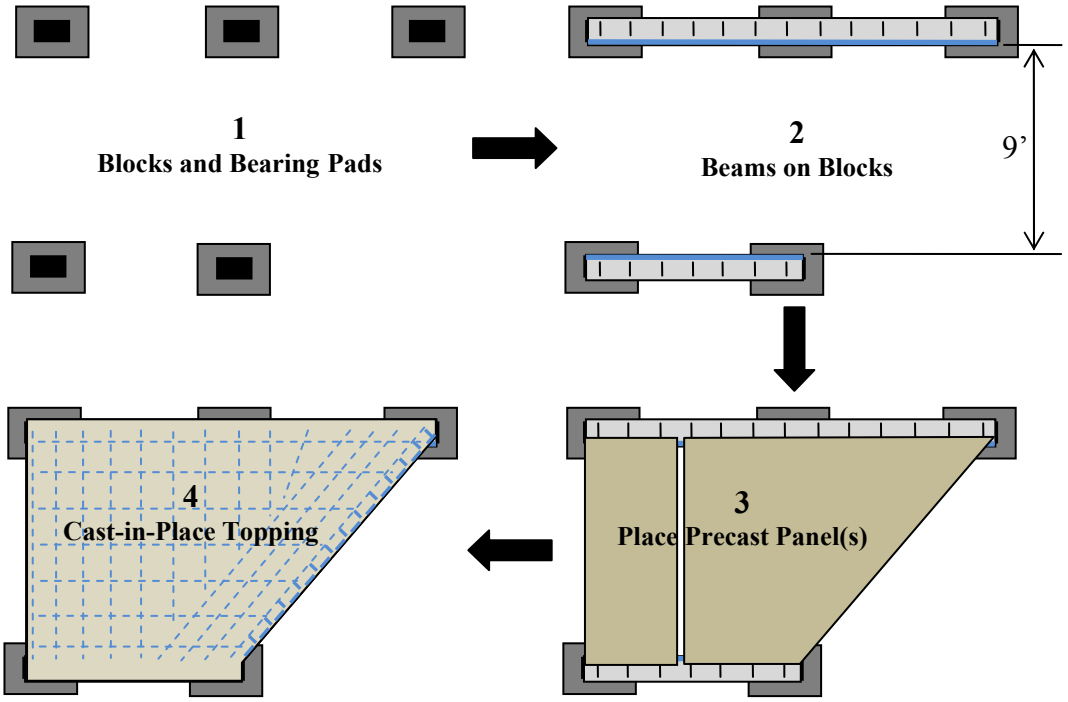

Figure 4.11: General Construction Sequence

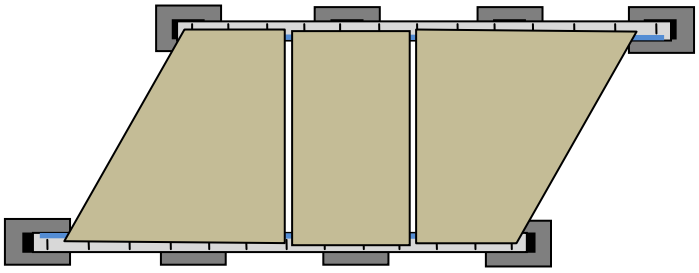

Figure 4.12: Panel Layout for Specimen 10

4.3.1 Placement of Panels

The panels were placed on bedding strips on the supporting beams as shown in Figure 4.13. When trapezoidal panels are used in the field, some tolerance in the spacing between PCPs will be needed. It was decided to leave a ¾ in. space between panels and to seal the gap with a backer rod as shown in Figure 4.14.

Figure 4.13: Precast Panels in Place

Figure 4.14: Backer Rod between Adjacent Panels

4.3.2 Sealed Expansion Joint (SEJ)

The most common expansion joint rail used in Texas bridge slabs is the SEJ-A detail and was used in the test specimens. The SEJ-A section is 3½ in. deep and fits within the space allowed by a 4-in. thick CIP topping. For this investigation, 6-in. steel studs were welded to the SEJ section at a spacing of 6 in. on center. Erection bolt holes were drilled every 4 ft along the member to connect to the formwork prior to placing the CIP topping. Details of the reinforcement and the expansion joint rail are shown in Figure 4.15.

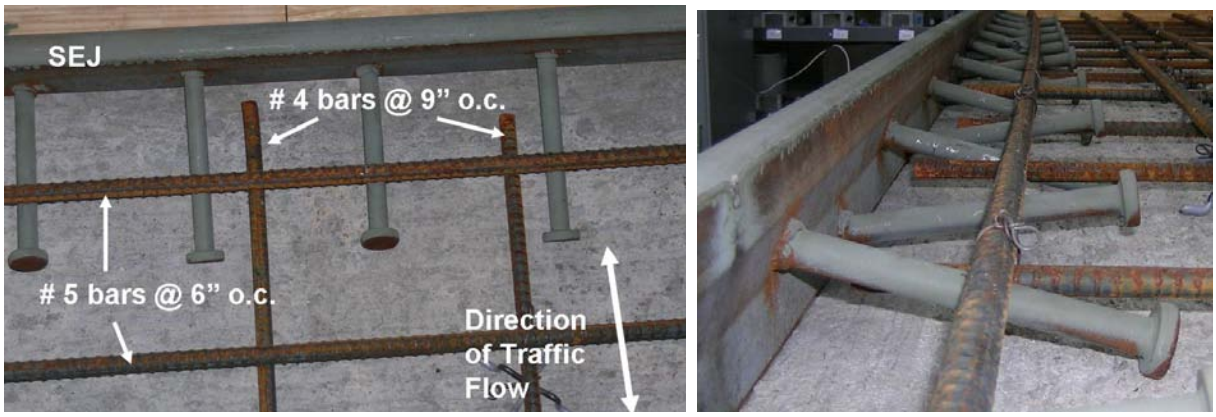

Figure 4.15: Expansion Joint and Reinforcement in Cast-in-Place Slab

4.3.3 Cast-in-Place Topping Slab

The layout of the Grade 60 steel reinforcement for the cast-in-place topping slab was designed according to standard TxDOT details. In the longitudinal direction of the slab, #4 bars were placed at 9 in. on center throughout the entire 10 ft width. In the transverse direction, #5 bars were placed at 6-in. on center throughout the entire 8 ft length. The bars were placed on 7/8-in. rebar chairs to provide a 2-in. clear cover to the top surface of the slab (Figure 4.15). Class S structural concrete was used for the topping slabs. The minimum specified compressive strength was 4000 psi, and the maximum water to cementitious material (w/cm) ratio was 0.45. It should also be noted that the surface of the precast panels must be wetted as required by TxDOT Standard Specifications prior to placing the topping slab.

All concrete was provided by a ready-mix plant. A test specimen ready for concrete placement is shown in Figure 4.16. After the topping slab was placed, the slab was covered with plastic sheeting for about a week to permit moist-curing of the concrete.

Figure 4.16: Expansion Joint and Reinforcement in Cast-in-Place Slab

4.4 Test Setup and Instrumentation

A simple frame was used to apply the vertical loads to the test specimens (Figure 4.17). The columns were tied to the strong floor using four, 3/4-in. threaded rods, and the cross beams

comprised two, W-sections bolted to the flanges of the columns. A 150-ton hydraulic ram was secured to the bottom flanges of the cross beam and a 100-kip load cell was used to measure the applied load. A steel plate (10 in. wide by 20 in. long by 2.5 in. thick) was positioned on top of an elastomeric bearing pad (Figure 4.17) to simulate the bearing area of a wheel from the HL-93 Design Truck. The position of wheel load at the expansion joint is shown in Figure 4.17. Figure 4.18 shows the position of the wheel load when the load was applied at the joint between the skewed and rectangular panels.

Figure 4.17: Load Frame and Apparatus

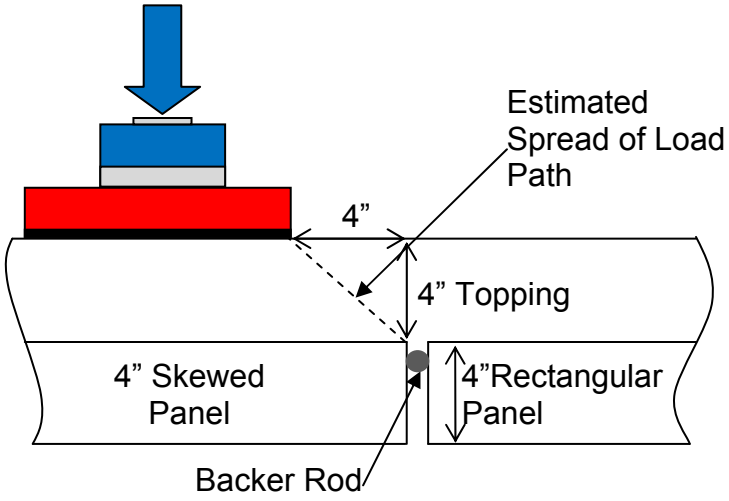

Figure 4.18: Wheel Position at Joint Between Panels

Several types of instruments were used to measure the response of the test specimens under the applied loads. Linear potentiometers and dial gages were used to measure vertical

deflections along the expansion joint and along the joint between panels. In some of the panels, strain gages were attached on the bottom surface of the concrete panels, on the SEJ, on the strand in the panels, and on the reinforcing bars. In general the strain gages were installed at the locations where highest strains were expected. However, with the formation of cracks, the strain gage data was often of little value. Strain gages on the SEJ were useful because the strains gave an indication the stiffening effect of the SEJ on the edge of the deck.

Chapter 5. Performance of Rectangular Panels Subjected to Fatigue

The measured response of Specimens 1-4 is summarized in terms of loading history. The applied loading histories include: initial static test, periodic static tests, static overload test (after at least two million fatigue cycles), additional periodic static tests, and static test to failure (after at least five million fatigue cycles). The implications of the results are discussed.

5.1 Specimen 1—Positive Moment Loading

Eleven static tests were conducted before, during, and after the fatigue test (Table 5.1). During the fatigue test, the applied loads varied between 1 and 7 kip at a frequency of 2 Hz. During the periodic static tests, a maximum load of 16 kip was applied, which corresponds to the wheel load for the rear axle of the HL-93 Design Truck. It was originally planned to apply a maximum load of 32 kip during the overload test, but flexural cracks were not observed at this level of load. Therefore, a maximum applied load of 50 kip was applied.

Table 5.1: Static Loading History for Specimen 1

Type of Static Test	Accumulated Fatigue Cycles*	Maximum Applied Load (kip)	Condition at Conclusion of Test
Initial	0	16	Uncracked
Periodic	250,000	16	
Periodic	1,240,000	16	
Periodic	2,000,000	16	
Overload	2,000,000	50	Cracked
Periodic	2,200,000	16	
Periodic	3,000,000	16	
Periodic	3,500,000	16	
Periodic	4,750,000	16	
Periodic	5,000,000	16	
Failure	5,000,000	88	Punching Failure

- Limiting fatigue loads: P_{min} = 1 kip and P_{max} = 7 kip

The load-deflection response was not sensitive to the number of fatigue cycles for the first 2 million cycles. The maximum deflection was less than 0.03 in. at an applied load of 16 kip during all four static tests. The tensile strains measured on the surface of the PC panel were also independent of the number of loading cycles. Slight variations were observed in the strain response of the SEJ, but these were considered to be insignificant.

After 2 million fatigue cycles, a static overload test was conducted to crack the test specimen. Subsequent fatigue tests were used to determine if the stiffness of the cracked slab deteriorated under fatigue loading. First, the load was increased to 32 kip, which corresponds to two times the wheel load for the rear axle of the HL-93 Design Truck. The overall load-deflection response was nearly linear during this cycle, as was the strain response in the SEJ. No

cracks were observed so the load was increased to 50 kip. The overall stiffness decreased gradually with increasing load during this cycle as shown in Figure 5.1. No cracks were observed on the top of the slab, but several cracks were observed on the bottom of the PC panel as shown in Figure 5.1.

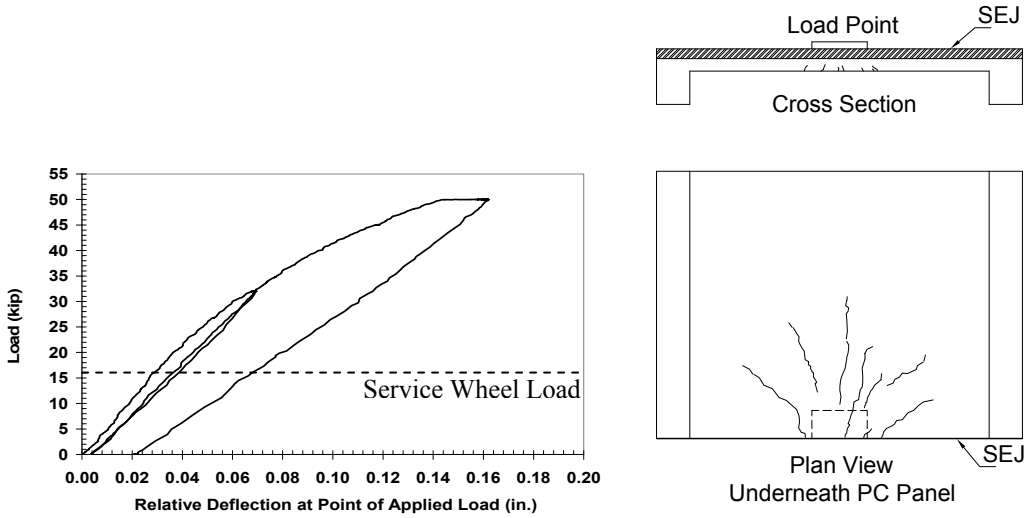

(a) Load-Deflection Response *(b) Crack Pattern*

Figure 5.1: Response of Specimen1 during Static Overload Test to 50k

After the overload test to 50k, the fatigue test was stopped five times between two million and five million cycles for additional static tests. The specimen was loaded statically to a maximum of 16 kip during each static test. The measured response during these static tests is shown in Figure 5.2. The stiffness of the specimen was slightly reduced, but the nature of the response did not change appreciably as the number of loading cycles increased. The overall load-displacement response was linear and the compressive strains in the SEJ increased linearly with increasing load.

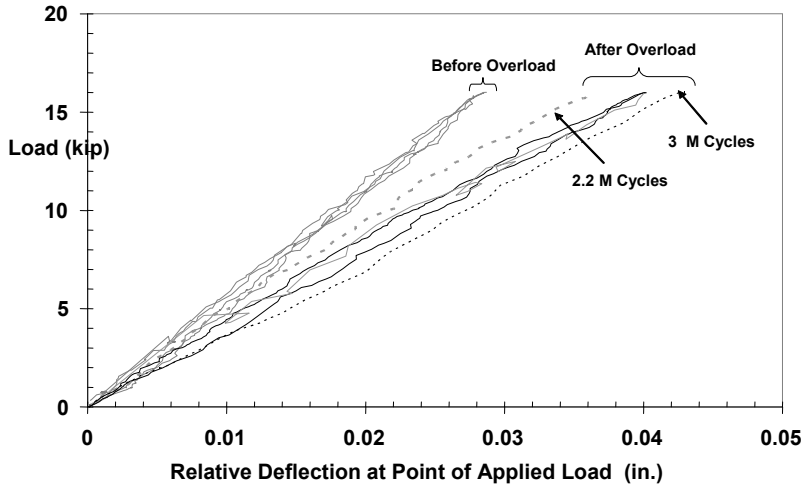

Figure 5.2: Load-Deflection Response of Specimen 1 during Periodic Static Tests after Overload to 50k

After completion of the fatigue test, the specimen was tested to failure. The specimen failed in punching shear at an applied load of 88 kip, which corresponds to more than 5 times the wheel load for the rear axle of the HL-93 Design Truck. However, the response of the specimen was the result of delamination near the corners of the specimen away from the loaded edge where large cracks formed at an applied load of 77 kip as the CIP slab pulled away from the support beams. The overall load-displacement response and strains in the SEJ were essentially linear for applied loads less than 65 kip (Figures 5.3 a, b). Above this load, the displacement increased rapidly with increasing load. Photographs of the specimen after failure are shown in Figure 5.3c.

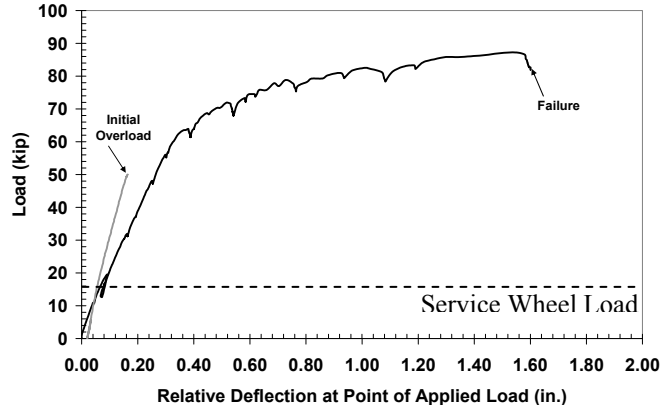

(a) Strains in SEJ

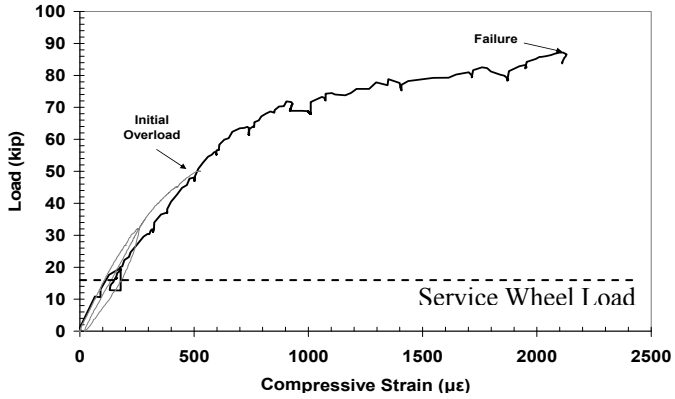

(b) Load-Deflection Response

(c) Appearance at Failure

Figure 5.3: Response of Specimen 1 during Static Test to Failure

5.2 Specimen 2—Positive Moment Loading

Specimen 2 was subjected to a total of thirteen static tests before, during, and after the fatigue test (Table 5.2). During the fatigue test, the applied loads producing positive moment along the expansion joint varied between 1 and 17 kip at a frequency of 3 Hz. The maximum applied load during the periodic static tests (16 kip) corresponded to the wheel load for the rear axle of the HL-93 Design Truck. During the overload test, a maximum load of 50 kip was applied. The overall load-displacement response was linear, and all strains increased linearly with increasing load. After 2.5 million fatigue cycles, a static overload test (three loading cycles) was conducted to crack the test specimen. The maximum applied load was 16 kip in the first cycle and 50 kip in the second and third cycles. The overall load-deflection response was nearly linear for applied loads less than 30 kip. The stiffness decreased above this load level and residual displacements on the order of 0.2 in. were observed at the conclusion of the test.

Table 5.2: Static Loading History for Specimen 2

Type of Static Test	Accumulated Fatigue Cycles*	Maximum Applied Load (kip)	Condition at Conclusion of Test
Initial	0	16	Uncracked
Periodic	500,000	16	
Periodic	760,000	16	
Periodic	1,000,000	16	
Periodic	1,250,000	16	
Periodic	2,000,000	16	
Periodic	2,190,000	16	
Overload	2,500,000	50	Cracked
Periodic	2,750,000	16	
Periodic	3,000,000	16	
Periodic	3,250,000	16	
Periodic	4,000,000	16	
Periodic	6,000,000	16	
Failure	6,000,000	90	Punching Failure

- Limiting fatigue loads: P_{min} = 1 kip and P_{max} = 17 kip

As indicated in Table 5.2, the fatigue test was stopped a number of times during the first two million cycles when an overload test to 50 kips was run. Between two million and six million cycles, additional static tests to 16 kips were carried out. The measured response during these static tests is shown in Figure 5.4. Similarly to specimen 1, the load-deflection responses and measured strain responses were not sensitive to the number of fatigue cycles. The load-deflection response during the overload test to 50k is shown in Figure 5.5.

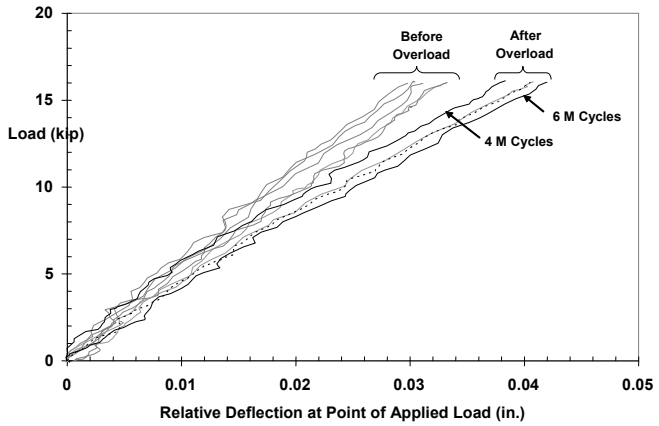

Figure 5.4: Response of Specimen 2 under Static Overload Tests

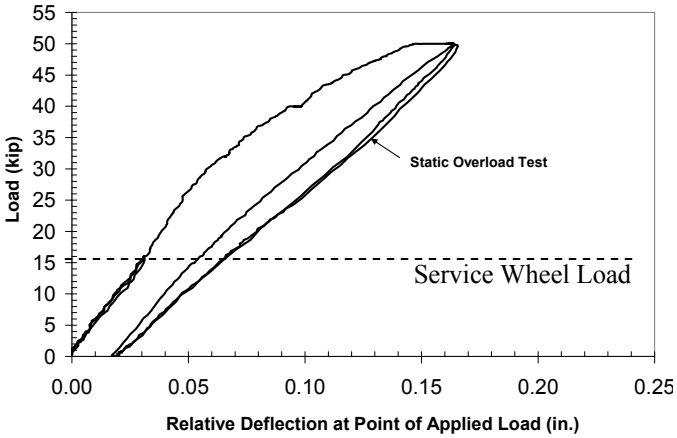

Figure 5.5: Response of Specimen 2 during Static Overload Test to 50k

After completion of the fatigue test, the specimen was tested to failure. The measured response is shown in Figure 5.6. The specimen failed abruptly in punching shear at an applied load of 90 kip, which corresponds to more than 5 times the wheel load for the rear axle of the HL-93 Design Truck. Similarly to Specimen 1, large cracks formed as the CIP slab pulled away from the loaded edge of the specimen and the stiffness of the load-displacement curve decreased abruptly at an applied of 60 kip. The compressive strains in the SEJ were nearly linear for applied loads less than 60 kip. Photographs of specimen 2 at failure are shown in Figure 5.7.

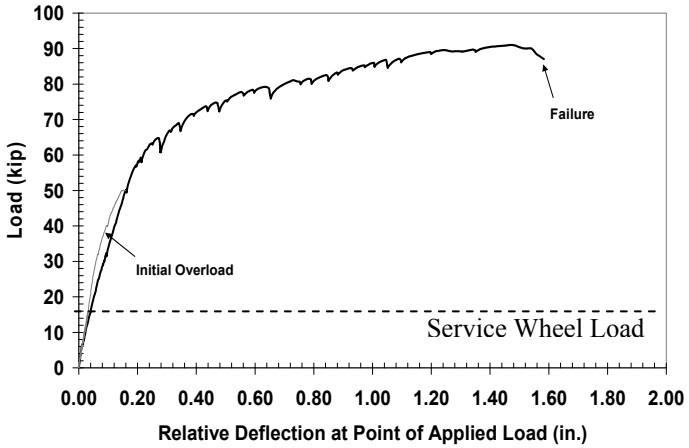

Figure 5.6: Response of Specimen 2 during Static Test to Failure

Figure 5.7: Photographs of Specimen 2 after Punching Shear Failure

5.3 Specimen 3—Negative Moment Loading

Specimen 3 was subjected to a total of 16 static tests before, during, and after the fatigue test (Table 5.3). During the fatigue test, the applied loads varied between 2 and 34 kip at a frequency of 3 Hz. The maximum applied load during the periodic static tests (32 kip) corresponded to the rear axle of the HL-93 Design Truck. During the overload static test to 50 kip, the negative moment specimens did not exhibit as many cracks as the positive moment specimens. The overload of 50 kip was only 1.5 times the rear axle of the HL-93 Design Truck, while for the positive moment specimens, the overload of 50 kip corresponded to 3 times the wheel load for the rear axle of the HL-93 Design Truck. However, before the initial static test, cracks were observed on the top of the slab directly above the edges of the center beam (Figure 5.8). These cracks corresponded closely to the shrinkage cracks observed by Coselli (2004) in project 0-4418. Overload to 50 kips did not cause an appreciable change in the measured response. The highest strains were less than 300 με and were measured in the first bar above the edges of the center support beam.

Table 5.3: Static Loading History for Specimen 3

Type of Static Test	Accumulated Fatigue Cycles*	Maximum Applied Load (kip)	Condition at Conclusion of Test
Initial	0	32	Shrinkage Crack
Periodic	250,000	32	
Periodic	600,000	32	
Periodic	875,000	32	
Periodic	1,100,000	32	
Periodic	1,443,000	32	
Periodic	1,750,000	32	
Overload	2,000,000	50	
Periodic	2,250,000	32	
Periodic	3,000,000	32	
Periodic	3,290,000	32	
Periodic	3,680,000	32	
Periodic	4,000,000	32	
Periodic	4,425,000	32	
Periodic	5,000,000	32	
Failure	6,000,000	130	Punching Failure

* Limiting fatigue loads: P_{min} = 2 kip and P_{max} = 34 kip

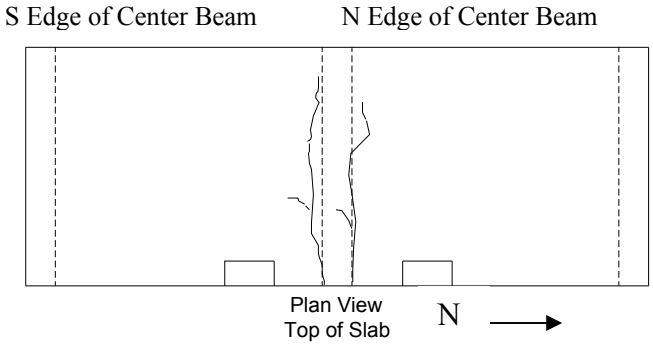

Figure 5.8: Cracks Observed in Specimen 3 before Initial Static Test

The load-deflection responses during the periodic static tests to 50k are shown in Figure 5.9. Similar to Specimens 1 and 2, the load-deflection responses were not sensitive to the number of fatigue cycles.

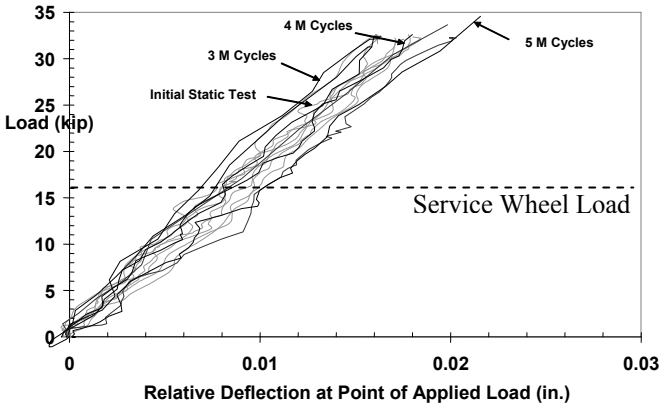

Figure 5.9: Response of Specimen 3 during Periodic Static Tests

After completion of the fatigue test, the specimen was tested to failure. The measured response is shown in Figure 5.10. The specimen failed abruptly in punching shear at an applied load of 130 kip, which corresponds to approximately four times the rear axle load from the HL-93 Design Truck. The load-displacement response was essentially linear for applied loads less than 85 kip. Above this load, the displacement increased rapidly with increasing load, indicating that the prestressed reinforcement in the PC panel had yielded. The tensile strain response of the SEJ was essentially linear for applied loads less than 110 kip, after which the response changed abruptly signifying initial yield of the cross section. Photographs of Specimen 3 are shown in Figure 5.11.

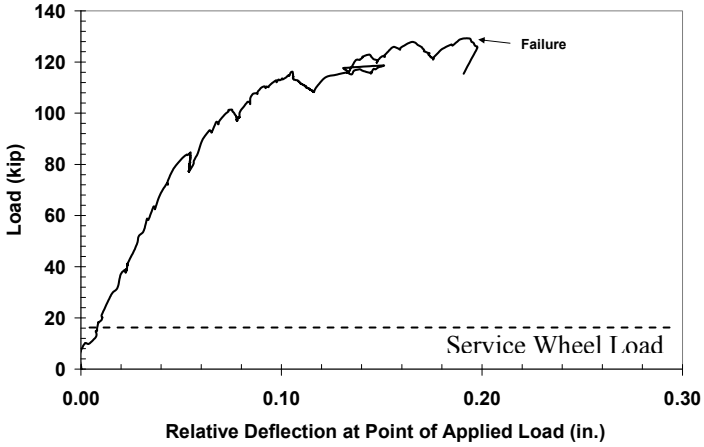

Figure 5.10: Response of Specimen 3 during Static Test to Failure

Figure 5.11: Photograph of Specimen N0P1 after Punching Shear Failure

5.4 Specimen 4—Negative Moment Loading

The applied load history for Specimen 4 differs from the previous three test specimens. Because the structural behavior of the specimens did not change significantly with increasing applied loads and number of cycles, it was decided to increase the fatigue load and static loads for all the tests of Specimen 4. Also, because the previous static overload test did not appreciably change the behavior of the specimen, the maximum applied load was 50 kip for all periodic static tests. Specimen 4 was subjected to a total of 12 periodic static tests (Table 5.4). During the fatigue test, the applied loads varied between 2 and 48 kip at a frequency of 3.5 Hz. The periodic static tests (50 kip) corresponded to the rear axle of the HL-93 Design Truck multiplied by an overload factor (1.25) and by the AASHTO dynamic impact factor for fatigue design of bridge decks, (1+I) where I=0.15. Before the initial static test, cracks were observed in the top of the slab directly above the edges of the center support beam (as in Specimen 3, Figure 5.8).

Table 5.4: Static Loading History for Specimen 3

Type of Static Test	Accumulated Fatigue Cycles*	Maximum Applied Load (kip)	Condition at Conclusion of Test
Initial	0	50	Shrinkage Cracks
Periodic	250,000	50	
Periodic	830,000	50	
Periodic	1,000,000	50	
Periodic	1,500,000	50	
Periodic	1,760,000	50	
Periodic	2,271,000	50	
Periodic	2,457,000	50	
Periodic	3,800,000	50	
Periodic	4,290,000	50	
Periodic	5,370,000	50	
Failure	5,370,000	140	Punching Failure

* Limiting fatigue loads: P_{min} = 2 kip and P_{max} = 48 kip

As indicated in Table 5.4, the fatigue test was stopped periodically for static loading. Due to an error with the data acquisition system, the measured strain response for most of the static tests was not collected. However, data were collected from the initial static test, after 250,000 cycles, and the test to failure after 5.37 million fatigue cycles. The load-deflection responses in Figure 5.12 were not sensitive to the number of fatigue cycles. For the strain gages placed along an edge of the center support beam, there was a slight increase in measured strain after the initial static test, however, the response was essentially the same after 250,000 cycles as it was after 5.37 million cycles, and the maximum tensile strain was less than 500 με. Strains measured on the SEJ were essentially the same as measured during the test to failure for Specimen 3. The maximum strain was approximately 300 με at an applied load of 50 kip.

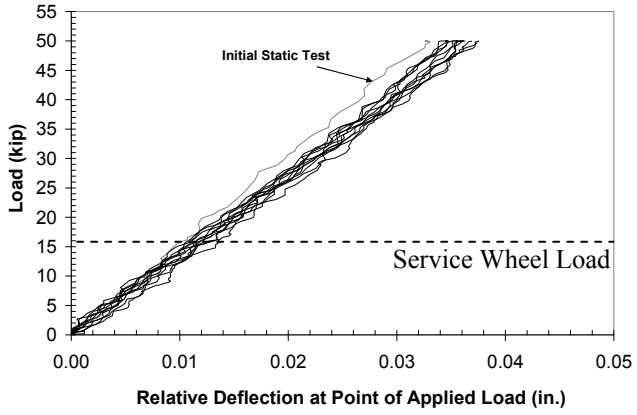

Figure 5.12: Response of Specimen 4 during Periodic Static Tests

After completion of the fatigue test, the specimen was tested to failure. The measured response is shown in Figure 5.13. The specimen failed abruptly in punching shear at an applied load of 140 kip, which corresponds to more than four times the rear axle weight of the HL-93 Design Truck. The load-displacement response was linear for applied loads less than 100 kip. Above this load, the displacement increased rapidly with increasing load. The maximum relative deflection was less than 0.25 in. The measured tensile strains in the slab reinforcement were essentially linear up to an applied load of 120 kip. The maximum strain (N1) was less than 1320 με which is approximately 58% of the yield strain. Strains measured in the SEJ reached yield at an applied load of 100 kip. Photographs of specimen 4 after failure are shown in Figure 5.14.

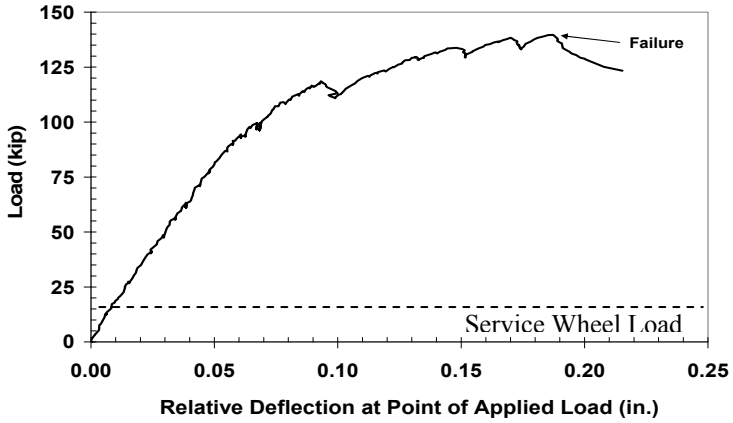

Figure 5.13: Measured Response of Specimen 4 during Static Test to Failure

Figure 5.14: Photograph of Specimen 4 after Shear Failure near Center Support

5.5 Discussion of Results

5.5.1 Comparison of Positive Moment Specimens

Because of the excellent fatigue response of Specimen1, service-level fatigue loads were increased to design-level fatigue loads for Specimen 2. After five million cycles, the maximum deflection for Specimen 1 was 0.043 in. at an applied load of 16 kip. The response of Specimen 2 was quite similar, and the maximum deflection after six million cycles was 0.042 in. at an applied load of 16 kip. The deflection-to-span ratios were less than 1/2500 for both specimens. These very small deflections are significant because they indicate that the stiffness of the test specimens did not degrade appreciably during the fatigue tests. Also, the larger fatigue loads used for Specimen 2 did not influence the load-deflection behavior.

After the static overload test, changes in stiffness were observed due to cracking of the PC panels, but the overall response did not change appreciably during additional fatigue cycles. The larger fatigue loads used for Specimen 2 did not influence the measured strain response. No indications of crack propagation were observed as the number of fatigue cycles was increased, and no evidence of delamination was observed at the interface of the PC panel and CIP slab.

During the tests to failure, there was no significant deterioration or delamination along the interface of the PC panel and CIP slab until the applied loads exceeded four times the design loads. When the applied loads approached the failure load, some delamination was observed at the interface near the support beams for both specimens. However, the capacities of both specimens were greater than 4.8 times the design loads, and delamination at such a high level of applied load was not considered significant. The larger fatigue loads used for Specimen 2 did not affect the capacity. A summary of the failure loads is included in Table 5.5. The overall load-displacement responses of the test specimens are compared with the measured responses of the larger-scale specimens tested by Coselli (2004) (Figure 5.15).

Table 5.5: Summary of Response of Positive Moment Specimens

Specimen	Type of Load	Design Wheel Load (kip)	Applied Load at First Observed Crack (kip)	Applied Load at Failure (kip)	Failure Load / Design Wheel Load (kip)
1	Design Truck	16	32	77	4.8
2	Design Truck	16	32	79	4.9
Coselli without SEJ	Design Tandem	12.5	28	67	5.3
Coselli with SEJ	Design Tandem	12.5	28	84	6.7

There are some differences between the tests that should be kept in mind when making comparisons. In the study by Coselli (2004), two wheel loads were used to represent one half of each of the axles of the Design Tandem configuration. A single wheel load, representing the rear axle of the Design Truck, was used to test Specimens 1 and 2. However, the failure surfaces in both cases were nearly the same, and the crack patterns observed by Coselli (2004) were similar

to the crack patterns observed in P0P1 and P0P2. The failure loads included in Figure 5.15 corresponds to the wheel load nearest the failure surface at the expansion joint, and are reported as "load per load point." The simply supported boundary conditions for the single panel in Specimens 1 and 2 did not permit load redistribution as was possible in the multiple-girder, larger-scale specimen. Coselli (2004) used a deeper expansion joint rail in one portion of the test specimen than was used in Specimens 1 and 2. In another portion of the larger-scale test specimen, no rail was used. In Table 5.6 and Figure 5.15, these two tests are referred to as "Coselli without SEJ" and "Coselli with SEJ." Finally, the measured compressive strength of the concrete was higher for Specimens1 and 2 (5200 psi and 5700 psi) compared with the larger-scale specimen (4100-4400 psi). The deck reinforcement was the same in all three specimens, and the reinforcement in all of the PC panels was nominally identical. While there were some differences, the larger-scale specimen and the smaller specimens both performed in a similar manner. For the three tests including expansion joints, the maximum applied loads were within 10%. All specimens exhibited capacities that significantly exceeded design loads.

5.5.2 Comparison of Negative Moment Specimens

Because of the excellent fatigue response of Specimen 2, the fatigue loads for specimen 3 were design-level loads that corresponded to the rear axle of the HL-93 Design Truck (32 kip). Furthermore, based on the excellent fatigue response of specimen N0P1, the design-level fatigue loads were increase to 46 kip for Specimen 4. For both specimens, the static overload tests did not crack the specimen; therefore, the response of the specimens did not reflect a change in stiffness. After five million cycles, the maximum deflection for Specimen 3 was 0.021 in. at an applied load of 32 kip. The response of Specimen 4 was quite similar, even though the fatigue load was significantly increased, and the maximum deflection after 6 million cycles was 0.038 in. at an applied load of 50 kip. The deflection-to-span ratios were less than 1/2800 for both specimens. These small deflections are significant because they indicate that the stiffness of the test specimens did not appreciably degrade during the fatigue tests. Also, the overload-level fatigue loads used for Specimen 4 did not influence the load-deflection behavior.

Overall, the measured responses indicated linear behavior for applied loads less than 70 kip. For both specimens, the periodic static tests indicated essentially the same responses throughout the fatigue tests. There was no crack propagation as the number of fatigue cycles was increased, and no visible change in the appearance of the PC panel detail. At failure, the measured strains indicated that the reinforcement did not yield. However, when the applied load approached the failure load, yielding of the SEJ preceded failure of the specimen. During the test to failure, there was no significant deterioration or delamination along the interface of the PC panel and the CIP slab until the loads exceeded three times the design loads. Because the capacity of both specimens significantly exceeded four times the design loads, the delamination near the support beams was not considered a significant problem. The overload-level fatigue loads used for Specimen 4 did not affect the capacity. A summary of the failure loads is included in Table 5.6.

The overall load-displacement response tested of the test specimens are compared with the response measure of the larger-scale specimens tested by Coselli (2004) (Figure 5.15). Similar to Specimens 1 and 2, a difference between the two sets of specimens must be mentioned. Coselli (2004) used the Design Tandem configuration, and for Specimens 3 and 4 the Design Truck configuration was used. Even though there were four wheel loads, each punching shear failure surface occurred at a wheel load at the edge of the expansion joint, and the crack

patterns observed by Coselli (2004) were similar to the crack patterns observed in N0P1 and N0P2. The failure loads included in Figure 5.15 correspond to the wheel load nearest the failure surface at the expansion joint, and are reported as "load per load point." The girder spacing was 10 ft in Specimens 3 and 4 and 8 ft in the larger-scale specimen. Coselli (2004) used an armor joint rail in one test, and at another test location, no rail was used. In Figure 6.2, these two tests are indicated "Coselli without Armor Joint" and Coselli with Armor Joint." The measured compressive strengths of the concrete were higher for Specimens 3 and 4 (5500 psi and 5900 psi) compared with the larger-scale specimen (4100-4400 psi). The deck reinforcement was the same in all three specimens, and the reinforcement in all of the PC panels was the same. Even though the test specimens are not equivalent, Figure 5.15 generally illustrates that the larger-scale specimen and the smaller specimens both performed in a similar manner, and all specimens exhibited capacities that significantly exceeded the design-level loads.

Table 5.6: Summary of Failure Response of Negative Moment Specimens

Specimen	Type of Load	Design Wheel Load (kip)	Applied Load at Failure (kip)	Failure Load / Design Wheel Load (kip)
3	Design Truck	16	65	4.1
4	Design Truck	16	70	4.4
Coselli without AJ	Design Tandem	12.5	70	5.6
Coselli with AJ	Design Tandem	12.5	90	7.2

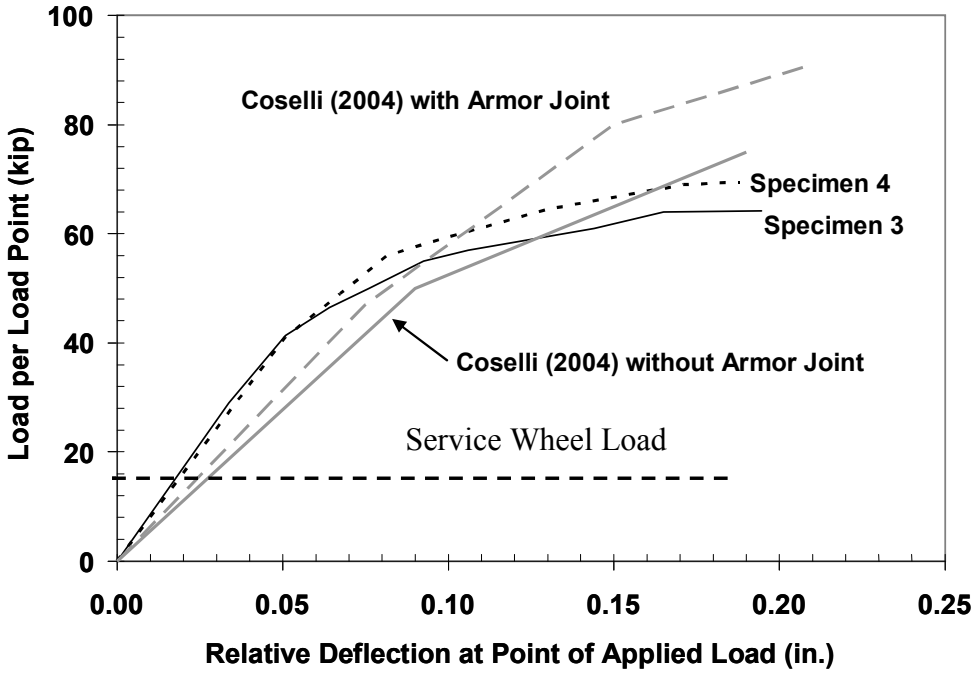

Figure 5.15: Comparison of Capacities of Specimens 3 and 4 with Larger-Scale Specimen

Chapter 6. Performance of Skewed (Trapezoidal) Panels

The behavior of prestressed concrete panels used adjacent to 30º and 45º skewed expansion joints is described. An overview of the test program was provided in Chapter 2. Six specimens were constructed and subjected to static loading to failure. One specimen was subjected to fatigue loading prior to static loading to failure. Construction of the test specimens was described in Chapter 4. Table 6.1 and Figure 6.1 contain details of the tests that are discussed in this chapter.

Table 6.1: Details of Test Specimens with Skewed (Trapezoidal) Panels

Test Specimen	Direction of Applied Moment	Skew Angle (deg)	Strand Arrangement	Length of Short Side (in.)	Relative Surface Roughness	Fatigue Test	Static Test to Failure
5	Positive	45	Fanned	60	Rough	—	X
6	Positive	45	Parallel	60	Rough	—	X
7	Positive	45	Parallel	45	Rough	X	X
8	Positive	30	Parallel	45	Smooth	—	X
9	Positive	30	Parallel	45	Smooth	—	X
10A	Positive	30	Parallel	45	Rough	—	X
10B	Positive	30	Parallel	45	Rough	—	X

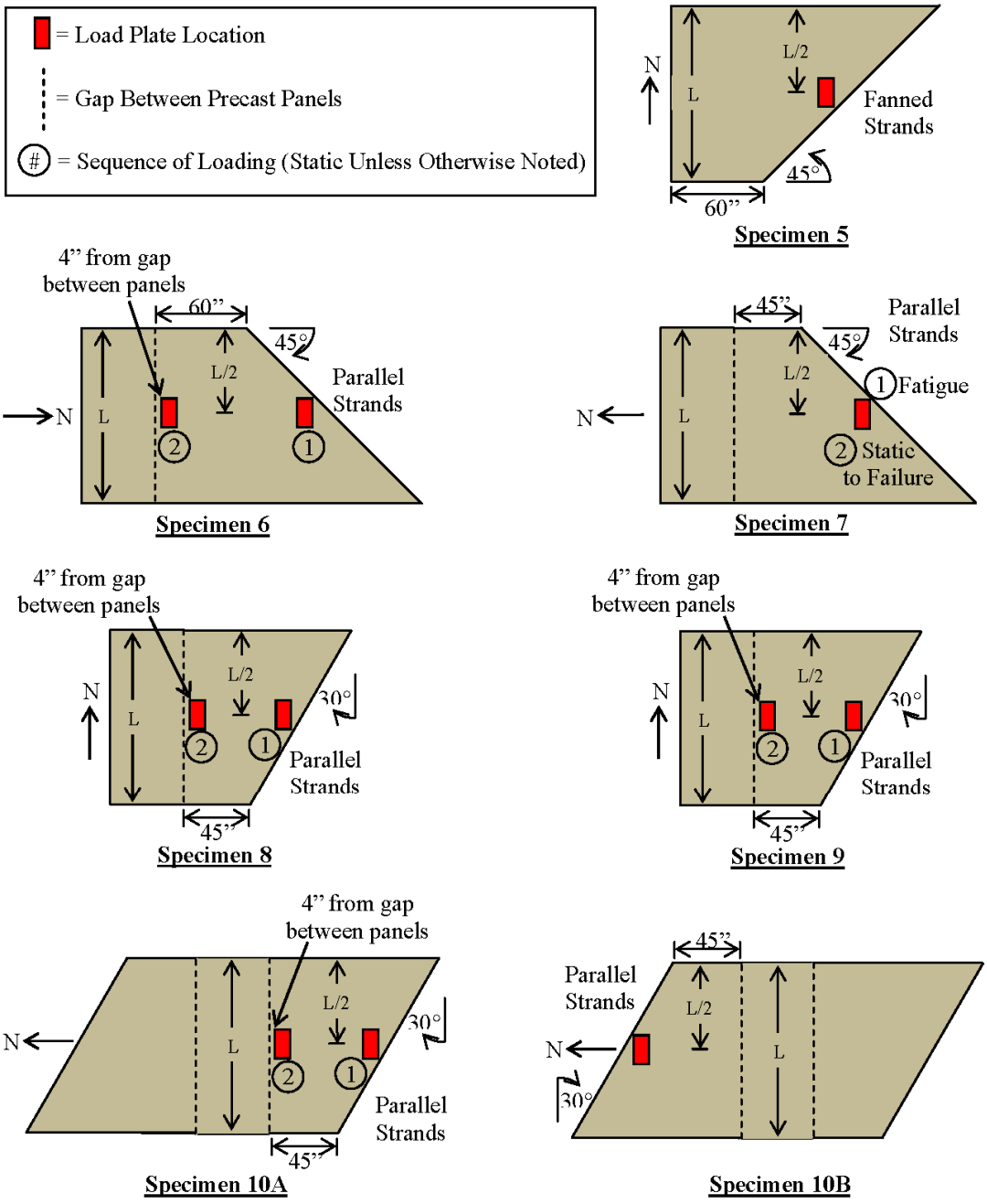

Figure 6.1: Location of Load Plate and Order of Loading for Specimens 5 to 10

Vertical loads were applied at midspan of the skewed end or the joint between the skewed panel and the rectangular adjacent precast panel. The behavior of the specimens is presented using the measured loads and deflections and observed crack patterns. Where measured strains provide further insight, they are discussed.

In discussing the response of the test specimens, several loads are used for comparison. With respect to the HL-93 Design Truck, three loads are considered, as defined in Table 6.2. The Service Wheel Load, P_W, refers to one half of the rear axle load for the HL-93 Design Truck. The Design Wheel Load corresponds to the Service Wheel Load amplified for impact, where I = 0.33. The Factored Wheel Load is the product of the live load factor and the Design Wheel Load.

Table 6.2: Loads Corresponding to HL-93 Design Truck

Load	Designation	Expression	Numerical Value
Service Wheel Load	P_W	P_W	16 kip
Design Wheel Load	P_L	(1+I) P_W	21.3 kip
Factored Wheel Load	P_U	1.75 P_L	37.3kip

6.2 Measured Response of Specimens with 45-Degree Skewed Panels

6.2.1 Response of Specimen 5 (45˚ Skew, Fanned Strands)

Specimen 5 was tested only at midspan of the skewed end. Specimen 5 consisted of an isolated panel. In subsequent tests, a rectangular panel abutted the straight end of the specimen. The load was applied monotonically to failure. The relative displacement at midspan of the skewed end under the applied load is shown in Figure 6.2.

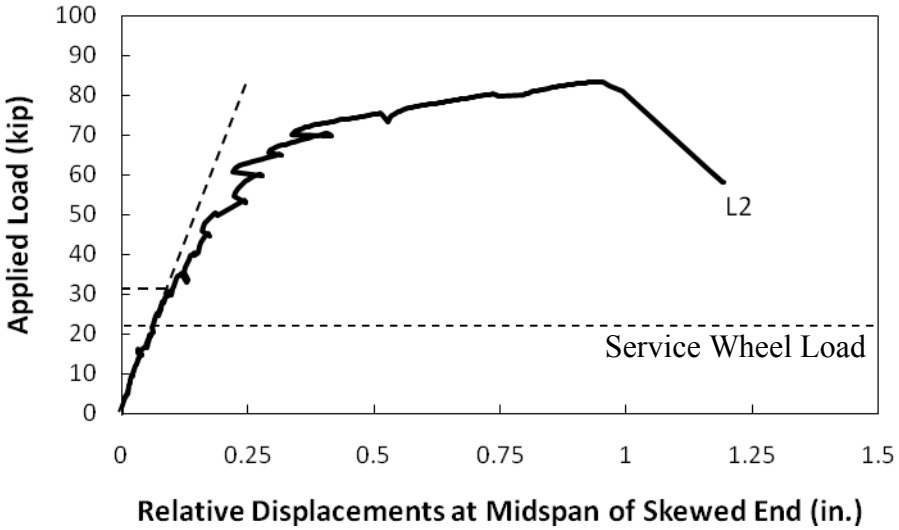

Figure 6.2: Load-Displacement Response of Specimen 5 for Load Applied at Midspan of Skewed End

The load-displacement plot in Figure 6.2 shows a cracking load of approximately 31 kip. Observed cracks at the conclusion of the static test are shown in Figure 6.3. It should be noted that these figures show the crack patterns corresponding to the major cracks only. The specimen failed in shear at the short side support. The precast trapezoidal panel pulled away from the topping slab at failure (Figure 6.4).

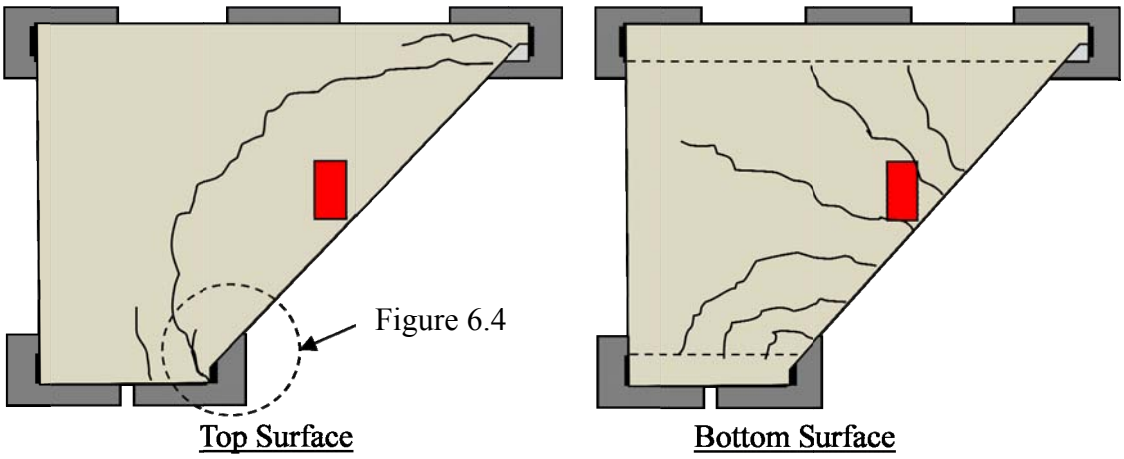

Figure 6.3: Observed Crack Pattern at Failure of Specimen 5

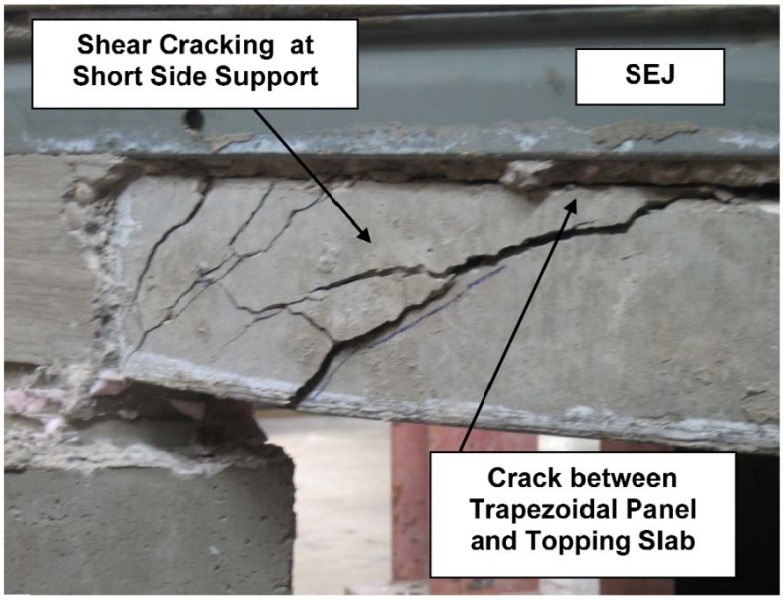

Figure 6.4: Shear Failure of Specimen 5

6.2.2 Response of Specimen 6 (45º Skew, Parallel Strands)

During the first test Specimen 6, the load was applied near midspan of the skewed end of the trapezoidal panel. For the second test, load was applied near midspan of the perpendicular end of the trapezoidal panel.

The relative displacement at midspan of the skewed end is shown in Figure 6.5. From the load-displacement data, the specimen cracked at approximately 31 kip, but cracks were not visible until the applied load reached 37 kip.

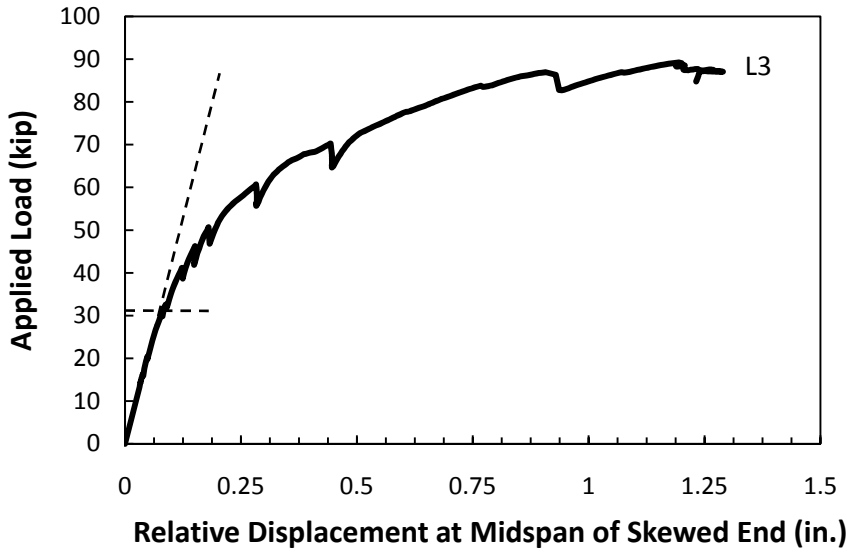

Figure 6.5: Displacement of Specimen 6 under Load at Midspan of Skewed End

The SEJ did not yield under the applied load. The strain gage data on the prestressing strands indicated that the cracking load for the skewed end was approximately 28 kip as shown in Figure 6.6. The changes in strains in the strands are highest under the load point and decrease sharply as distance from the loaded end increases as shown in Figure 6.7.

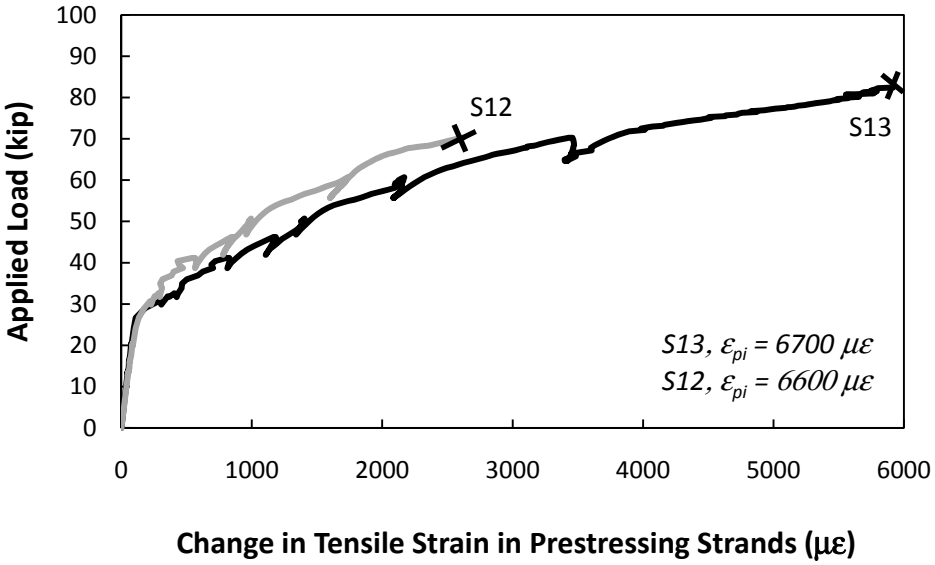

Figure 6.6: Change in Tensile Strain in Prestressing Strand in Specimen 6 for Load at Midspan of Skewed End

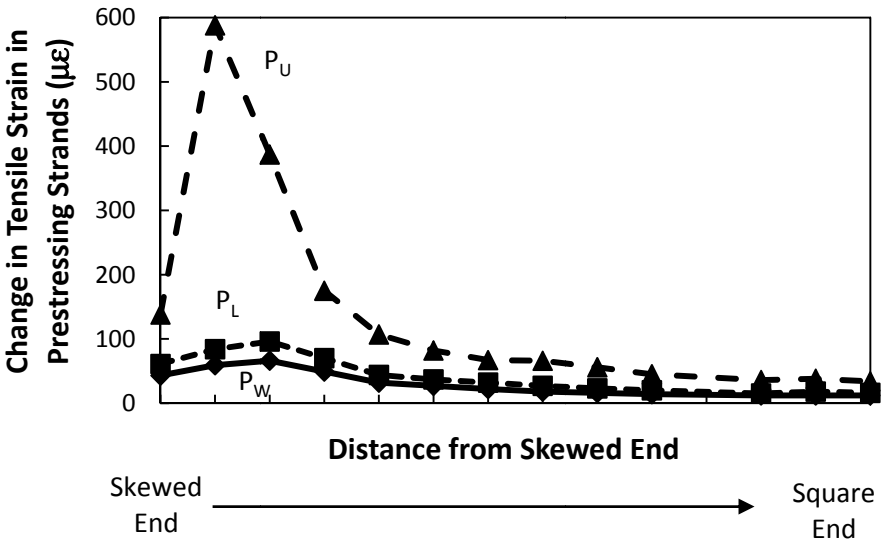

Figure 6.7: Variation of Measured Strain in Prestressing Strands for Load at Midspan of Skewed End of Specimen 6

Observed cracks at the conclusion of the static test at midspan of the skewed end are shown in Figure 6.8. A diagonal shear crack formed at the support on the short side of the trapezoidal panel and propagated to the top surface of the specimen as shown in Figure 6.9.

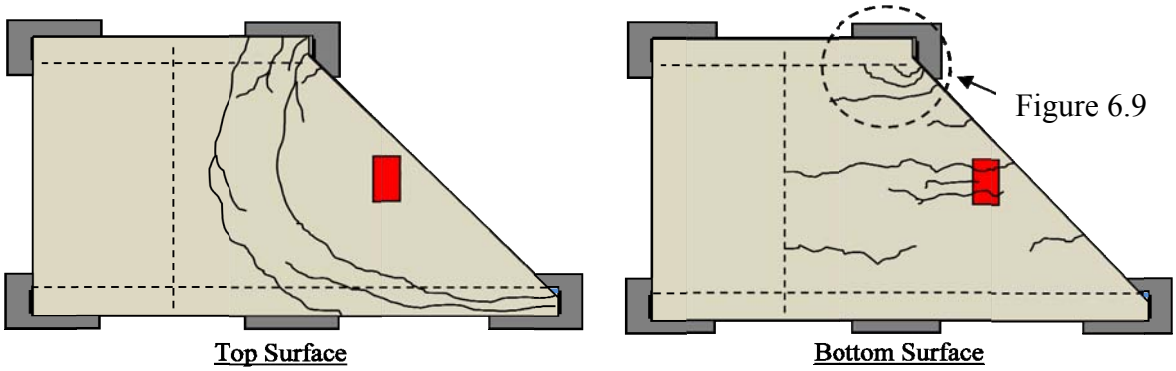

Figure 6.8: Observed Crack Pattern at Failure of Specimen 6

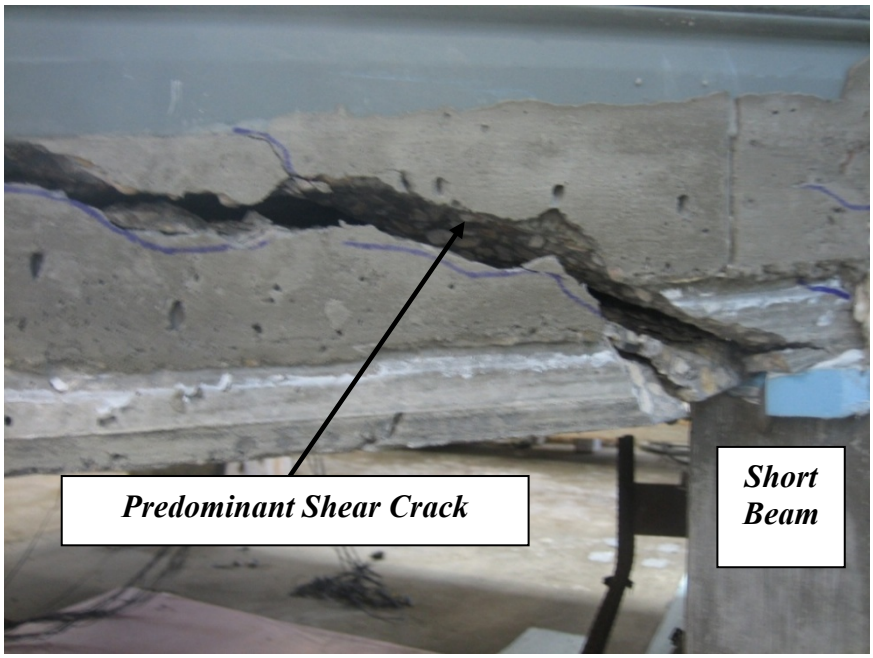

Figure 6.9: Shear Failure of Specimen 6 under Load at Midspan of Skewed End

Following the completion of the test at the expansion joint, load was applied at midspan of the square end of the trapezoidal panel. During this test, the specimen had to be unloaded and reloaded when load cell were changed. Thus, there are two curves in the load-displacement plot in Figure 6.10.

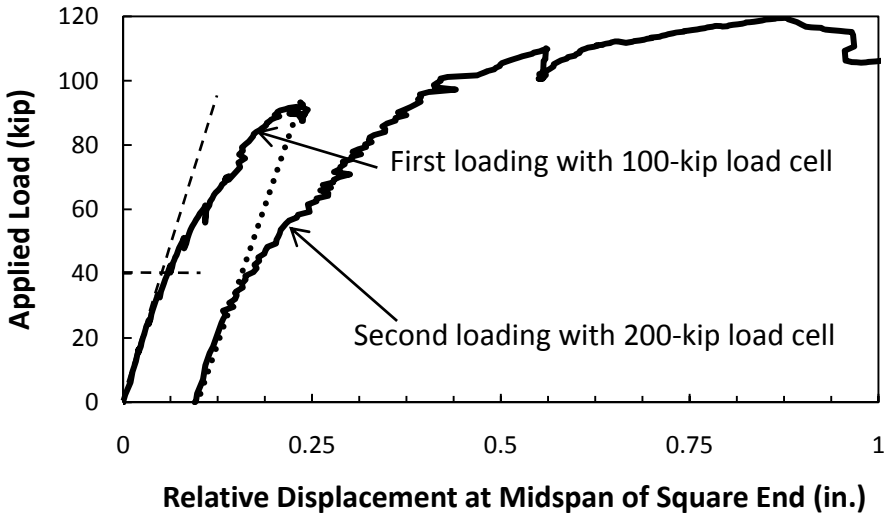

Figure 6.10: Displacement of Specimen 6 under Load at Midspan of Square End

Strains were measured on the deformed reinforcement place parallel to the straight end of the trapezoidal panel. The strains shown in Figure 6.11 indicate that at service wheel loads, the bars reached about 10% of yield.

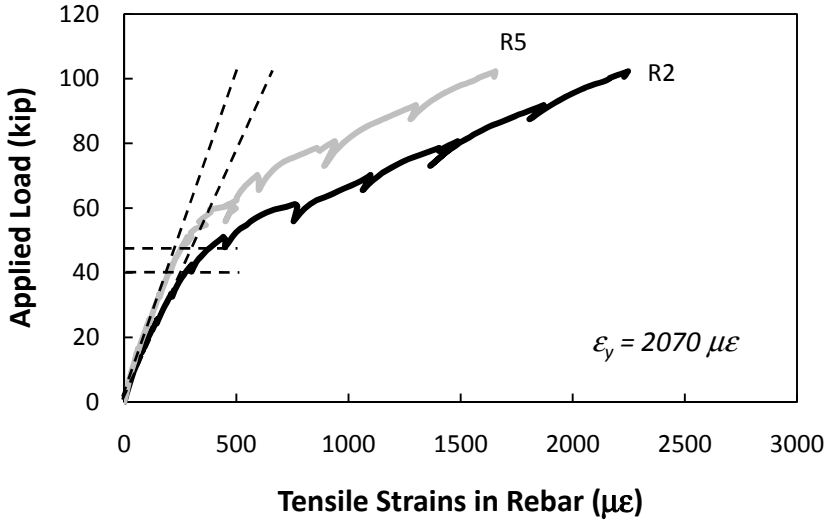

Figure 6.11: Tensile Strains in Deformed Bars along Straight End of Specimen 6 for Load at Midspan

It should be noted that the load plate was positioned 4 in. from the edge of the skewed panel to avoid the possibility that the load would be transferred directly to the adjacent rectangular panel. The displacements of the trapezoidal and rectangular panels were nearly identical as shown in Figure 6.12.

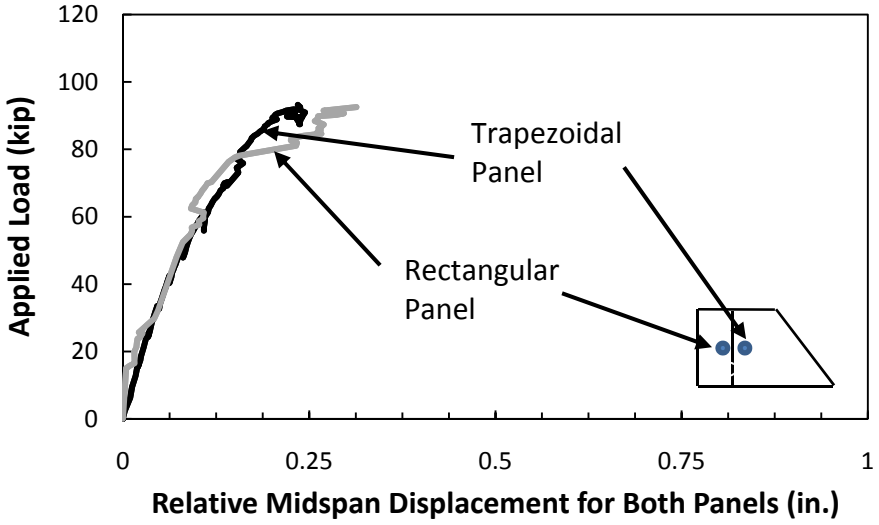

Figure 6.12: Displacements at Midspan of Trapezoidal and Rectangular Panels in Specimen 6 under Load at Midspan of Square End

Specimen 6 failed in punching shear at a load of 120 kip. Concrete on the bottom of the panel spalled off, exposing the bottom layer of reinforcement. Photographs of the failure (Figure

6.13) show the punching shear crack around the load plate on the top side of the specimen and spalled concrete on the bottom side.

Figure 6.13: Failure of Specimen 6 under Loading at Joint Between Panels

6.2.3 Response of Specimen 7 (45º Skew, Parallel Strands, Fatigue Loading)

Specimen 7 was subjected first to fatigue load applied at midspan of the skewed end of the trapezoidal panel. The specimen was subjected to four million loading cycles during the fatigue test. Subsequently, the specimen was loaded monotonically to failure.

During the fatigue test, the peak-to-peak amplitude of the applied load was 16 kip. In the first phase of the test, the specimen was subjected to two million loading cycles. The fatigue tested was stopped periodically—approximately every 250,000 cycles—to measure the static response of the specimen. No cracks were observed during the first phase of the fatigue test. After two million fatigue cycles, the specimen was loaded until flexural cracks formed. The maximum applied load was 43 kip and was considered to be representative of an overload. After cracking, the specimen was subjected to two million additional fatigue cycles. Periodic static tests were again conducted to detect changes in specimen stiffness. The complete load history for Specimen 7 is summarized in Table 6.3.

Table 6.3: Periodic Static Tests Conducted During Fatigue Test for Specimen 7

Type of Static Test	Accumulated Fatigue Cycles	Maximum Applied Load (kip)	Condition at Conclusion of Test
Initial	0	16	Uncracked
Periodic	250,000	16	
Periodic	500,000	16	
Periodic	850,000	16	
Periodic	1,100,000	16	
Periodic	1,400,000	16	
Periodic	1,700,000	16	
Periodic	2,000,000	16	
Overload	2,000,000	43	Cracked
Periodic	2,000,000	16	
Periodic	2,225,000	16	
Periodic	2,500,000	16	
Periodic	2,850,000	16	
Periodic	3,100,000	16	
Periodic	3,300,000	16	
Periodic	3,500,000	16	
Periodic	3,850,000	16	
Periodic	4,000,000	16	

The measured displacement response of Specimen 7 during selected periodic tests is presented in Figure 6.14. Cracking occurred at a load of approximately 32 kip. The overall stiffness of the test specimen did not change appreciably during the fatigue test.

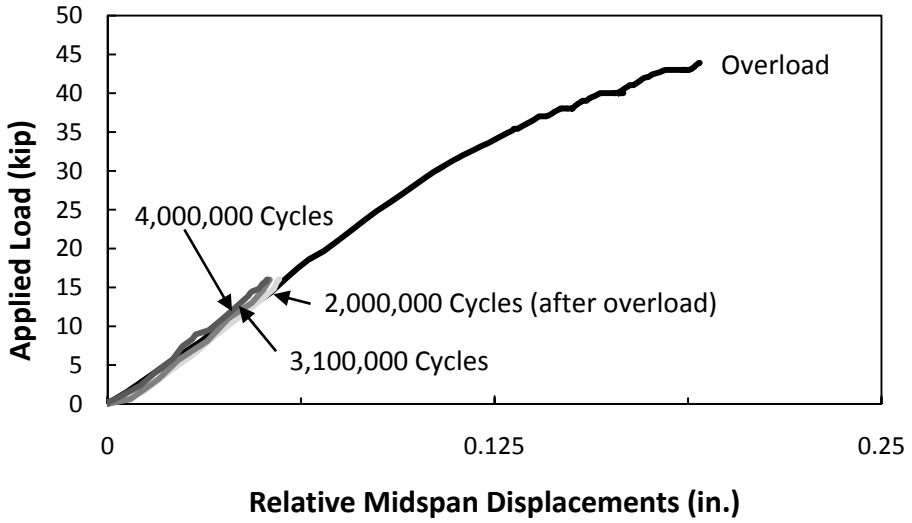

Figure 6.14: Displacement at Midspan of Skewed End for Specimen 7 during Periodic Static Tests

Variation of strain in the prestressing strands during the overload test from the loaded end towards the interior of the panel is shown in Figure 6.15. The largest changes in strain were observed directly beneath the load point and then quickly drop off as distance from the loaded end increases.

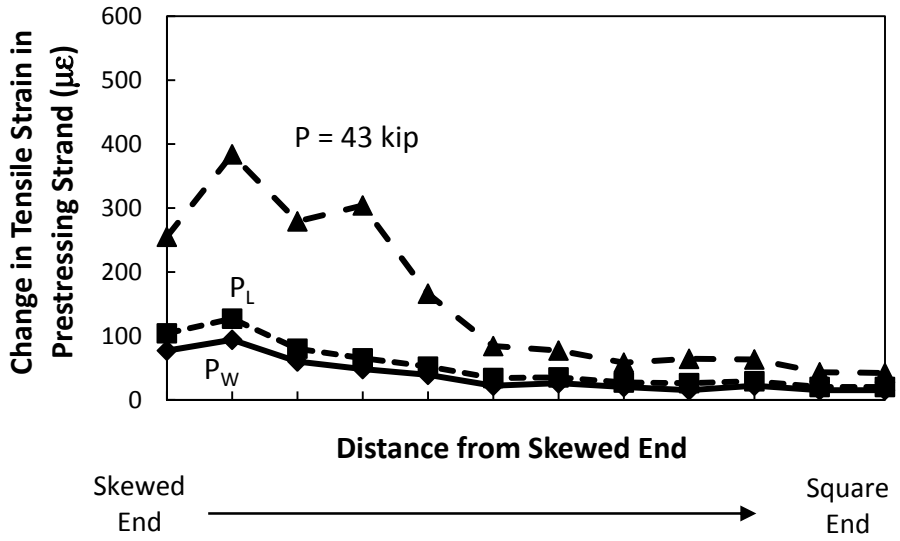

Figure 6.15: Variation of Measured Strain in Prestressing Strands in Specimen 7 during Static Overload Test

At the conclusion of the fatigue test, the few cracks that formed during the static overload test had not propagated and no delamination was observed between the precast panels and the topping slab. Specimen 7 was then loaded statically to failure. Displacements at midspan of the skewed end are plotted in Figure 6.16.

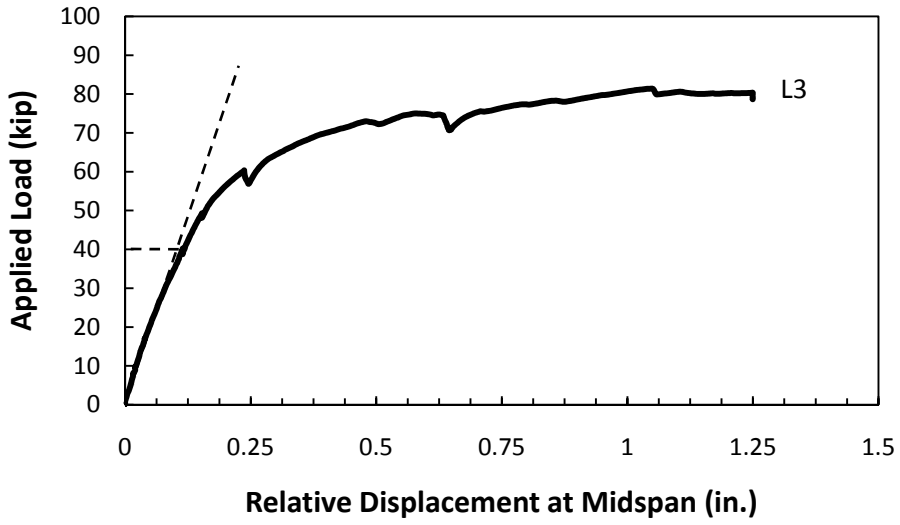

Figure 6.16: Displacement of Specimen 7 under Load at Midspan of Skewed End after Fatigue Test

Variation of the measured strains in the prestressing strand strain from the interior of the panel to the loaded end is presented in Figure 6.17. Strain changes are largest under the load point and drop off quickly as distance away from the loaded end increases.

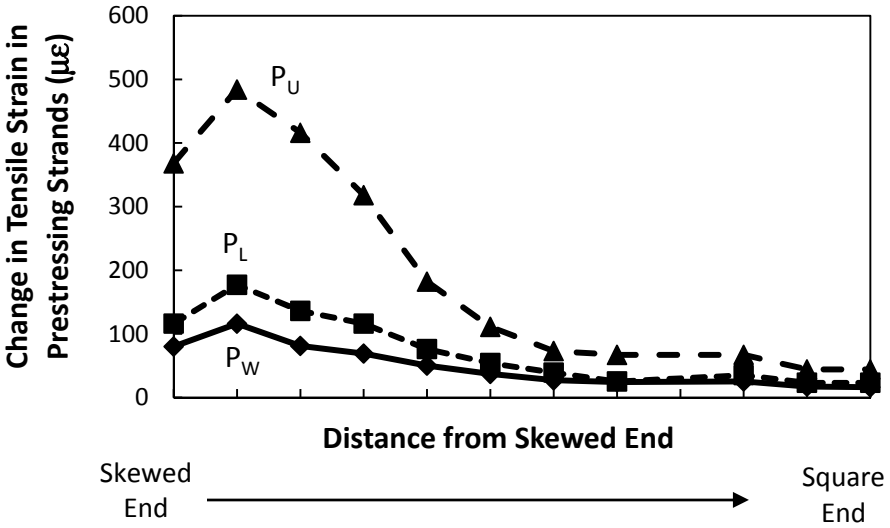

Figure 6.17: Variation of Measured Strain in Prestressing Strands under Load at Midspan of Skewed End for Specimen 7 after Fatigue Test

The specimen failed in shear. No delamination between the panel and topping slab was observed. The appearance of the specimen at after failure is shown in Figure 6.18.

Figure 6.18: Cracking of Specimen 7 at Failure

6.3 Measured Response of the 30-Degree Specimens

6.3.1 Specimen 8 and 9 (30º Skew, Parallel Strands, Smooth Surface)

Specimens 8 and 9 were first tested to failure with the load applied near midspan of the skewed end of the trapezoidal panel. Specimen 8 was subsequently loaded near midspan of the square end of the trapezoidal panel.

The measured displacement response of Specimen 8 at midspan of the skewed end is shown in Figure 6.19. The cracking load was about 32 kip, but the stiffness quickly decreased as load increased. As the load approached 50 kip, the panel delaminated from the topping slab. Only a few cracks were visible on the surface of the specimen. After delamination, the specimen was unable to carry a maximum applied load higher than 50 kip. It should also be noted that the surface of the precast panels was not wetted as required by TxDOT Standard Specifications. It is not known whether proper wetting would have prevented or delayed delamination of the topping slab.

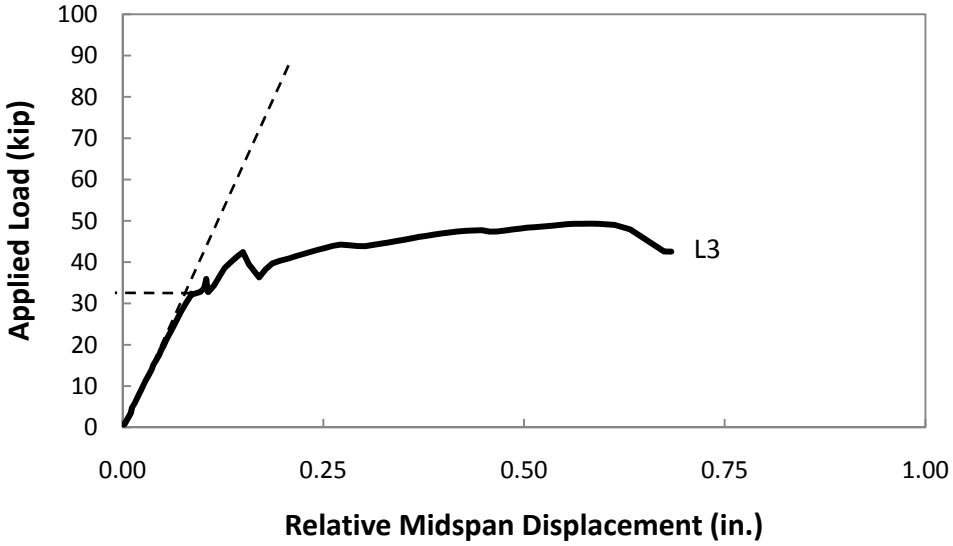

Figure 6.19: Displacement of Specimen 8 under Load at Midspan of Skewed End

The gap between the panel the topping slab due to the delamination is provided in Figure 6.20.

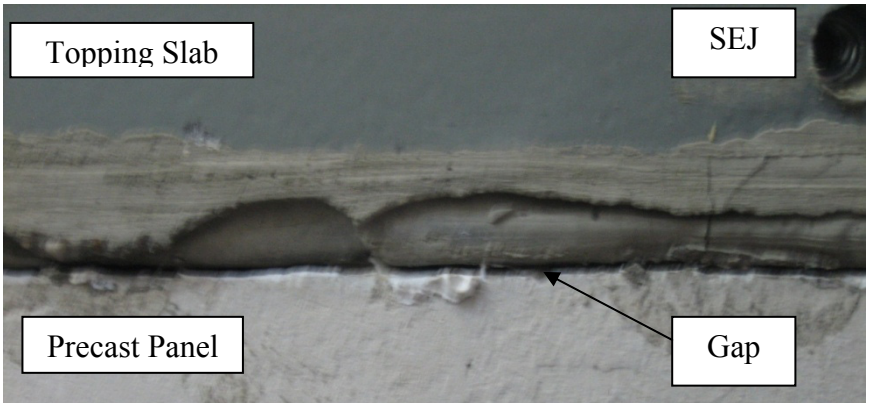

Figure 6.20: Gap Between Topping Slab and Precast Panel at Failure of Specimen 8

Testing of Specimen 9 duplicated that of Specimen 8. The performance was nearly identical to that of Specimen 8 and will not be repeated here.

Specimen 8 and 9 were loaded at midspan of the square end after failure of the skewed end. Displacement for Specimen 9 is plotted in Figure 6.21. The maximum applied load of 84 kip resulted in a midspan displacement of more than 1.5 in., which is approximately L/80 for a centerline beam spacing of 10 ft. The specimen failed due to punching shear. Figure 6.22 shows the punching shear cracks on the top surface of Specimen 8.

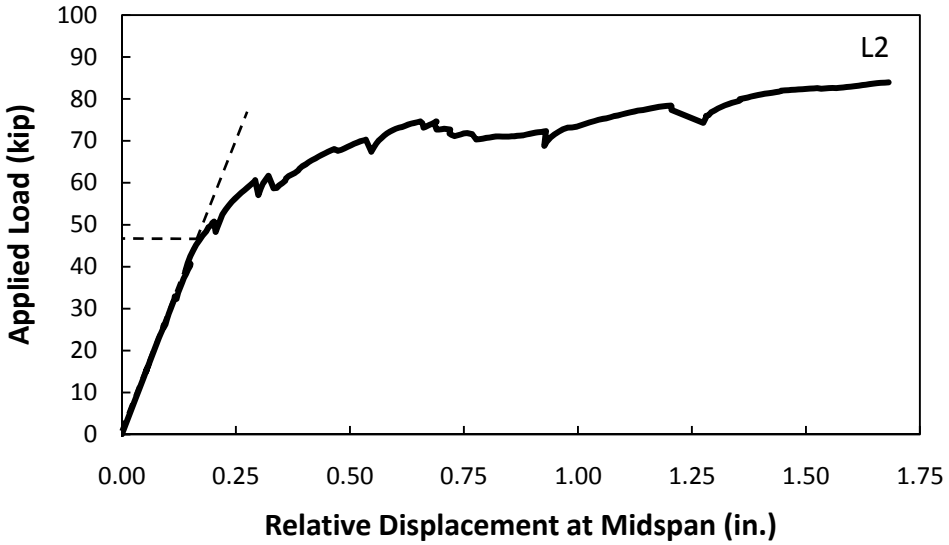

Figure 6.21: Displacement at Midspan of Square End of Specimen 8

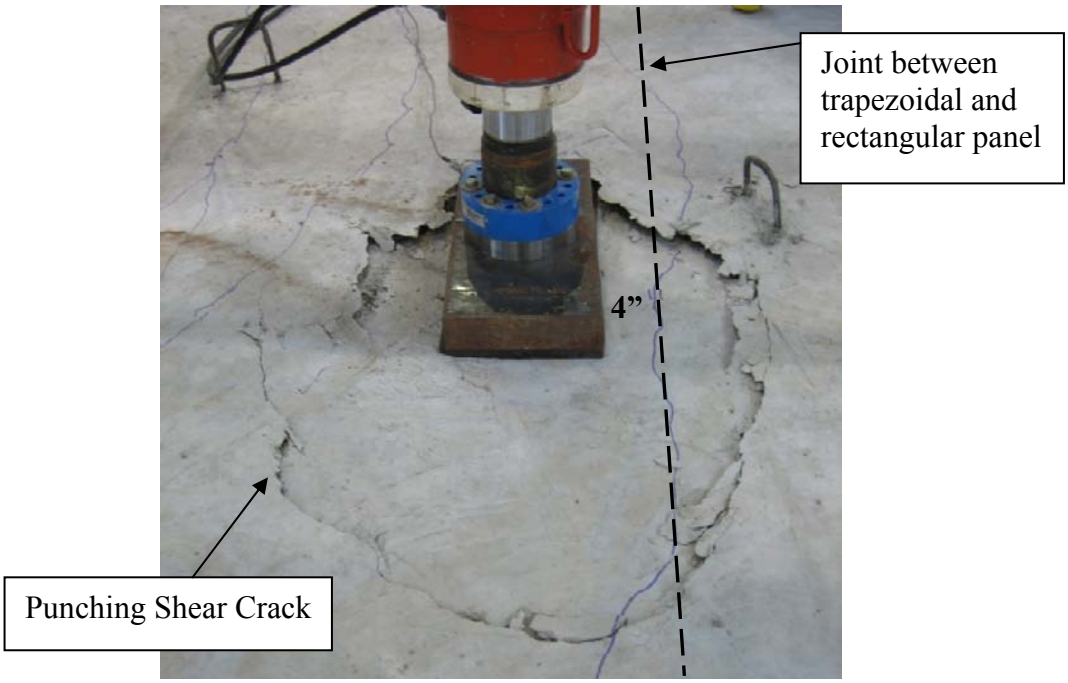

Figure 6.22: Punching Shear Failure of Specimen 8 under Load at Midspan of Square End

6.3.2 Specimen 10A and B (30º Skew, Parallel Strands, Rough Surface)

The construction of these Specimens 10A and B was similar to that of Specimens 8 and 9. The 30° PC panels had a rougher surface and the surfaces were wetted properly prior to casting the topping slab. No delamination was observed.

Specimen 10 was subjected to three different loadings to failure. During the first test (10A), load was applied at midspan of the SEJ along one skewed end of the specimen. In Test 10B, load was applied at midspan of the SEJ along the other skewed end of the specimen. In the third test, load was applied at midspan of the square end of the southern trapezoidal panel (10A end).

Test 10A Skewed End

The displacement at midspan of the skewed end is shown in Figure 6.23. The cracking load was approximately 20 kip and failure occurred at about 79 kip.

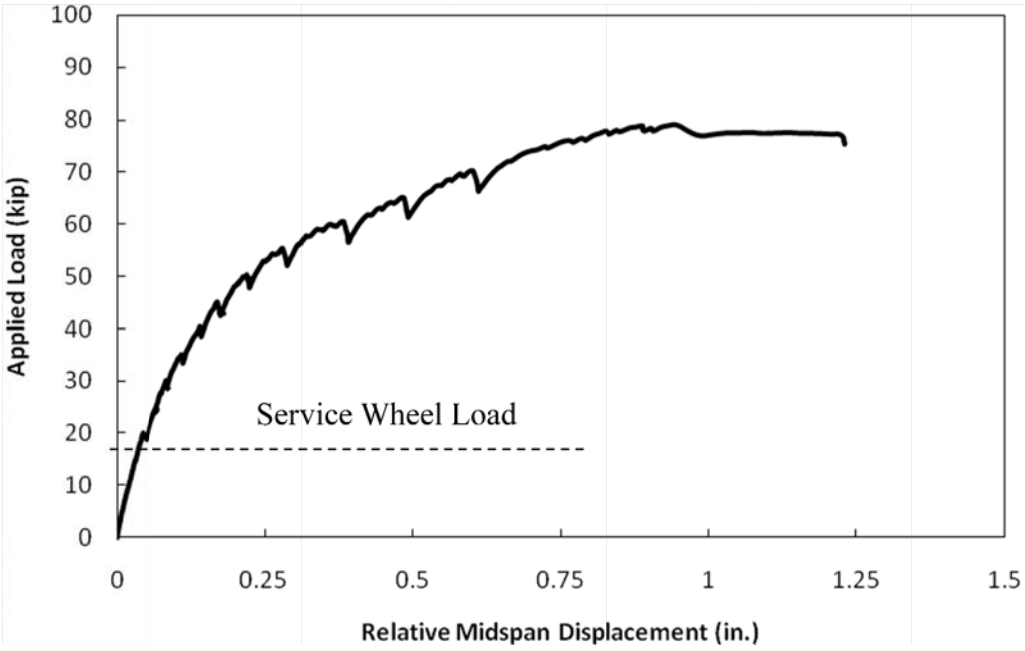

Figure 6.23: Displacement of Skewed End 10A under Load Applied at Midspan

Observed cracks in the specimen at the conclusion of the static test to failure are shown in Figure 6.24. A shear failure occurred at the short side support, and no delamination between the panel and topping slab was observed. Photographs of the specimen at the conclusion of the test are provided in Figures 6.25.

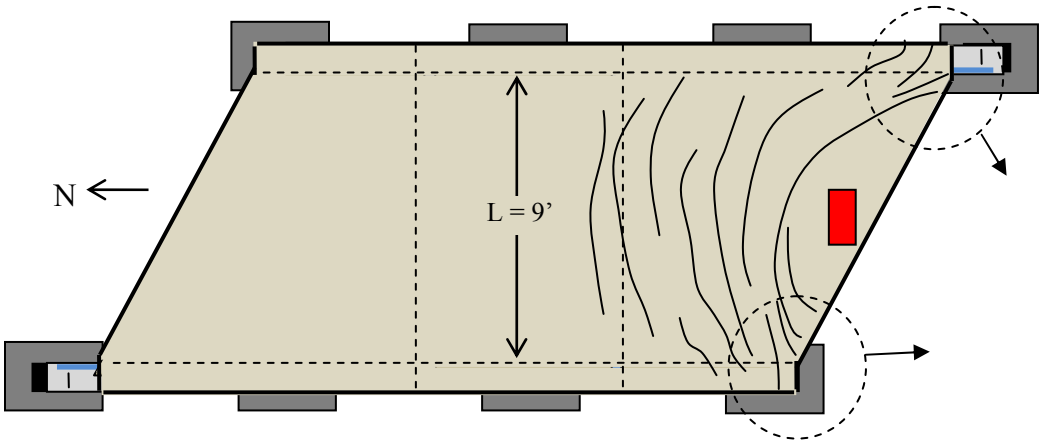

Top Surface

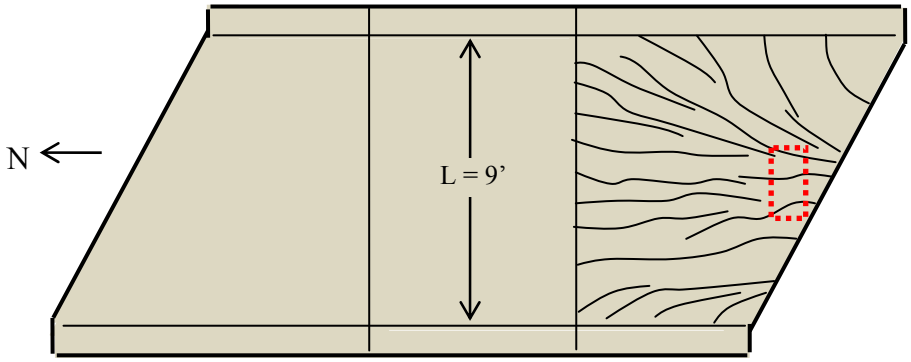

Bottom Surface

Figure 6.24: Cracking at Failure of Skewed End 10A under Load at Midspan

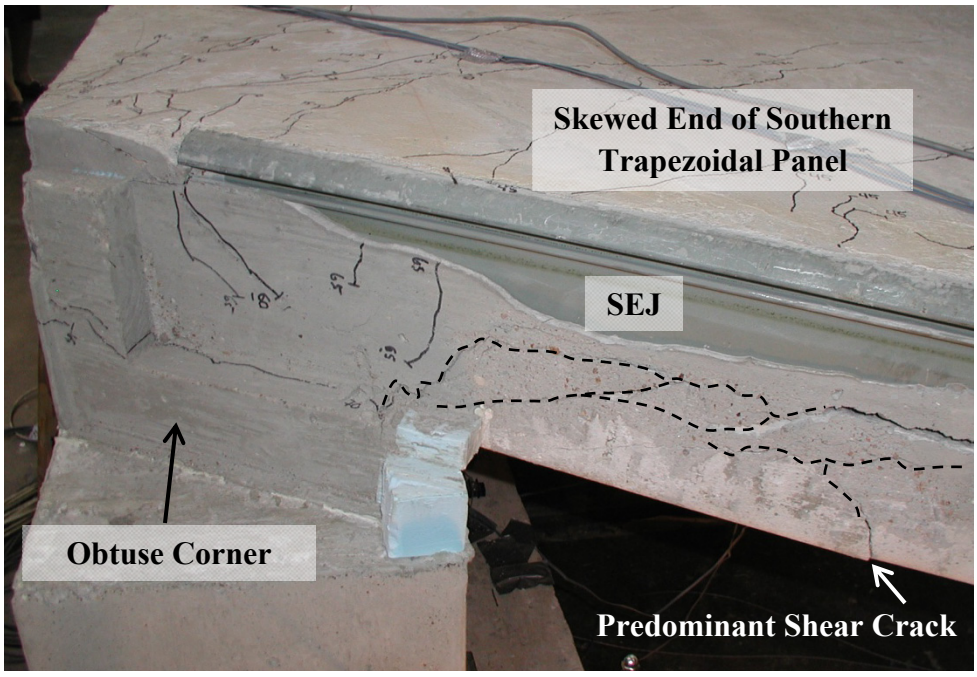

Figure 6.25: Cracking at Failure of Skewed End 10A

Test 10B Skewed End

The performance of skewed end 10B was nearly identical to that of 10A. Therefore, the deflections and crack patterns and appearance at failure will not be repeated here.

Test 10A Joint between Skewed and Rectangular Panels

The joint between the rectangular panel and the panel with edge 10A was loaded at midspan of the square end after the two skewed ends of the specimen had been tested. Measured relative displacements at midspan of the rectangular and trapezoidal panels are plotted in Figure 6.26. The specimen failed due to punching shear in the topping slab at a load of approximately 115 kip, although the linear potentiometers were removed at around 70 kip to avoid damaging them.

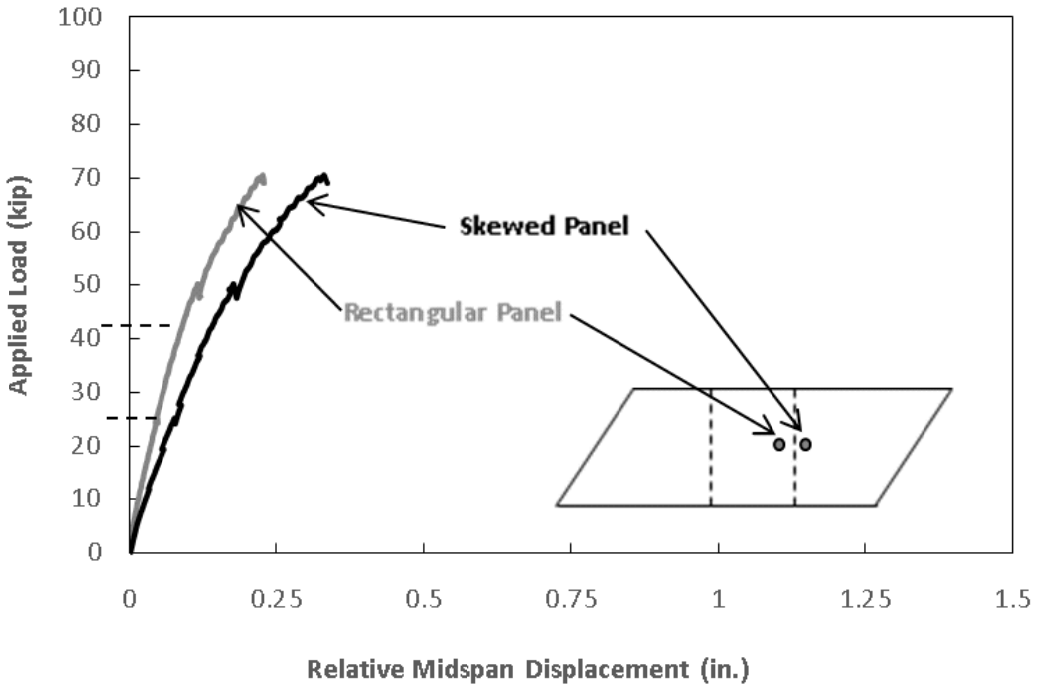

Figure 6.26: Displacement at Midspan of Square End of Specimen 10A

The specimen failed in punching shear as shown in Figure 6.27. Figure 6.28 shows the concrete that spalled off of the bottom of the rectangular panel at failure.

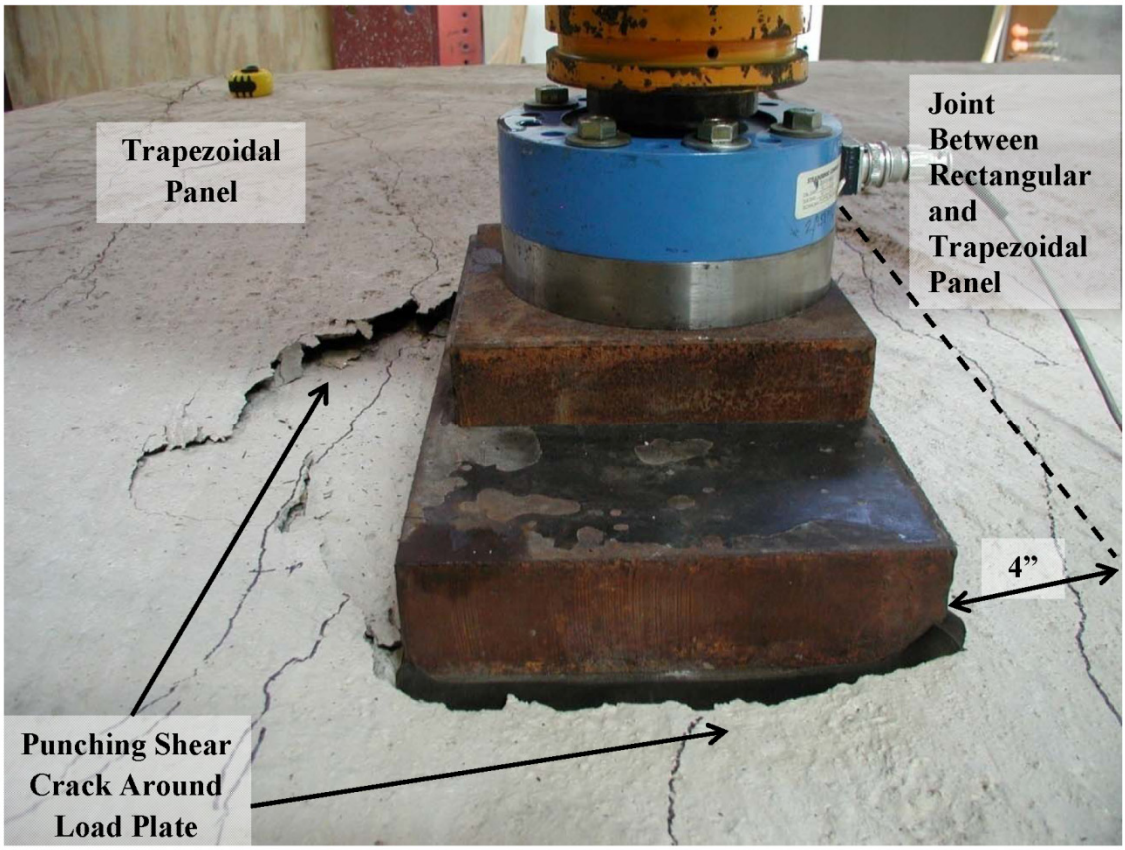

Figure 6.27: Punching Shear Failure for at Joint Between Panels

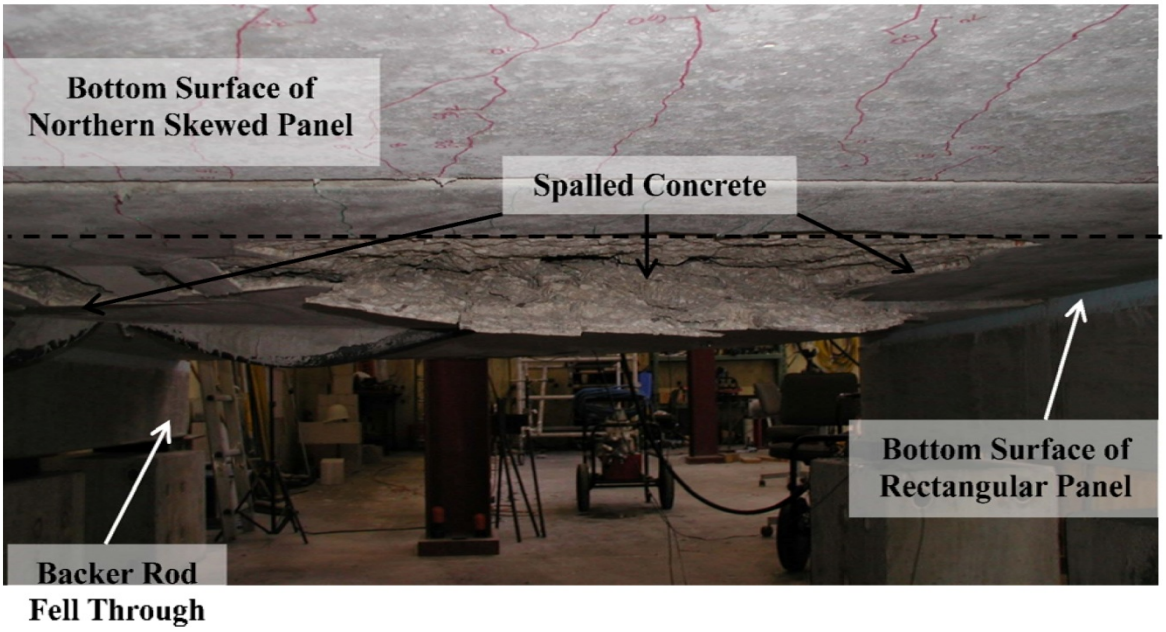

Figure 6.28: Photograph of Spalled Concrete at Conclusion of Test of Specimen 10A for Load Applied at Midspan of Square End

6.4 Discussion of Results

6.4.1 Load Applied Along Skewed End

The three 45° specimens exhibited similar response to loads applied at midspan of the skewed end. The load-displacement plots for the 45° specimens are shown in Figure 6.29. Significant observations from the tests of the 45° specimens are listed below:

- Deflections at midspan of skewed end under the Design Wheel Load (P_L) were approximately 1/16 in., which corresponds to approximately L/2400 for a 9-ft clear span between girder flanges.
- Maximum applied loads were approximately 4 times the Design Wheel Load, P_L.
- The arrangement of the prestressing strands within the precast panel did not influence the strength or initial stiffness of the test specimens. Specimen 5 with fanned strands behaved essentially the same as the Specimens 6 and 7 with prestressing strands parallel to the skewed end of the panel.
- Fatigue loading of Specimen 7 did not significantly influence the stiffness of the specimen for load applied at midspan of the skewed end.

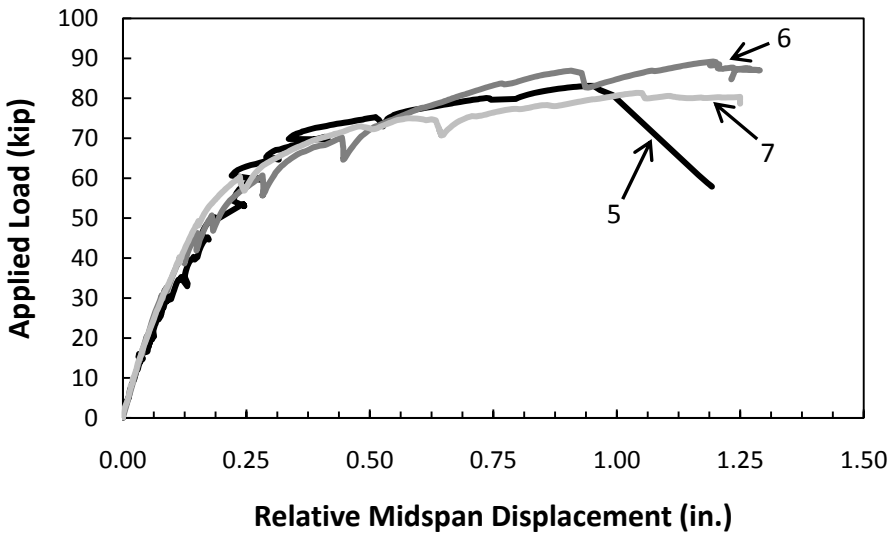

Figure 6.29: Displacement Response of 45° Specimens under Load at Midspan of Skewed End

The response of the 45° specimens is compared with the 0° specimens subjected to positive moment in Figure 6.30. The 0° specimens (1 and 2) achieved slightly higher loads and slightly larger displacements at failure; however, the overall response was essentially the same.

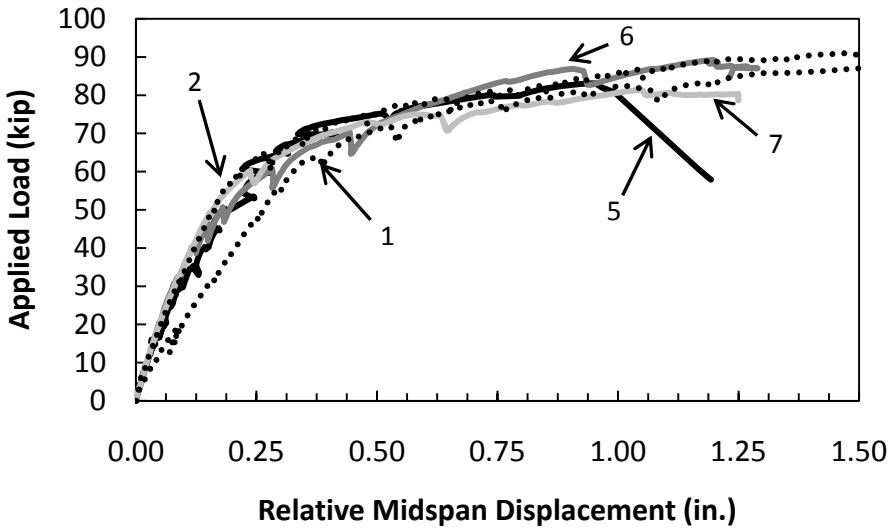

Figure 6.30: Comparison of Displacement Response of 0° and 45° Specimens

The behavior of the 30° specimens under loads applied at midspan of the skewed end was markedly different depending on the surface roughness of the panels and wetting the surface of the panel prior to casting the topping slab. The load-displacement response for the 30° specimens is provided in Figure 6.31.

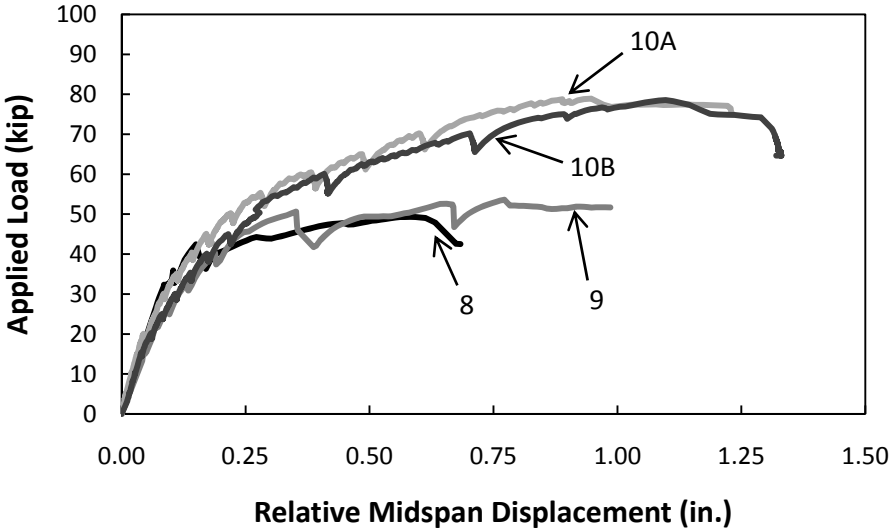

Figure 6.31: Displacement of 30° Specimens for Load at Midspan of Skewed End

Significant points from the skewed end behavior of the 30° specimens are listed below:

- The capacity of the 30° specimens was limited by the delamination of the panels from the cast-in-place topping slabs. Maximum applied loads were

approximately 2.5 times the Design Wheel Load, P_L for panels with a smooth, unwetted surface (Specimens 8 and 9) and about 4 times for the panels with rough, wetted surfaces (Specimens 10A and 10B).

- Deflections at midspan of skewed end under the Design Wheel Load (P_L) were approximately 1/16 in, which corresponds to L/2000 for a 9-ft. clear span between girder flanges.

The response of the 30° specimens is compared with the 45° specimens in Figure 6.32. The initial stiffness of all the specimens is comparable; however, the strength of the 30° specimens with smooth panels (Specimens 8 and 9) was considerably less than the strength of the 45° specimens because of the delamination of those panels from the cast-in-place topping.

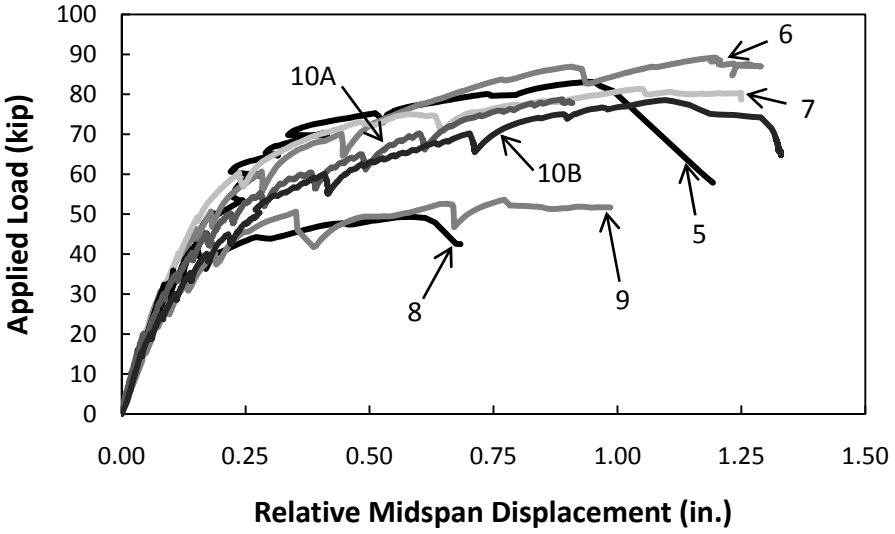

Figure 6.32: Comparison of Measured Displacement Response of 30° and 45° Specimens

The response of the 30° specimens is compared with the 0° specimens in Figure 6.33. Again, the differences in the strength due to the panels with smooth, unwetted surface are apparent.

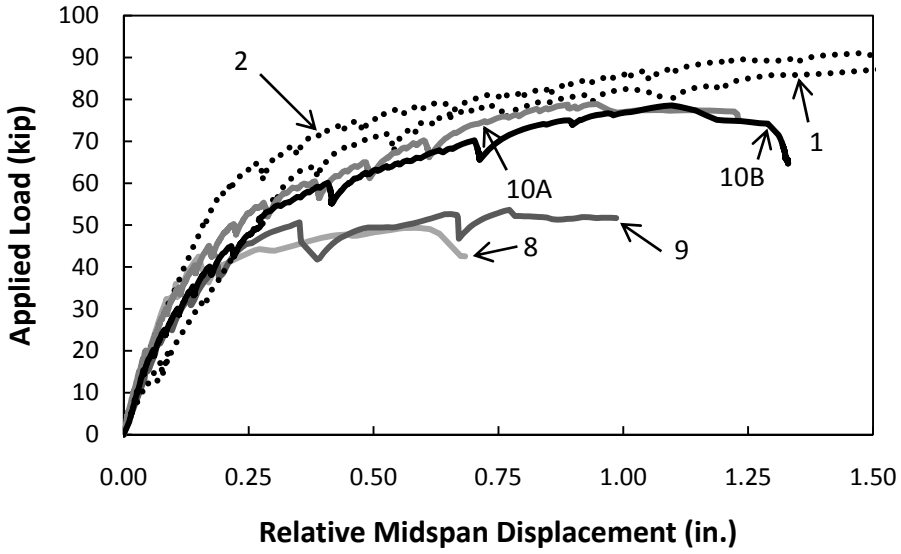

Figure 6.33: Comparison of Displacement Response of 30^o and 0^o Specimens

6.4.2 Load Applied at Joint between Panels

Four of the five skewed specimens were loaded at the joint between panels midspan (on the trapezoidal panel) after they had been loaded to failure at the skewed end. The displacement response of those specimens is plotted in Figure 6.34.

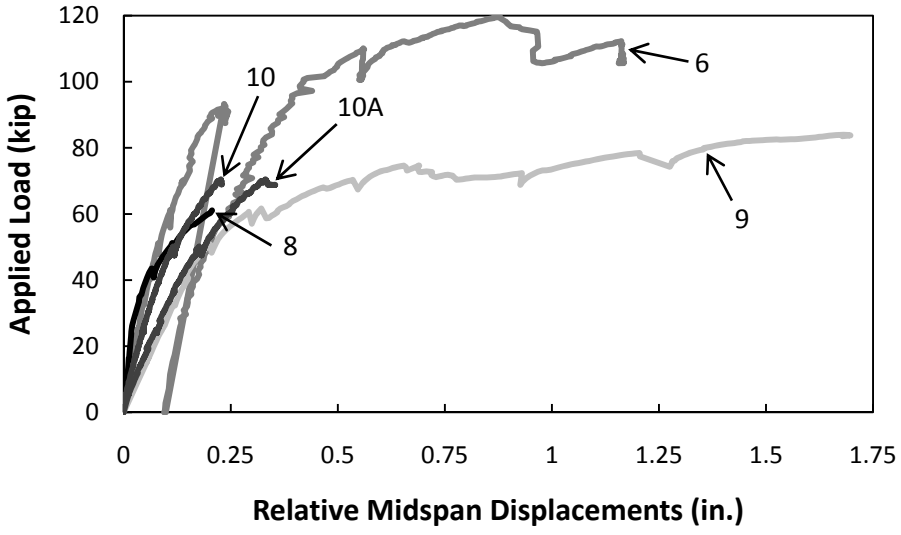

Figure 6.34: Displacement Response of Specimens Loaded at Joint between Panels

Important observations from these tests are summarized below:

- The test results were less consistent when the load was applied along the square end of the trapezoidal panel than the skewed end. This difference is

likely due to the level of damage induced during previous tests along the skewed end and resulted in lower failure loads in Specimens 8 and 9.

- In spite of the damage induced in the earlier tests, the maximum applied load at midspan of the square end always exceeded the maximum applied load at midspan of the skewed end.
- The maximum applied load along the square end was always limited by a punching shear failure.
- The non-prestressed corner of the skewed panels (with strands running parallel to the skewed end) did not limit of the punching shear strength of the specimens.

Chapter 7. Summary and Conclusions

7.1 Summary

Over the past eight years, the Texas Department of Transportation has funded two investigations regarding the use of precast concrete panels as stay-in-place formwork adjacent to expansion joints in bridge deck construction. Prestressed concrete panels have been used by the bridge construction industry in the state of Texas for many years to increase speed and improve safety and economy. The panels serve as stay-in-place formwork and become a part of a composite deck after a topping slab is cast. At expansion joint locations, however, TxDOT currently uses the IBTS detail rather than prestressed panels. This cast-in-place detail requires temporary formwork and slows construction processes. In TxDOT Project 0-4418, reconstructed three full-scale bridge decks were constructed. One of the specimens included precast panels at a 0^o skew and the results indicated that the precast panel system provided adequate strength and reduced construction costs compared with the traditional cast-in-place details at the expansion joint. As a result, prestressed panels have been used at the expansion joints of a few 0^o skew bridge decks using a new detail developed under Project 0-4418. In this investigation (TxDOT Project 0-5367) two areas that were not covered in Project 0-4418 were studied: fatigue performance of bridge decks using precast panels at the expansion joints and the use of precast panels at skewed expansion joints.

In the first phase of the investigation reported here, the fatigue response of precast panels was evaluated at the expansion joint in 0^o skew bridges. In the second phase, the response of skewed precast panels at expansion joints was tested under static and fatigue loads. Two skew angles were tested: 30^o and 45^o. Six specimens were constructed and subjected to a total of eleven tests. Loads were applied at midspan of the skewed end of each specimen, and some specimens were also tested at midspan of the square end of the trapezoidal panels.

7.2 Conclusions

7.2.1 Phase 1: Fatigue Tests

The PC panels for 0° and 45° skew bridge decks exhibited excellent fatigue response. The specific responses are summarized below.

- Service-Level Fatigue Behavior
  - The overall system response (load vs. deflection) and the measured strain response remained linear throughout the fatigue test and did not change appreciably with increasing fatigue cycles.
  - The stiffness of specimens was lower after being subjected to static overload, but the fatigue response did not change appreciably with increasing fatigue cycles.
  - No delamination or deterioration was observed along the interface of the PC panel and the CIP slab during the fatigue tests.
- Design-Level Fatigue Behavior
  - The overall system response (load vs. deflection) and the measured strain responses remained linear throughout the fatigue tests, and did not change appreciably with increasing fatigue cycles.

- The stiffness of specimen reduced after the static overload test (three times the design wheel load), but the fatigue response did not change appreciably with increasing fatigue cycles.

7.2.2 Phase 2: Skewed Precast Panels

Constructibility issues

The experiences gained from production of the trapezoidal panels and the construction of full-scale test specimens provided valuable information regarding the implementation of skewed precast panels. Constructibility issues were also discussed with bridge designers, fabricators and contractors at the start of the project. The following conclusions can be drawn regarding the practicality and constructibility of trapezoidal prestressed panels.

- Fanned Prestressing Pattern
  - Trapezoidal panels using a fanned prestressing pattern cannot be mass produced on a long-line casting bed.
  - Custom formwork is required for any change in panel geometry.
  - The spacing of prestressing strands will be different for each combination of skew angle and panel width and will require casting beds to be capable of shifting bearing locations to accommodate variations in strand spacing. Moreover, since each strand layout is unique to the panel geometry, standard drawings cannot be developed.
  - Non-parallel prestressing strands create difficult bearing conditions because each strand exits the edge at a different angle. On the short edge of the panel, strands converge after exiting the edge of the panel and create congestion of the anchorages.
  - In the laboratory, no cracking was observed in highly stressed regions after strand release at the TxDOT specified release strength for panels with concrete strength of 4,000 psi despite lack of bursting reinforcement.
- Parallel Prestressing Pattern
  - Trapezoidal panels using a parallel prestressing strand pattern can be mass produced on a long-line casting bed. However, panels with large widths and skew angles would require casting beds wider than the 8 ft. standard.
  - Custom formwork is required for any change in panel geometry.
  - Standard bulkheads could be used since strand spacing remains constant for all panel geometries.
  - Standard spacing of prestressing strands parallel to the skewed end allows implementation with any skew angle.
  - Due to lack of required development length, some strands may require de-bonding or omission, which creates a region with partially prestressed concrete.
  - Placing reinforcing bars beneath the prestressing strands to provide moment capacity where strands are debonded or omitted is simple and requires minimal time during panel fabrication.

- In the laboratory, no cracking was observed at interface of prestressed and non-prestressed regions where strands were de-bonded or omitted.

- Construction
  - Setting trapezoidal panels on support beams and aligning the skewed end is not difficult.
  - Compression of the bedding strip under high bearing pressures is not a concern to TxDOT engineers as long as minimum clearance requirements are met. However, the compression capacity of bedding strips should be carefully considered for the short dimension of the panel.
  - The expansion joint armor is supported on the girders; therefore, removal of conventional formwork does not affect the placement of the armor.
  - Minimal formwork would still be required at the ends of the girders and between the expansion joint armor and precast panel.
  - Panel fit-up errors require a standard solution. Potential solutions include permitting gaps between panels that are filled with backer rods or custom cutting panels on site with a concrete saw.

It was demonstrated that producing trapezoidal prestressed panels can be economical while accommodating a wide range of geometries. Due to the complexity of the fanned prestressing bearings, the variability of strand spacing, and the inability to use a long-line casting bed, the parallel prestressing pattern is the suggested design alternative. The parallel prestressing strand pattern allows concurrent fabrication techniques and procedures to be utilized thereby maintaining the efficiency of the precast industry.

It was also shown that trapezoidal prestressed panels can be used as stay-in-place formwork at skewed expansion joints. Compression of the bedding strip was deemed acceptable when using a 9 ft. 6 in. wide panel with a 45 in. short edge length and 60 psi bedding strip.

Performance of Skewed Panels

From the research results, it was shown that trapezoidal precast panels used as stay-in-place formwork adjacent to expansion joints in bridge decks provide sufficient strength and stiffness for current design loads. Important observations from this investigation are summarized below:

- General Observations
  - The orientation (fanned or parallel) of the strands in the precast panel did not influence the strength or stiffness of the test specimens.
  - Even though the length of the free end of skewed panels is greater than that of rectangular panels, the skewed panels exhibited similar strength and stiffness to rectangular panels when the surface roughness was sufficient and the panel surface was wetted to prevent delamination of the panel from the topping slab.

- Response of Specimens for Load Applied at Midspan of Skewed End
  - Test specimens with a 45^{o} skew angle exhibited maximum load carrying capacities 4 times greater than the 21.3-kip Design Wheel Load for the HL-93 Design Truck, and they failed in diagonal shear at the short side support.

- The overall system response remained linear throughout the duration of the fatigue loading at service level loads, and no delamination or reduction of stiffness was observed with increasing fatigue loading.
- Fatigue loading did not significantly affect overall system stiffness or the maximum load carrying capacity for the specimens compared to specimens with no previous load history.
- In two tests of 30^o panels, the topping slab delaminated from the panels. Because of the delamination, the maximum load carrying capacities were only 2.5 times greater than the Design Wheel Load. Panel surface roughness and lack of pre-wetting of the surface prior to placement of the topping slab were likely causes of panel delamination. When the same tests were repeated with two 30^o specimen that had panels with a rough surface and were pre-wetted, maximum applied loads were 3.7 times the Design Wheel Load, a strength that better correlates with the 45^o specimens.
- All specimens loaded at midspan of the square end failed in punching shear.

- Response of Specimens for Load Applied at Midspan of Joint Between Skewed and Rectangular Panels

  In addition to loading at the skewed edge, loading was applied at joint between the skewed and rectangular panels. At that joint, parallel strands in the skewed panels did not provide a load path to the girders and ordinary deformed reinforcement was added to provide a load path. Therefore, it was important to assess the performance of the panel with load applied at the joint.
  - The test specimens loaded at midspan of the joint between the skewed and rectangular panels exhibited higher load carrying capacities than when loaded at the skewed end. The maximum load carrying capacity was reached when punching shear failure occurred.
  - The non-prestressed corner of the skewed panels (with strands running parallel to the skewed end) did not reduce the punching shear strength limit of the specimens for load applied at midspan of the joint between the skewed and rectangular panels.

Appendix A: Design Recommendations

The results of this research project demonstrate that precast concrete (PC) panels can be used adjacent to expansion joints in bridges with skew angles between 0° and 45° without compromising the strength or fatigue performance of the bridge deck. Recommendations for the design of skewed panels are summarized in this appendix. Limits on the geometry of the panels are discussed in Section A.1. Recommended reinforcement is presented in Section A.2. Issues related to construction of the PC panels and of the composite bridge deck are summarized in Section A.3 and Section A.4, respectively. Throughout this appendix, the geometry of the panels will be described using the terms shown in Figure A.1.

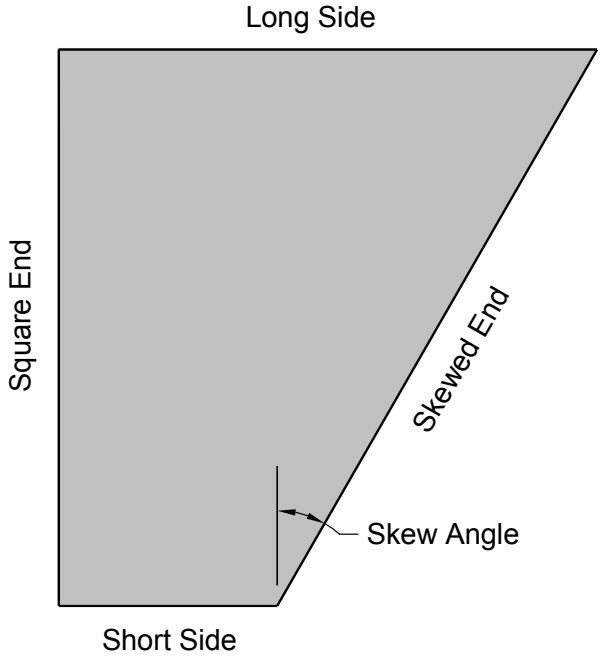

Figure A.1 Terminology Used to Define Geometry of Skewed PC Panels

A.1 Geometric Limits

The length of the short side of the precast trapezoidal panels should be at least 3'-9". This dimension was selected to ensure a reasonable bearing length for the PC panel during construction of the bridge deck. The length of the square end of the precast trapezoidal panels should not exceed 9'-6", which corresponds to a centerline girder spacing of 10'-0" for traditional, I-shaped, prestressed concrete girders. All trapezoidal panels tested as part of this investigation satisfied these geometric limits.

The dimensions of trapezoidal panels with a short size equal to 3'-9" and a square end length equal to 9'-6" are shown in Figure A.2, Figure A.3, and Figure A.4, for skew angles of 45°, 30°, and 15° respectively. The length of the long side varies depending on the skew angle.

Dimensions of the skewed panels are summarized in Table A.1 for girder spacing of eight or ten feet.

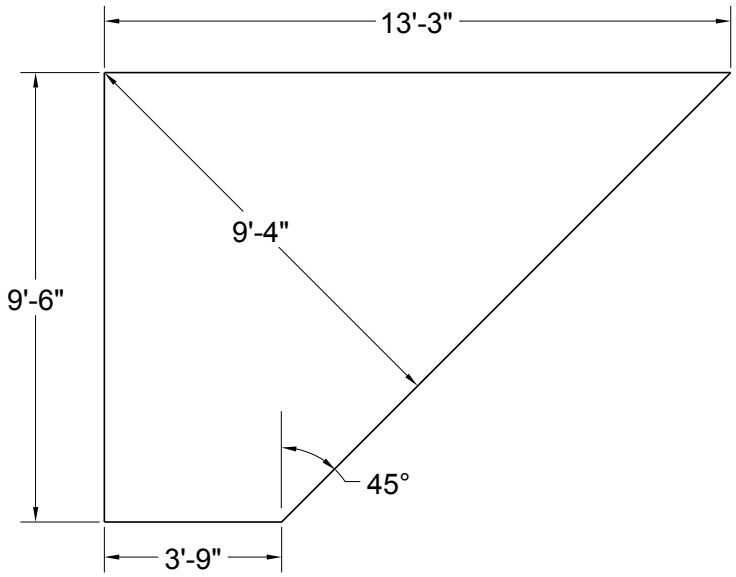

Figure A.2 Dimensions of PC Panel with 45° Skew

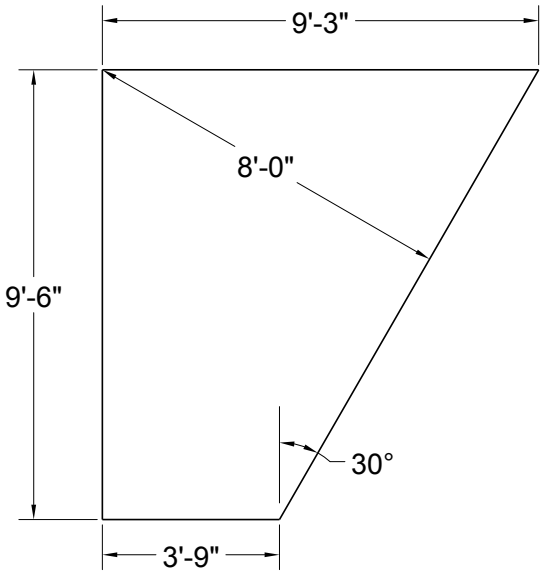

Figure A.3 Dimensions of PC Panel with 30° Skew

Table A.1 Geometry of Skewed Precast Panels

Skew Angle	Short Side (Min)	Length of Square End = 9'-6" Girder Spacing = 10'-0"		Length of Square End = 7'-6" Girder Spacing = 8'-0"	
		Long Side	Required Width of Prestressing Bed	Long Side	Required Width of Prestressing Bed
45°	3'-9"	13'-3"	9'-4"	11'-3"	7'-11"
30°	3'-9"	9'-3"	8'-0"	8'-1"	7'-0"
15°	3'-9"	6'-4"	6'-1"	5'-9"	5'-7"

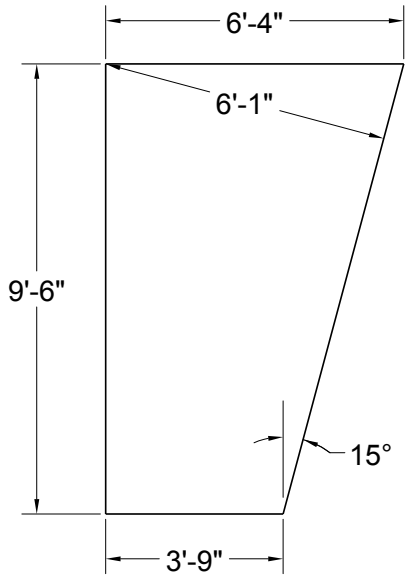

Figure A.4 Dimensions of PC Panel with 15° Skew

The corresponding layouts of the formwork for skewed panels with square end lengths of 9'-6" on a casting bed are shown in Figure A.5. Panels with skew angles of 15° and 30° can be accommodated within a standard 8-ft prestressing bed. A wider bed will be required to construct panels with a skew angle of 45°. However, if the length of the square end is reduced to 7'-6", the 45° panels can also be constructed using a standard 8-ft prestressing bed.

A.2 Recommended Reinforcement

A.2.1 Prestressing Strand

The recommended configuration of the trapezoidal PC panels includes ⅜-in. prestressing strand at mid-depth of the panel. The strands are oriented parallel to the skewed end of the panel and spaced at 6 in. on center. Strands with an embedded length less than 48 in. should be debonded because the embedded length is less than two times the transfer length of the strand. The layouts of the strands for panels with skew angles of 45°, 30°, and 15° are shown in Figure A.6, Figure A.7, and Figure A.8, respectively.

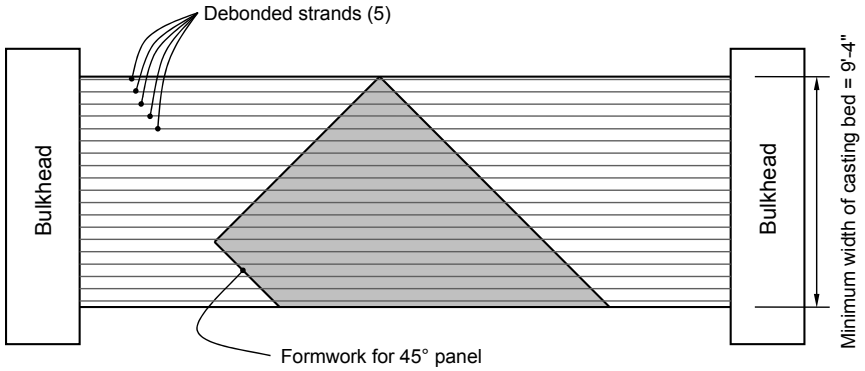

(a) 45° Skew

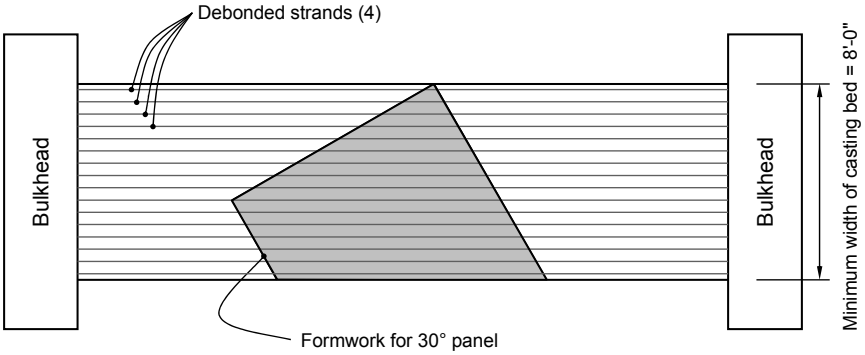

(b) 30° Skew

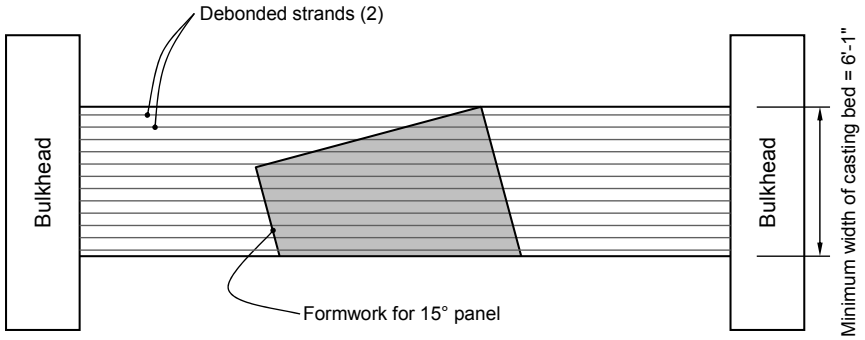

(c) 15° Skew

Figure A.5 Configuration of Skewed PC Panels with a Square End Length of 9'-6" within Casting Bed

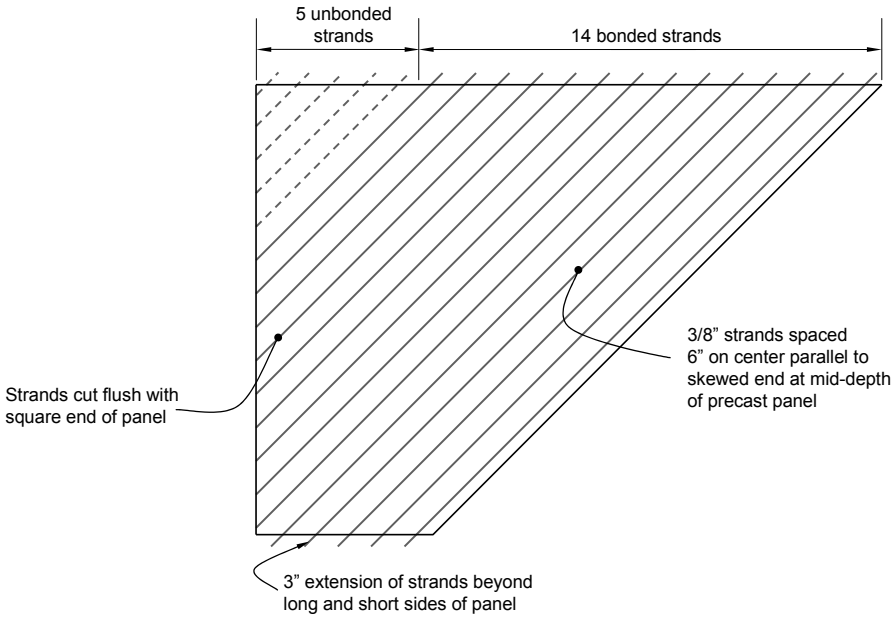

Figure A.6 Layout of Prestressing Strands in PC Panel with 45° Skew

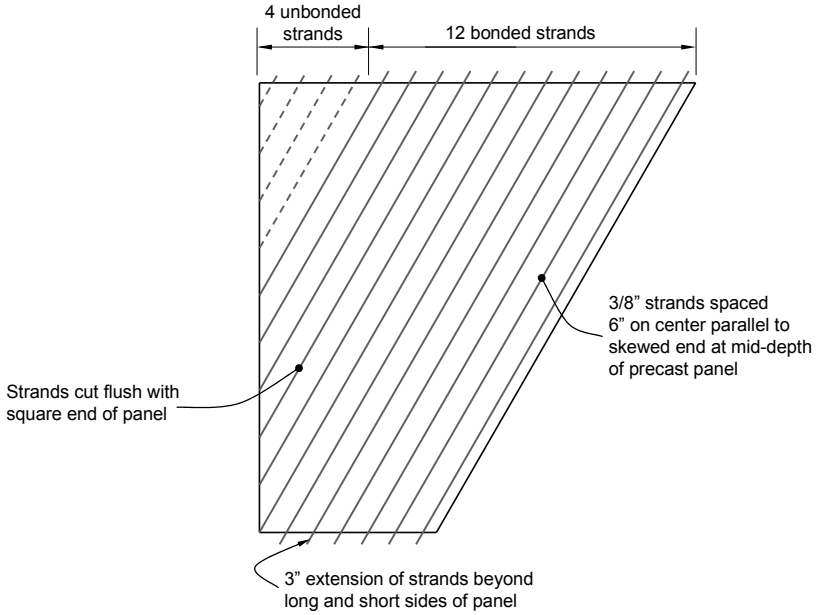

Figure A.7 Layout of Prestressing Strands in PC Panel with 30° Skew

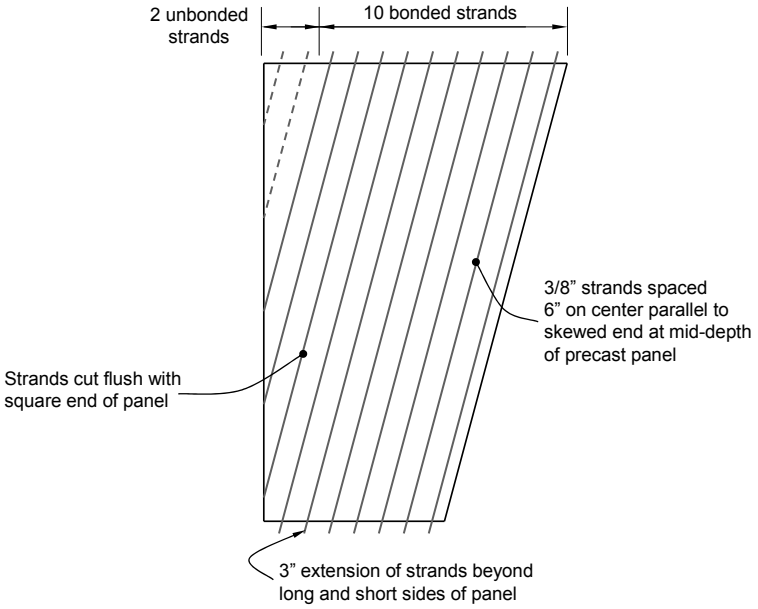

Figure A.8 Layout of Prestressing Strands in PC Panel with 15° Skew

A.2.2 Deformed Reinforcement

Trapezoidal PC panels also include two layers of deformed reinforcement. Number 4 bars should be placed immediately below the strands and oriented parallel to the square end of the panel. These bars are needed to provide a force path for loads along square edge where strands are debonded or where the bonded strands do not extend to the supported sides of the PC panel. The #4 bars are spaced at 4 in. on center. For the larger skew angles (Figure A.9 and Figure A.10), the bars are distributed over the length of the short side of the panel. For the 15° skew, fewer bars are required (Figure A.11).

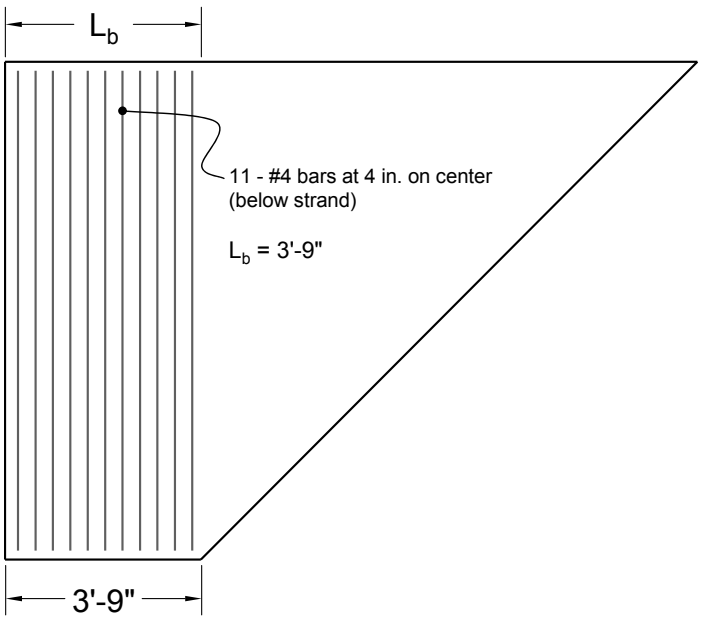

Figure A.9 Layout of #4 Deformed Bars in PC Panel with 45° Skew

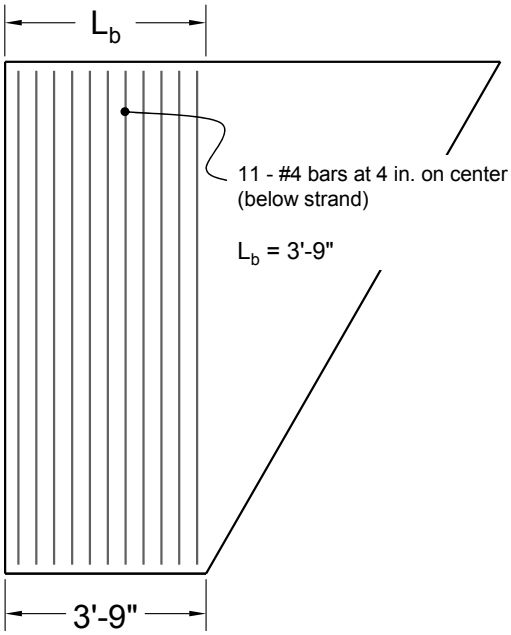

Figure A.10 Layout of #4 Deformed Bars in PC Panel with 30° Skew

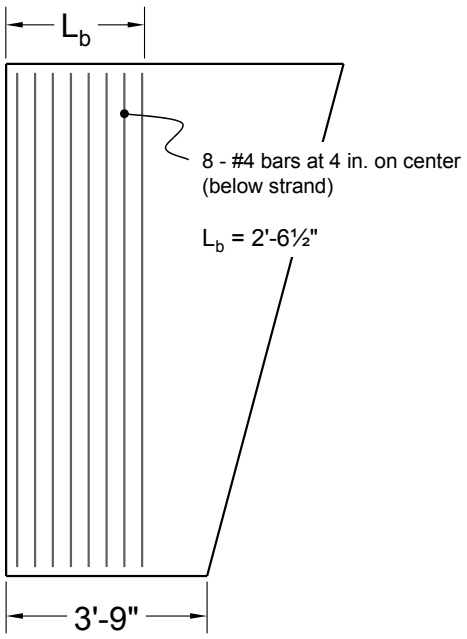

Figure A.11 Layout of #4 Deformed Bars in PC Panel with 15° Skew

The distance over which the #4 bars must be distributed, L_b, is determined by the dimensions of the shaded parallelogram in Figure A.12, which is defined by the length of the short side of the panel, L_{sh}, and the skew angle, θ. The critical skew angle, θ_{cr}, corresponds to the case where $L_b = L_{sh}$:

$$\tan \theta_{cr} = L_{sh} / L_{sq} \qquad \text{(A.1)}$$

where L_{sq} is the length of the square end of the panel. If the skew angle is less than θ_{cr}, the required length of the #4 bars is less than the short side of the panel. If the skew angle exceeds θ_{cr}, the #4 bars must be distributed along the length of the short side of the panel. The required number of #4 bars is summarized in Table A.2 for various skew angles. When the skew angle is less than θ_{min} , the #4 bars are no longer required.

$$\tan \theta_{min} = (4 \text{ in})/L_{sq} \qquad \text{(A.1)}$$

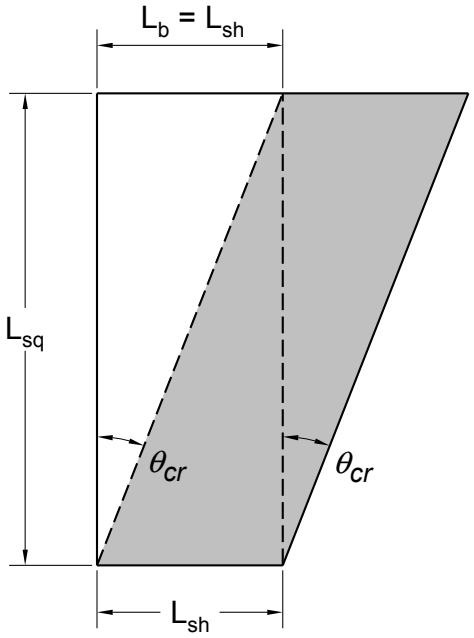

Figure A.12 Definition of Critical Skew Angle

Table A.2 Number of #4 Bars Required in Bottom Layer of Reinforcement

Length of Square End = 9'-6" Length of Short Side = 3'-9"			Length of Square End = 7'-6" Length of Short Side = 3'-9"		
Skew Angle	L_b (ft)	Number of #4 Bars	Skew Angle	L_b (ft)	Number of #4 Bars
≥ 21.5°	3.75	11	≥ 26.6°	3.75	11
20°	3.46	10	25°	3.50	10
15°	2.55	8	20°	2.73	8
10°	1.68	5	15°	2.01	6
5°	0.83	2	10°	1.32	4
< 2°	—	0	5°	0.66	2
			< 2°	—	0

Number 3 bars should be placed immediately above the strands and oriented parallel to the sides of the panel as is standard TxDOT practice for rectangular PCP details. The bars are spaced at 6 in. on center. For a square end length of 9'-6", nineteen #3 bars are placed in all panels, regardless of the skew angle (Figure A.13). For panels with a square end length of 7'-6", fifteen #3 bars are required.

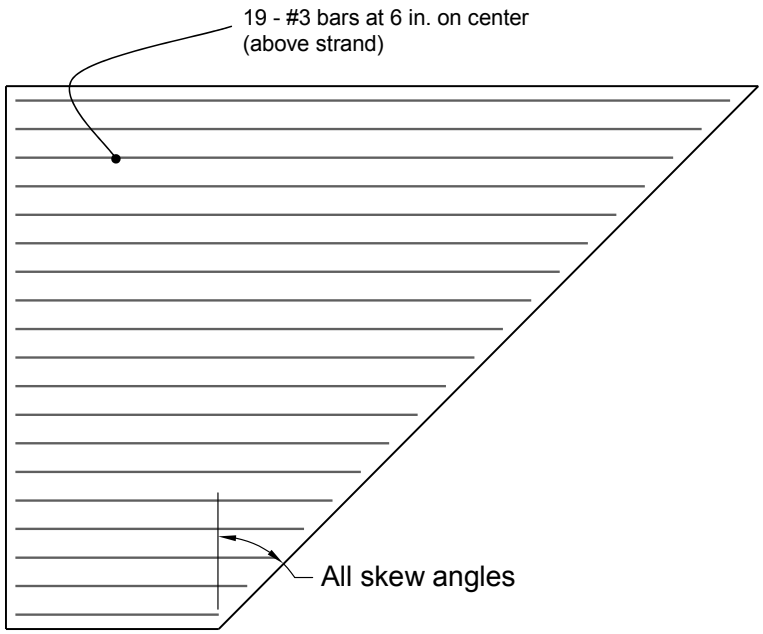

Figure A.13 Layout of #3 Deformed Bars in PC Panel with 45° Skew

A.3 Construction of PC Panels

The test results indicated that the performance of the composite bridge deck is sensitive to the surface roughness of the precast panels. The precast panels constructed by the research team and the second set of 30° PC panels fabricated at a commercial precast yard had well-defined deformations on the top surface, and the specimens performed satisfactorily. However, the test specimens constructed using the first set of 30° PC panels fabricated at a commercial precast yard failed by delamination of the topping slab from the precast panel. Although these panels had a broom finish that presumably satisfied TxDOT Specifications, the deformations on the top surface of the concrete was quite smooth. It is believed that the practice of flooding the panels with water immediately after placing the concrete may have reduced the roughness of the surface of the precast panel. It should also be noted that the surface of the precast panels was not pre-wetted prior to placement of the topping slab as required by TxDOT Standard Specifications. It is not known whether proper wetting would have prevented or delayed delamination of the topping slab. The second set of 30° PC panels had a rougher surface and the surfaces were pre-wetted prior to casting the topping slab. No delamination was observed.

Minimum requirements for surface roughness of the PC panels to ensure satisfactory response of the composite bridge were not within the scope of this study. It is, however, recommended that the TxDOT Specifications for surface roughness of PCP units be reviewed. It may be desirable to specify minimum requirements for the amplitude and spacing of the deformations on the top surface of the PC panels. ACI 318-08 includes a requirement that "…the interface for shear transfer shall be clean and free of laitance. If μ {*coefficient of friction*} is assumed to be 1.0, interface shall be roughened to a full amplitude of approximately ¼ in."

While this provision provides guidance regarding the amplitude of the roughened surface, there is no guidance regarding the distance over which the amplitude should be measured.

A.4 Construction of Composite Bridge Decks

Two issues related to the constructibility of composite bridge decks with PC panels were identified during this research project—bedding strips and spacing between panels.

A.4.1 Bedding strips

Currently, bedding strips are typically cut from sheets of 40-psi Styrofoam. Preliminary calculations indicated that this material had sufficient strength to support the PC panels and topping slab. However, crushing of the bedding strips was observed during the construction of the test specimens. Since bottom of the panels may not be true plane or the alignment of panel and the supporting girder may not result in a uniform spacing between the two elements, it is not possible to ensure that the dead load is uniformly distributed along the bedding strips during placement of the PC panels. Inevitably, one corner of the trapezoidal panel will contact the bedding strip first. In the test program, crushing of the Styrofoam was observed at those locations. The observed deformations were appreciably less when 60-psi Styrofoam was used for the bedding strips. Therefore, 60-psi Styrofoam is recommended for use with trapezoidal PC panels.

A.4.2 Spacing between panels and use of backer rods

With the IBTS detail at expansion joints, PCP units could be butted against each other and any dimensional variations were accounted for by cast-in-place concrete. With the use of panels over the entire length of the bridge, some tolerance should be provided for spacing between panels. In the test program, ¾ in. spacing was the desired gap between the skewed panels and adjacent rectangular panels. In the case of the 30º skew panels, the spacing had to be increased. The trapezoidal panels constructed at a commercial precast yard had dimensions and angles that were not true. Lumber was used to construct the formwork for the short side, square end, and long side. Because lumber is not as stiff as the metal formwork used for rectangular panels, the edges of the trapezoidal panels were not straight and the angles between sides varied. It was possible to accommodate these variations by permitting larger gaps between panels. These gaps were filled with backer bars to prevent leakage of concrete from the cast-in-place deck and did not influence the overall response of the composite bridge deck. In one instance the gap was nearly two inches wide and was filled with backing material. When the specimens were tested, there was no indication that the width of the gap had any influence on the load carrying capacity of the panels.

References

Agnew, L.S. (2007). "Evaluation of the Fatigue Behavior of Bridge Decks with Precast Panels at Expansion Joints," M.S. Thesis, Department of Civil, Architectural and Environmental Engineering, The University of Texas at Austin, 152 p. (http://fsel.engr.utexas.edu/publications/detail.cfm?pubid=326165804)

Boswell, C.A. (2008). "Simple Design Details using Precast Concrete Panels at Skewed Expansion Joints," M.S. Thesis, Department of Civil, Architectural and Environmental Engineering, The University of Texas at Austin. (http://fsel.engr.utexas.edu/publications/detail.cfm?pubid=605113705)

Coselli, C.J.; Griffith, E.M.; Ryan, J.L.; Bayrak, O.; Jirsa, J.O.; Breen, J.E.; and Klingner, R.E. (2006). "Bridge Slab Behavior at Expansion Joints," Research Report 0-4418-1, Center for Transportation Research, The University of Texas at Austin, 101 p. (http://www.utexas.edu/research/ctr/pdf_reports/0_4418_1.pdf)

Kreisa, A.R., (2008). "Constructibility of Prestressed Concrete Panels for Use at Skewed Expansion Joints," M.S. Thesis, Department of Civil, Architectural and Environmental Engineering, The University of Texas at Austin. (http://fsel.engr.utexas.edu/publications/detail.cfm?pubid=605113100)